ESCUELA TÉCNICA SUPERIOR DE INGENIERÍA (ICAI)

INGENIERO INDUSTRIAL

OFFSHORE ENERGY GENERATION: JOINT RECUPERATION OF WIND AND TIDAL POWER

Autor: Laura Miranda Lasa
Director: Aymeric Vié, Fernando de Cuadra Garcia

Madrid
Julio 2017

OFFSHORE ENERGY GENERATION: JOINT RECUPERATION OF WIND AND TIDAL POWER

Laura Miranda Lasa

AUTHORIZATION FOR DIGITALIZATION, STORAGE AND DISSEMINATION IN THE NETWORK OF END-OF-DEGREE PROJECTS, MASTER PROJECTS, DISSERTATIONS OR BACHILLERATO REPORTS

1. Declaration of authorship and accreditation thereof.

The author Mr. /Ms. Laura Miranda Lasa

HEREBY DECLARES that he/she owns the intellectual property rights regarding the piece of work: Offshore Energy Recuperation : Joint Recuperation of Wind and Tidal Power
that this is an original piece of work, and that he/she holds the status of author, in the sense granted by the Intellectual Property Law.

2. Subject matter and purpose of this assignment.

With the aim of disseminating the aforementioned piece of work as widely as possible using the University's Institutional Repository the author hereby **GRANTS** Comillas Pontifical University, on a royalty-free and non-exclusive basis, for the maximum legal term and with universal scope, the digitization, archiving, reproduction, distribution and public communication rights, including the right to make it electronically available, as described in the Intellectual Property Law. Transformation rights are assigned solely for the purposes described in a) of the following section.

3. Transfer and access terms

Without prejudice to the ownership of the work, which remains with its author, the transfer of rights covered by this license enables:

a) Transform it in order to adapt it to any technology suitable for sharing it online, as well as including metadata to register the piece of work and include "watermarks" or any other security or protection system.

b) Reproduce it in any digital medium in order to be included on an electronic database, including the right to reproduce and store the work on servers for the purposes of guaranteeing its security, maintaining it and preserving its format.

c) Communicate it, by default, by means of an institutional open archive, which has open and cost-free online access.

d) Any other way of access (restricted, embargoed, closed) shall be explicitly requested and requires that good cause be demonstrated.

e) Assign these pieces of work a Creative Commons license by default.

f) Assign these pieces of work a HANDLE (*persistent* URL). by default.

4. Copyright.

The author, as the owner of a piece of work, has the right to:

a) Have his/her name clearly identified by the University as the author

b) Communicate and publish the work in the version assigned and in other subsequent versions using any medium.

c) Request that the work be withdrawn from the repository for just cause.

d) Receive reliable communication of any claims third parties may make in relation to the work and, in particular, any claims relating to its intellectual property rights.

5. Duties of the author.

The author agrees to:

a) Guarantee that the commitment undertaken by means of this official document does not infringe any third party rights, regardless of whether they relate to industrial or intellectual property or any other type.

b) Guarantee that the content of the work does not infringe any third party honor, privacy or image rights.
c) Take responsibility for all claims and liability, including compensation for any damages, which may be brought against the University by third parties who believe that their rights and interests have been infringed by the assignment.
d) Take responsibility in the event that the institutions are found guilty of a rights infringement regarding the work subject to assignment.

6. Institutional Repository purposes and functioning.

The work shall be made available to the users so that they may use it in a fair and respectful way with regards to the copyright, according to the allowances given in the relevant legislation, and for study or research purposes, or any other legal use. With this aim in mind, the University undertakes the following duties and reserves the following powers:

a) The University shall inform the archive users of the permitted uses; however, it shall not guarantee or take any responsibility for any other subsequent ways the work may be used by users, which are non-compliant with the legislation in force. Any subsequent use, beyond private copying, shall require the source to be cited and authorship to be recognized, as well as the guarantee not to use it to gain commercial profit or carry out any derivative works.
b) The University shall not review the content of the works, which shall at all times fall under the exclusive responsibility of the author and it shall not be obligated to take part in lawsuits on behalf of the author in the event of any infringement of intellectual property rights deriving from storing and archiving the works. The author hereby waives any claim against the University due to any way the users may use the works that is not in keeping with the legislation in force.
c) The University shall adopt the necessary measures to safeguard the work in the future.
d) The University reserves the right to withdraw the work, after notifying the author, in sufficiently justified cases, or in the event of third party claims.

Madrid, on ..18….. of ..July 2017……..., …….

HEREBY ACCEPTS

Signed…… 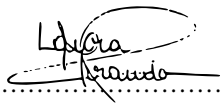 ……

Reasons for requesting the restricted, closed or embargoed access to the work in the Institution's Repository

Declaro, bajo mi responsabilidad, que el Proyecto presentado con el título: *Offshore Energy Generation: Joint Recuperation of Wind and Tidal Power*, en la ETS de Ingeniería - ICAI de la Universidad Pontificia Comillas en el curso académico 2016/2017 es de mi autoría, original e inédito y no ha sido presentado con anterioridad a otros efectos. El Proyecto no es plagio de otro, ni total ni parcialmente y la información que ha sido tomada de otros documentos está debidamente referenciada.

Fdo.: Laura Miranda Lasa Fecha: 18/ 07/ 2017

Autorizada la entrega del proyecto

EL DIRECTOR DEL PROYECTO

Fdo.: Aymeric Vié Fecha: 7/ 13/ 2017

Vº Bº del Coordinador de Proyectos

Fdo.: Fernando de Cuadra Garcia Fecha: ...../ ...../ .....

DISEÑO DE UN PARQUE DE RECUPERACION DE ENERGIA OFFSHORE: APROVECHAMIENTO CONJUNTO DE LA ENERGIA EOLICA Y MAREOMOTRIZ

Autor: Miranda Lasa, Laura.

Director: Vié, Aymeric.

Entidad Colaboradora: ICAI – Universidad Pontificia Comillas, Ecole Centrale Paris

RESUMEN DEL PROYECTO

INTRODUCCIÓN

El crecimiento de la población mundial *[1]* supone un incremento de la demanda de producción de energía. La Agencia Internacional de la Energía (IEA) prevé que la demanda mundial de electricidad aumentará un 70% hasta 2040 *[2]*. El aumento de la demanda se yuxtapone a una desaforada explotación de los escasos recursos fósiles, origen de la producción de las energías tradicionales. Estas dos condiciones tienen consecuencias humanas y medio ambientales - destrucción de ecosistemas, calentamiento del planeta, hambrunas, dependencia energética de países productores de petróleo etc.

Las energías renovables son fuentes de energía limpias, inagotables y crecientemente competitivas. Representan cerca de la mitad de la nueva capacidad de generación eléctrica instalada en 2014 según la IEA *[2]*. Por añadidura, el coste de su generación evoluciona a la baja, contrariamente a los costes de los combustibles fósiles.

Dentro de las fuentes de energías renovables, los océanos – constituyendo el 71% de la superficie terrestre *[3]* - tienen un inmenso potencial de generación de tres tipos de energías: mareomotriz, undimotriz y eólica offshore. Sin embargo, la recuperación de estas energías conlleva nuevos desafíos tecnológicos: mantenimiento de turbinas en condiciones de elevada humedad, problemas de corrosión o instalación de cableado submarino. Por ende, los costes de instalación y mantenimiento de estos equipos son importantes.

Este proyecto nace en el seno de una intuición industrial, que se ha querido estudiar y validar cualitativamente. En la actualidad, existen iniciativas industriales, que investigan el potencial de reducción de costes de una instalación conjunta offshore. Es el caso de CENIT-E OCEAN LIDER de Iberdrola *[4],* cuyo objetivo es crear conocimiento sobre tecnologías rupturistas, para el aprovechamiento eficiente e integral de las energías oceánicas, a través de la creación de sistemas híbridos como energía de las corrientes/eólica o undimotriz/eólica.

En esta línea, este proyecto propone el diseño un parque de recuperación de energía del mar en Normandía, para el aprovechamiento conjunto de la energía eólica offshore y de la energía mareomotriz. La proyección de dicho parque se justifica bajo la hipótesis de

una reducción de costes, debido a la posibilidad de mutualizar elementos de ambas tecnologías en un mismo parque**.** Además, la tentativa de proponer un parque de recuperación de energía mareomotriz y eólica offshore en Raz Blanchard (Normandía), responde al gran potencial energético de estas dos energías en el Canal de la Mancha *[5]* y a la voluntad política de desarrollar ambas tecnologías en la zona *[6,7]*.

La energía eólica –dado el fuerte apoyo económico recibido por parte de las autoridades políticas desde los años 80- es una tecnología madura, barata y de fuerte rendimiento. La variabilidad del viento, fuera del control del humano, permanece su gran desventaja. Al contrario, la energía de las corrientes marinas sigue a estado de prueba, con la construcción, actualmente, de los primeros parques mareomotores. La apuesta de los industriales y de las autoridades por este nuevo tipo de energía renovable augura grandes posibilidades de desarrollo. Efectivamente, la previsibilidad de las corrientes marinas representa su gran ventaja.

La complementariedad de estas dos energías es indudable.

Los costes de estas instalaciones, tanto eólicas como mareomotrices, siguen representando una gran inversión. Las reparticiones de costes de estas energías difieren. Sin embargo, una gran parte se puede atribuir a la construcción del parque (fundaciones, sistema eléctrico, cableado…) y a su mantenimiento. Las posibilidades de mutualización de estos son los motores de este proyecto.

El riesgo rupturista de este proyecto puede quedar en parte minimizado, si como esperan el autor del mismo y la industria, las autoridades de diferentes gobiernos mantienen y/o aumentan el apoyo reciente a este tipo de instalaciones. Así pues, en consecuencia, proyectos como este son necesarios para anticipar el cambio de políticas energéticas, apoyando el desarrollo de energías renovables con mayor carácter de predictibilidad que las actuales.

En resumen, este proyecto trata de maximizar la recuperación una energía madura pero fluctuante, como la eólica, con una energía todavía innovadora, pero predictible, como la mareomotriz. En un parque offshore conjunto, la rentabilidad económica de la energía eólica supone, para los inversores privados, una renta segura, mientras que, para la energía mareomotriz, un gran impulso a su desarrollo.

METODOLOGÍA

En primer lugar, se realizó un estudio meteorológico y se establecieron criterios de decisión para la selección del emplazamiento del parque. La elección de un área de 50 km^2 entre Auderville y la isla de Sainte-Anne responde, ante todo, al optimo potencial de recuperación de ambas energías en esta área. Para encontrar una zona con fuertes vientos y corrientes marinas, se estableció una colaboración con OpenOcean *[8]* (empresa de simulación de datos marinos, para la ayuda a la decisión de industrias offshore). De manera iterativa, se fueron comparando las simulaciones digitales de regímenes de viento y corrientes marinas, proporcionados por OpenOcean, para elegir la mejor de las zonas en Raz Blanchard. Además, esta área final tiene en cuenta una superposición de restricciones geográficas (barimetría, suelo marino), comerciales (cableado submarino, rutas de paso) y sociales (visibilidad y distancia a la costa). Se dispone de datos horarios

y anuales simulados, de tanto la magnitud, como la orientación del viento y las corrientes marinas en el área seleccionada.

Figura 1: Emplazamiento del parque offshore

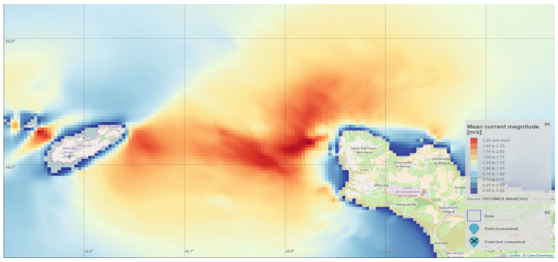

Figura 2: Magnitud media de la corriente marina en el área [8]

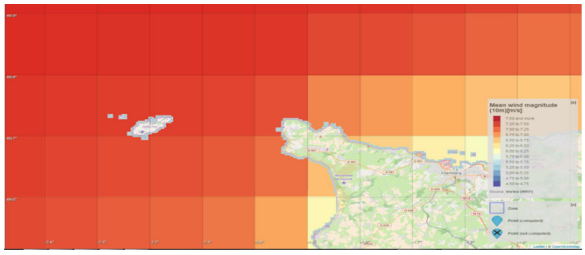

Figura 3: Magnitud media del viento en el área [8]

Una vez elegido el emplazamiento optimo, se realizó un estudio teórico del proceso de transformación de la energía del viento o de las corrientes a energía eléctrica. Se determinaron los componentes clave de este sistema, disponiendo así de criterios de decisión para la selección del modelo de turbinas eólicas e hidráulicas que constituirían el parque. Siguiendo las tendencias actuales en materia de energía eólica offshore y *[9],* la turbina eólica Siemens Sapiens 6MW de generador síncrono a imanes permanentes, y la turbina hidráulica SeaGen 2MW de generador asíncrono fueron seleccionadas para esta instalación.

El diseño del parque offshore se basa en el dimensionamiento del espacio óptimo entre las unidades de recuperación de energía eólica y mareomotriz. Para ello, se tuvo en cuenta por un lado las indicaciones dadas por la literatura *[10, 11]*. En efecto, las interacciones entre unas mismas turbinas de viento y entre unas mismas turbinas de hidráulicas han estudiadas y pautadas por los industriales. Sin embargo, dado el carácter innovador y nunca realizado de este proyecto, el estudio de las interacciones entre una turbina de viento y una hidráulica no consta. Por esta razón, se llevó a cabo una simulación de mecánica de fluidos - mediante el programa ANSYS Fluent - para el cálculo de los efectos turbulentos, provocados por el mástil de la turbina eólica, en el océano (ver Figura 4).

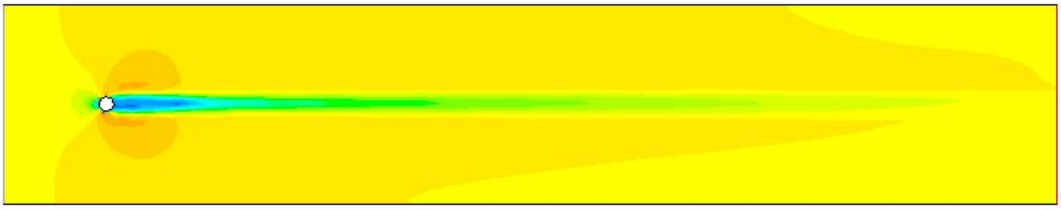

Figura 4: Perturbación de la corriente marina por el mástil de la turbina eólica Resultados obtenidos con ANSYS – FLUENT

Disponiendo, así, de los parámetros limitantes de espaciamiento entre unidades, y de los datos meteorológicos del área seleccionada (tanto magnitud como orientación del viento y de la corriente), se diseñó el parque. Se concluyó con la decisión de instalar 100 turbinas mareomotrices y 50 turbinas eólicas, de capacidad total de 500MW. En la Figura 5 se aprecia la superposición de las coacciones de espaciamiento: en rojo la cuadricula de espaciamiento de las turbinas hidráulicas y en azul la de las turbinas eólicas.

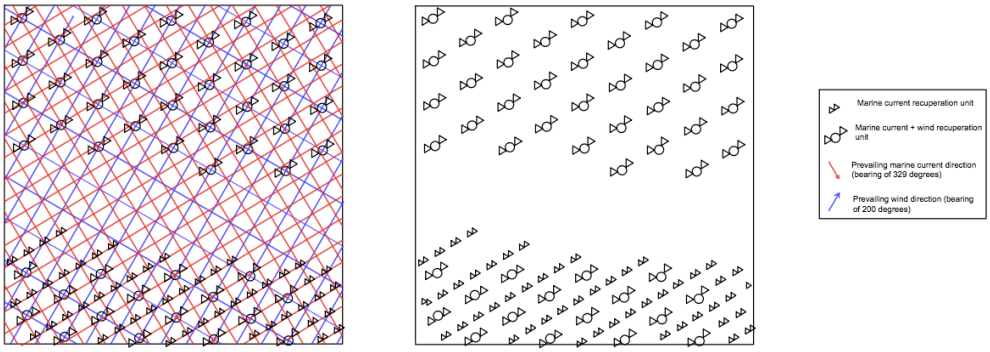

Figura 5: Disposición de los elementos de recuperación de energía del parque offshore

Por añadidura, para calcular el potencial de producción de energía anual del parque diseñado en función de la meteorología, el trabajo cuenta con el desarrollo de dos programas SIMULINK -uno para simular las turbinas eólicas, y otro para simular las turbinas hidráulicas. Estos sirven de modelo eléctrico de las tecnologías elegidas, y permiten comprender y cuantificar la transformación mecánico-eléctrica de la energía eólica y mareomotriz de la zona elegida. Estos programas reciben en entrada los datos del viento y de las corrientes marinas, para simular el comportamiento del parque cada hora a lo largo de un año.

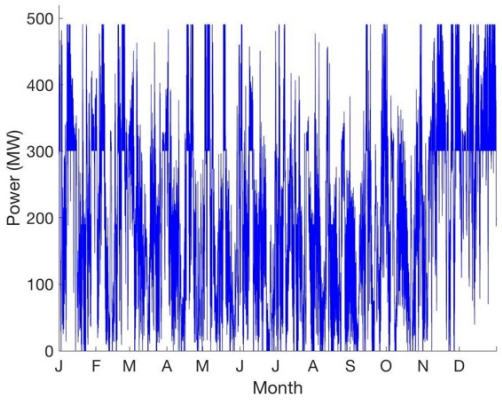

Figura 6: Potencial anual extraída del parque offshore diseñado
Resultados obtenidos con los modelos SIMULINK

Finalmente, la pertinencia de este proyecto depende de su viabilidad económica. Para extraer estas conclusiones e investigar la hipótesis inicial de reducción de costes, se creó un indicador económico de Levelised Cost of Energy (LCoE). Se siguieron las pautas marcadas por curso en línea de la Universidad Técnica de Dinamarca *[12],* para

comprender la estructura de costes de ambas tecnologías y calcular el coste del MWh de éstas. Dicho indicador se utiliza en la parte final del proyecto, como punto de partida, para un análisis de diferentes hipótesis de reducción de costes debidas a la recuperación conjunta de ambas energías –reparto de instalaciones eléctricas, cableado submarino, instalación, o costes de mantenimiento, entre otros.

RESULTADOS Y CONCLUSIONES

El diseño del parque desde un punto de vista eléctrico, logístico y mecánico concluye con resultados tanto cuantitativos como cualitativos.

De este modo, el estudio técnico-económico del parque compartido obtiene resultados cuantitativos para el emplazamiento de éste, su distribución, la energía generada anual y el coste de esta energía por MWh. Sin embargo, dicho estudio proporciona resultados cualitativos para las oportunidades de reducción de costes, mediante un análisis de sensibilidad de éstos, bajo hipótesis de sinergias entre las tecnologías.

El proyecto propone un parque integrado e innovador, que complementa la recuperación de energía mediante una tecnología madura, competitiva y fluctuante (eólica) con la de una tecnología aún experimental, más cara, pero previsible (mareomotriz). Además de señalar las posibles reducciones de costes que la co-localización de la recuperación de estas energías supondría, este trabajo implica un apoyo a la energía mareomotriz, que promocionaría su desarrollo y permitiría que fuera económicamente competitiva.

REFERENCIAS

[1] Estadísticas Banco Mundial, 2015. Online : datos.bancomundial.org/indicator/SP.POP.TOTL?end=2015&start=1960&view=chart
[2] World Energy Outlook 2014, International Energy Agency.
[3] Surface area of our planet covered by oceans and continents, 2006. Pidwirny, Michael, University of British Columbia, Okanagan.
[4]: 3rd International Conference on Ocean Energy. “OCEAN LIDER: Ocean Renewable Energy Leaders” J. Amate López, 2010
[5] Éolien en Mer, France Énergie Éolienne. Online: www.fee.asso.fr/politique-de-leolien/eolien-en-mer/
[6] Resumen regional de desarrollo de energías renovables, Réseau de transport d’électricité Rte France. Online: www.rtefrance.com/sites/default/files/be_regional_2013_bretagne.pdf
[7] L’Éolien Offshore Français Monte en Puissance : Où en est-on ?, Niels de Grival 2015. Revista: E-RSE. Online: www.e-rse.net/leolien-offshore-monte-en-puissance-19419/amp
[8] Open Ocean: Marine Data Intelligence. Official website: www.openocean.fr/
[9] 4coffshore, 2016. Online: www.4coffshore.com/
[10]: *The wind Farm Layout Optimization Problem*, 2013, Michele Samorani.
[11] *SeaGen Environmental Monitoring Programme*, 2012, Royal HASKONING.
[12]: MOOC: Wind Energy, Danish Technical University. Available online at: www.coursera.org

DESIGN OF AN OFFSHORE ENERGY GENERATION PARK: JOINT RECUPERATION OF WIND AND TIDAL POWER

Author: Miranda Lasa, Laura.

Director: Vié, Aymeric.

Collaborating Entity: ICAI – Universidad Pontificia Comillas, Ecole Centrale Paris

ABSTRACT

INTRODUCTION

The growth of the world's population *[1]* involves an increase in the energy production demand. The International Energy Agency (IEA) predicts a risen of 70% of the global demand for electricity until 2040 *[2]*. The increase of the demand juxtaposes itself to an unbridled utilisation of scarce fossil resources, traditional source of energy production. These two conditions have human and environmental consequences – ecosystem destructions, global warming, famines, energy dependency on fuel producer countries etc.

Renewable energies are a clean, endless and growingly competitive source of energy. They represent almost half of the new electric generation capacity installed in 2014, according to the IEA *[2]*. In addition to this, the cost of its generation evolves downwards, contrary to the cost of fossil fuels.

Among renewable energies, oceans – constituent 71% of the earth's surface *[3]* – have an immense generation potential of three types of energy : tidal, wave and wind offshore. However, the recuperation of this energy implies new technological challenges: turbine maintenance in high humidity conditions, corrosion problems or installation of underwater cables. For that matter, the installation costs and maintenance of these equipment are significant.

This project was born under the wing of an industrial intuition, to be studied and validated qualitatively. Currently, there are industrial initiatives that explore the potential cost reductions of a joint offshore installation. It is the case of CENIT-E OCEAN LIDER by Iberdrola *[4],* whose objective is to create expertise of rupturist technologies, for the efficient and integral use of the oceanic energies, through the creation of hybrid systems such as tidal current/eolic or wave/eolic.

In this regard, this project suggests the design of an ocean energy recuperation park in Normandy, for the joint use of offshore wind energy and tidal energy. The forecast of this park justifies itself under the assumption of a cost reduction, due to the possibility of element mutualizing, between both technologies, in one park. Moreover, the attempt of proposing an offshore energy recuperation park for wind and tidal energy in Raz Blanchard (Normandy) responds to a huge energy potential of these two energies in the

English Channel *[5],* and to the political will of developing both technologies in the area *[6,7]*.

Wind energy – provided the strong economic support received from the political authorities since the 80's- represents a mature, affordable and high-performance technology. The wind's variability, out of human control, remains its major disadvantage. On the contrary, tidal current energy is still on a testing stage, with the construction currently, of the first tidal current energy parks. The bet of industrials and authorities on this new type of renewable energy promises strong possibilities of growth. Indeed, the predictability of tidal current represents its key benefit.

The complementarity of these two energies is undeniable.

The cost of these installations, wind as well as tidal current, still constitutes a significant investment. The cost sharing of these energies differs. However, a substantial part is assigned to the construction of the park (foundations, electric system, cabling…) and to its maintenance. The possibilities of mutualisation of these are the driving force of this project.

The rupturist risk of this project can be partly minimized, if as expected by the author and the industry, the authorities of different governments keep and/or increase their recent support to this type of facilities. Therefore, projects, such as this one, are necessary to anticipate the changes in the energy policies, promoting the development of renewable energies, with higher predictability than the existing ones.

In fine, this project aims to maximise the recuperation of a mature, but fluctuating energy, such as the offshore wind, with an innovative, but predictable energy, such as the tidal current. In an offshore joint park, the economic profitability of wind energy supposes, for private investors, a safe income, whereas, for tidal current energy, a major boost to its development.

METODOLOGY

Firstly, a meteorological study was furthered in order to establish decision criteria for the selection of the park's location. The choice of a 50 km^2 area between Auderville and Sainte-Anne island responds, first and foremost, to the optimal potential of both energies in this area. To find a location with strong wind and strong sea current, a collaboration was established with OpenOcean *[8]* (simulation company of marine data, for decision-making in offshore activities). Iteratively, the comparison of annual wind and sea current simulated regimes, given by OpenOcean, enabled the selection of the best and most adapted areas in Raz Blanchard (Normandy) for the installation of the park. Furthermore, the final area considers an overlap of geographical (barometer, sea floor), commercial (underwater cable, sea routes) and social constraints (visibility and distance to the coast). Hourly and annually simulated data of the selected area were given: magnitude as well as orientation of the wind and sea currents.

Figure 1: Selected area for the offshore park location

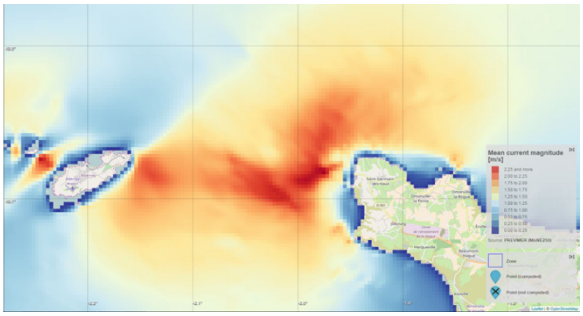

Figure 2: Mean sea current magnitude in the area [8]

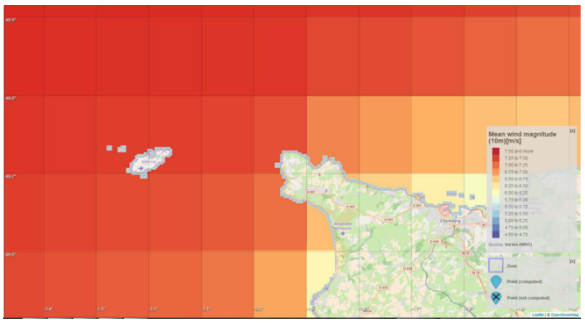

Figure 3: Annual wind magnitude in the area [8]

Once the optimal location had been selected, a theoretical study of the process of transformation of wind or tidal current energy into electrical energy was furthered. The key components of this process were determined, thus providing decisive criteria for the selection of the models the hydraulic and wind turbines, that would constitute the park. Following actual trends in terms of offshore wind energy and *[9],* the Siemens Sapiens 6MW wind turbine of synchronous generator with permanent magnet and SeaGen 2MW tidal current turbine of asynchronous generator were chosen for the facility.

The design of the offshore park is based on the dimensioning of the optimal spacing between the different energy recuperation units (wind and tidal). To do this, were considered indications given by literature *[10,11]*. Indeed, the interactions between the same wind turbines and between the same tidal current turbines have been studied and guidelined by the industry. However, because of its innovative nature, the study of the interaction between a wind turbine and a tidal current turbine does not feature. On this accound, a fluids mechanics simulation was driven – through the program ANSYS Fluent- for the estimation of the turbulent effects, caused by the wind turbine mast, in the ocean (see the Figure 4).

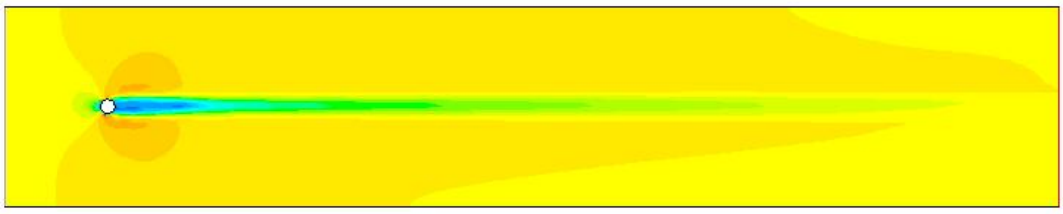

Figure 4: Disruption of the sea current by the mast of the wind turbine Results obtained with ANSYS - Fluent

We finally boast all the limiting parameters of the needed-spacing between the recuperation units, as well as the meteorological data of the chosen area (magnitude and orientation of the wind and tidal current). It was concluded to install 100 tidal current turbines and 50 wind turbines, for a total capacity of 500MW. On the Figure 5, on the left sketch is noticeable the overlap of the spacing constraints: in red, the grid of the tidal current turbines spacing, and in blue, the grid of the wind turbines spacing.

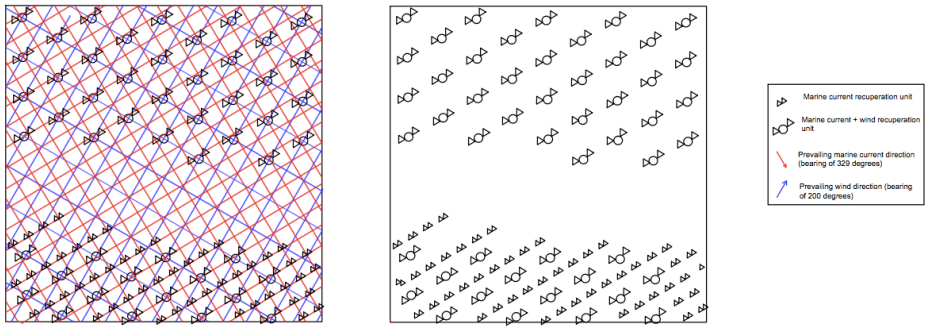

Figure 5: Allocation of the energy recuperation units for the park design

Also, to calculate the annual energy production of the designed park according to the weather, the study relies on the developing of two Simulink programs – one to model the wind turbine, and another to model the tidal current turbine. These function as an electric model of the chosen technologies, and allow the understanding and quantification of the mechanical-electrical transformation of the wind and sea current energy in the chosen area. These programs receive as input the wind and sea current magnitude data to simulate the performances of the park hourly for a year long.

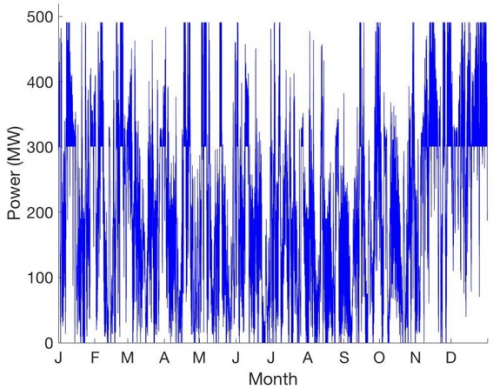

Figure 6: Annual power produced by the offshore designed park
Results obtained with the Simulink models

Finally, the relevance of this project depends on its economical sustainability. To draw these conclusions and explore the initial assumption of cost reductions, an economic indicator of Levelised Cost of Energy (LCoE) was created following the guidelines given by the online Course of the Danish Technical University *[12]*. This enabled the understanding of the cost structure for both technologies, just as, the calculation of the cost of the MWh. The LCoE indicator is used, in the final part of the study, as a starting point for an analysis of the different cost reduction assumptions, thanks to the joint

recuperation of energy – sharing of electrical installation, underwater cable, installations, among others.

RESULTS AND CONCLUSIONS

The design of the park, from an electrical, logistical and mechanical point of view, concludes with quantitative and qualitative results.

Thus, the technical-economical study of the jointed park reaches quantitative results for the location of the park, its design, the annual produced energy and the cost of this energy production per MWh. However, the study delivers qualitative results for the cost reduction opportunities, through a sensitivity analysis under the assumption of synergies between these two technologies.

The project proposes an integrated and innovative park, that complements the recuperation of energy through a mature, competitive and fluctuant energy (wind energy) with a technology that remains experimental, more expensive but foreseeable (tidal energy). Besides indicating the possible cost reductions that the co-location of the recuperation of these energies would enable, this park implies a support to the tidal energy, and would promote its growth and allow it to become economically more competitive.

REFERENCES

[1] Estadísticas Banco Mundial, 2015. Online : datos.bancomundial.org/indicator/SP.POP.TOTL?end=2015&start=1960&view=chart
[2] World Energy Outlook 2014, International Energy Agency.
[3] Surface area of our planet covered by oceans and continents, 2006. Pidwirny, Michael, University of British Columbia, Okanagan.
[4]: 3rd International Conference on Ocean Energy. "OCEAN LIDER: Ocean Renewable Energy Leaders" J. Amate López, 2010
[5] Éolien en Mer, France Énergie Éolienne. Online: www.fee.asso.fr/politique-de-leolien/eolien-en-mer/
[6] Resumen regional de desarrollo de enerías renovables, Réseau de transport d'électricité Rte France. Online: www.rtefrance.com/sites/default/files/be_regional_2013_bretagne.pdf
[7] L'Éolien Offshore Français Monte en Puissance : Où en est-on ?, Niels de Grival 2015. Revista: E-RSE. Online: www.e-rse.net/leolien-offshore-monte-en-puissance-19419/amp
[8] Open Ocean: Marine Data Intelligence. Official website: www.openocean.fr/
[9] 4coffshore, 2016. Online: www.4coffshore.com/
[10]: *The wind Farm Layout Optimization Problem*, 2013, Michele Samorani.
[11] *SeaGen Environmental Monitoring Programme*, 2012, Royal HASKONING.
[12]: MOOC: Wind Energy, Danish Technical University. Available online at: www.coursera.org

ESCUELA TÉCNICA SUPERIOR DE INGENIERÍA (ICAI)

INGENIERO INDUSTRIAL

OFFSHORE ENERGY GENERATION: JOINT RECUPERATION OF WIND AND TIDAL POWER

Autor: Laura Miranda Lasa
Director: Aymeric Vié, Fernando de Cuadra Garcia

Madrid
Julio 2017

OFFSHORE ENERGY GENERATION: JOINT RECUPERATION OF WIND AND TIDAL POWER

Laura Miranda Lasa

Acknowledgements

I would like to thank my supervisor, Aymeric Vie for guiding and supporting my work throughout the year.

Moreover, I would like to thank Amir Arzandé for his patience and help throughout this process; our discussions and ideas have been invaluable.

I am very grateful to Jean Claude Vannier and Pascal Da Costa for their feedback on this project.

Lastly, this project would not have been possible without the collaboration and advice of OpenOcean.

INDEX

LIST OF FIGURES

LIST OF EQUATIONS

LIST OF TABLES

1. INTRODUCTION

The growth of the world's population involves an increase in the energy production demand. The International Energy Agency (IEA) predicts a risen of 70% of the global demand for electricity until 2040. The increase of the demand juxtaposes itself to an unbridled utilisation of scarce fossil resources, traditional source of energy production. These two conditions have human and environmental consequences – ecosystem destructions, global warming, famines, energy dependency on fuel producer countries etc.

Renewable energies are a clean, endless and growingly competitive source of energy. They represent almost half of the new electric generation capacity installed in 2014, according to the IE. In addition to this, the cost of its generation evolves downwards, contrary to the cost of fossil fuels.

Among renewable energies, oceans – constituent 71% of the earth's surface– have an immense generation potential of three types of energy : tidal, wave and wind offshore. However, the recuperation of this energy implies new technological challenges: turbine maintenance in high humidity conditions, corrosion problems or installation of underwater cables. For that matter, the installation costs and maintenance of these equipment are significant.

This project was born under the wing of an industrial intuition, to be studied and validated qualitatively. Currently, there are industrial initiatives that explore the potential cost reductions of a joint offshore installation. It is the case of CENIT-E OCEAN LIDER by Iberdrola, whose objective is to create expertise of rupturist technologies, for the efficient and integral use of the oceanic energies, through the creation of hybrid systems such as tidal current/eolic or wave/eolic.

In this regard, this project suggests the design of an ocean energy recuperation park in Normandy, for the joint use of offshore wind energy and tidal energy. The forecast of this park justifies itself under the assumption of a cost reduction, due to the possibility of element mutualizing, between both technologies, in one park. Moreover, the attempt of proposing an offshore energy recuperation park for wind and tidal energy in Raz Blanchard (Normandy) responds to a huge energy potential of these two energies in the English Channel, and to the political will of developing both technologies in the area.

Wind energy – provided the strong economic support received from the political authorities since the 80's- represents a mature, affordable and high-performance technology. The wind's variability, out of human control, remains its major disadvantage. On the contrary, tidal current energy is still on a testing stage, with the construction currently, of the first tidal current energy parks. The bet of industrials and authorities on this new type of renewable

energy promises strong possibilities of growth. Indeed, the predictability of tidal current represents its key benefit.

The complementarity of these two energies is undeniable.

The cost of these installations, wind as well as tidal current, still constitutes a significant investment. The cost sharing of these energies differs. However, a substantial part is assigned to the construction of the park (foundations, electric system, cabling…) and to its maintenance. The possibilities of mutualisation of these are the driving force of this project.

The rupturist risk of this project can be partly minimized, if as expected by the author and the industry, the authorities of different governments keep and/or increase their recent support to this type of facilities. Therefore, projects, such as this one, are necessary to anticipate the changes in the energy policies, promoting the development of renewable energies, with higher predictability than the existing ones.

In fine, this project aims to maximise the recuperation of a mature, but fluctuating energy, such as the offshore wind, with an innovative, but predictable energy, such as the tidal current. In an offshore joint park, the economic profitability of wind energy supposes, for private investors, a safe income, whereas, for tidal current energy, a major boost to its development.

The key elements that have guided the educated decisions taken to find the best emplacement for our offshore facility, as well as its most economically profitable design, will be detailed throughout this report. Among these:

- Site selection. Were taken into account :
    - Meteorological study: energy maximisation of both energies (an optimal wind and optimal marine currents should be assured).
    - Constraints locations: such as greographical constraints (water depth) or political ones (impact on the landscape, view from the cost) as well as the environmental impact.
- Technology selection: selection of a wind turbine and tidal current turbine model
- Design of the park:
    - Study of the interferences between the installations: each energy recuperation unit should work at its maximum rate without being disturb by the surrounding units
    - Optimization of the available space
- Computation of the produced power: given the meteorological data of the park, the produced energy can be computed.
- Economical study: creation of a Life Cycle cost tool, that enables the calculation of potential cost reductions due to the coupling of both energies.

2.DOCUMENTARY REVIEW

2.1 Wind Energy and Technology

Wind energy refers to the transformation of the mechanical energy from the wind to electrical energy. The basic principle consists of an air flow which drives a generator and creates a current.

Wind energy has been a source of energy for humans since we put sails into wind. It has been used to ground grain, pump water and, recently, to generate electricity. In 1887, the first windmill for electricity conversion was deployed. Since then, this technology has advanced and evolved considerably. Even though, a positive trend and investments on wind energy are being made, in 2014, wind power only accounted for 3% of the energy mix, which is still a relatively low percentage *[1]*. In Europe, this percentage is much higher in many countries. In Spain in 2015, it accounted for nearly 20% of the generation mix came from wind power. In Denmark, this figure went up to 42%. *[2]*

The amount of energy in the wind is very important, and wind power can be a solution to our power needs. A study from Stanford University, proves that by 2030, "Wind power could meet many times world power demand". *[3]*

Despite the fact that wind energy is a renewable source of energy and pretty abundant, it does have a major drawback: its intermittence. As there has been no important development in the field of energy storage, energy consumption must meet energy production at any time. In the case of wind energy, it is difficult to adapt production to consumption, as it depends entirely on an external factor: the wind.

There are two main types of wind generators, which are HAWT (Horizontal Axis Wind Turbines) VAWT, yet other unconventional wind turbines are being developed. In our case, we only took into consideration the main existing types. Examples of these turbines are found in Figure 2.1.

Figure 2.1: Types of Wind Turbines; HAWT (left), VAWT (right)

2.1.1 HAWT

Horizontal Axis Wind Turbines (HAWT) are the most commonly used turbines, due to its effectiveness and performance. All of its components are found at the top of the tower. As its own name indicates, the blades are attached to a horizontal axis which move a generator. Normally HAWT have the ability to pitch the blades, providing the best attack angle and minimising the damage in case of a storm. HAWT are found onshore and offshore. *[4]*

2.1.2 VAWT

Vertical Axis Wind Turbines (VAWT), unlike HAWT, poses a vertical axis which makes the turbine non-directional. They are less efficient than horizontal ones and tend to be deployed in more turbulent wind. They are economically better than HAWT as construction and transportation cost are lower. In addition, they are easier to maintain.

2.2 Marine Energy and Technology

Marine energy – also referred to as ocean energy, energy power or marine and hydrokinetic energy – is a renewable source of energy, which is, currently, not very exploited. However, it is yet a form of energy which possesses great potential. They are, nonetheless, starting to be considered as an important element for renewable energy, due to its heavy load factor from the fluid characteristics. The predictable resource characteristics make marine currents

particularly attractive for power generation and advantageous, when compared to other renewable energies, such as wind power which is less predictable.

There are four main sources of ocean energy which are: ocean waves, current, salinity gradients and ocean temperature differences. Salinity and ocean temperature differences are two forms of energy generation which are currently less exploited. The principle behind ocean temperature difference is to use the difference between shallow and warmer water to run a heat engine and eventually produce electricity. There is only one operating OTEC (Ocean Thermal energy conversion) which uses this phenomenon to generate electricity in Japan.

Equally, salinity gradient energy production is a relatively new concept, which was discovered in 1970's and only recently has begun to make advances. The salinity based plants are based on the mixing of fresh and salt water to produce energy, thanks to a semi permeable membrane (ion specific membrane). This technology is nowadays considerably costly which discourages its use. The two main countries involved in the development of this technology are the Netherlands and Norway. *[5]*

In our case, we found interest in the two other forms of marine energy: wave energy and tides. The former uses the kinetic energy, captured in the wave, to produce work for electricity generation, water desalination or the pumping of water, amongst others. Although there has been a lot of attempts to use this technology (since 1890), wave power generation is not broadly employed nowadays. In 2008, Portugal launched the first experimental wave farm. Due to time limitations, and the greater production of energy that tidal energy produces, we decided to focus on tidal energy over wave energy – although the initial idea was to work on both of them. A complementary advantage of tidal energy was that most of the physical principles behind this form of energy production were the same, as the ones found in the wind turbines.

Tidal energy (tidal power) is a form of hydropower that converts energy from the tides into electricity. Although not widely used, recent advancements and cost reductions has made it a very attractive form of energy production. Economic and environmental costs have been brought to competitive levels, thus encouraging countries to invest in this form energy generation. Nowadays there are large-scale power plants across the globe.

There are four main turbine types or Tidal Energy Conversion Technology (TEC) as defined by EMEC (European Marine Energy Center) *[6]*. These four are: horizontal axis turbine, vertical axis turbine, venturi effect and oscillating hydrofoil as represented in Figure 2. Many of them use similar technology to those from wind turbines.

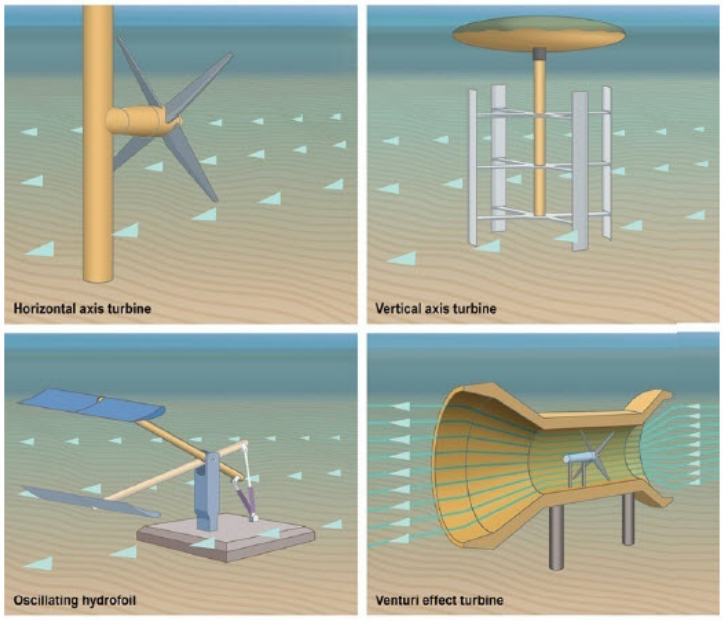

Figure 2.2: Types of tidal Turbines; horizontal axis turbine (top left), vertical axis turbine (top right), oscillating hydrofoil (bottom left) and venturi effect turbine (bottom right) [7]

2.2.1 Horizontal Axis Turbine

The horizontal axis turbine is similar to a wind turbine, and most of its physical equations and principles are the same. It is the most common type of tidal stream turbine. An example of a horizontal tidal turbine is found in Figure 2.2. The current impact the blade drives a generator, which converts energy harnessed from the ocean currents into power.

2.2.2 Vertical Axis Turbine

As its own name indicates, the vertical axis (similar to VAWT, Figure 2.1) moves has its axis vertically and has the advantage that, unlike the horizontal axis tidal, it does not need to be orientated in the direction of the flow. Curiously, it has the form of an eggbeater. An example of a vertical axis turbine can be found in Figure 2.2.

2.2.3 Venturi Axis Turbine

In Figure 2.2. an example of a venturi effect turbine is found. It is composed of a horizontal axis turbine in a symmetrical venturi duct. The shroud increases the water flow through the turbine (the mass of fluid must be kept constant between the inlet and outlet; as the area decreases. In order to ensure mass conservation, the fluid is accelerated in this section). As it is bi-directional, yawing is now required for ebb and flow.

2.2.4 Oscillating Hydrofoil

Thanks to the hydrofoil attached to an oscillating arm it is possible to harness motion. This motion drives the fluid in a hydraulic system to be converted into electricity.

2.3 Working principle of wind and tidal turbines

In this section, we will examine the aerodynamic forces driving the rotor around. The explanation of the lift and drag forces acting on a blade is crucial in order to understand a turbine's power coefficient, C_p. Once C_p is determined, the theoretical mechanical power recuperation formula from wind and tidal horizontal turbines will be understood. That is, we are going to comprehend the implications of the following formula:

$$P_{mec} = \frac{1}{2}\rho\, C_p\, A\, v^3 \tag{2.1}$$

Where ρ is the density of the air or the water, A is the swept area by the turbines, and v is the speed of the incoming current or wind. As we will later comment, this same physical phenomenon is the working principle of both turbines (tidal and wind). We will hence explain its implications for the wind turbine, knowing that the same concepts apply for the tidal turbine – some comments on the differences in the nature of this phenomenon will be addressed at the end of the section.

2.3.1 Power Coefficient: an introduction

Power Coefficient is a measure of wind turbine's efficiency, often used by the industry and the literature. C_p is the ratio of actual power captured by the wind turbine rotor divided by the total wind power flowing into the turbine blades at specific wind speed.

The maximum theoretical value of the coefficient of performance is 0.593. This value is determined by a fluid mechanics constraint known as the Betz limit. Actual coefficients of performance are less than this limit, due to various aerodynamic and mechanical losses. For a given turbine design, C_p is a function of tip speed ratio, which is, in turn defined the linear speed at the tip of the blade over the speed of the incident wind:

$$\lambda = \frac{R\Omega}{v} \tag{2.2}$$

The following section helps in the understanding and calculation of this C_p, and, therefore shed a light on the physical phenomena responsible for mechanical power recuperation at the turbine rotor blades.

2.3.2 Relative wind speed on the blade

The incident wind on the blade (V) is deviated by the blade so that the relative wind velocity acting on the blade (V_r) is the result of the incident wind velocity and the wind velocity created by the movement of the blade (V_m).

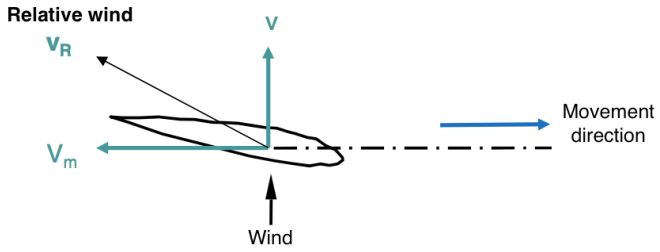

Figure 2.3: Airfoil velocity triangle [8]

$$\overrightarrow{V_R} = \vec{V} + \overrightarrow{V_m} \tag{2.3}$$

This relative wind can be projected into its two components:

$$\vec{V}_R \begin{vmatrix} V_{Rx} \\ V_{Ry} \end{vmatrix}$$

Moreover, the angle between the relative wind velocity direction, and the chord that passes through the profile of the blade, is known as the incident angle or angle of attack, α. The angle, between the chord that passes through the profile of the blade and the direction of movement of the blade, is called the angle of inclination of the blade, β. These two angles are very important in the determination of C_p. To adjust them, angle β is controlled by the rotation of blades (pitch angle) by the wind turbine's control system. This is to ensure a C_p as high as possible.

2.3.3 Lift and Drag forces on blade

There are two major forces that arise on the blade, when exposed to an incoming wind. On the one hand, according to Bernoulli's Theorem, air sliding along the upper surface of the blade will move faster than on the lower surface. The airfoil shape produces unequal lengths across the top and bottom of the wing. Air splitting at the front of the wing must re-join at the back of the wing, so as not to create a vacuum. Since the top surface is curved upward and is longer it forces the air to move faster across the top than the bottom.

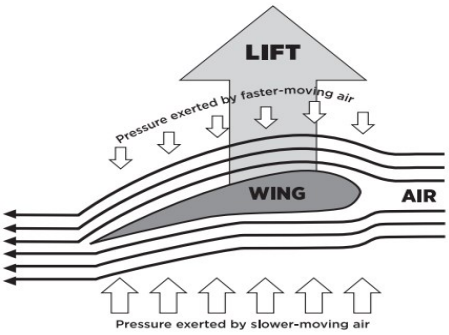

Figure 2.4 Lift, Source: scienceworld.ca

The lift is perpendicular to the direction of the wind.

On the other hand, there is the force of drag. Due to surface irregularities, air passing by the airfoil whirls around in an irregular vortex on its upper surface. This irregular vortex is indeed a turbulent flow of fluid (air). Therefore, the lift from the low pressure on the upper surface of the wing disappears. This phenomenon is known as stall.

A blade (airfoil) wing will stall if its shape tapers off too quickly as the air moves along its general direction of motion. Notice that the turbulence is created on the back side of the wing in relation to the air current. The stall phenomenon created a drag force.

A dent in the wing or rotor blade, or a piece of self-adhesive tape can be enough to start the turbulence on the backside, even if the angle of attack is fairly small. In order to control this stall, the control system of the wind turbine will regulate the pitch movements. This drag force is minimised, which gives rise to a resistive force in the blades.

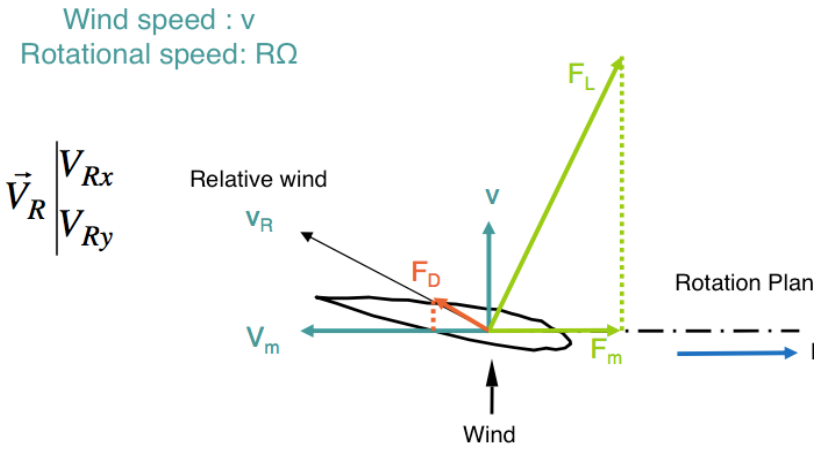

Figure 2.5: Lift (green) and Drag (orange) forces on an airfoil [8]

In all, up to this point, we have explained the existence of two forces:

- Lift force: $F_L = \frac{1}{2}\,\rho\, C_L\, A\; v_R^2$ (2.4)
- Drag force: $F_D = \frac{1}{2}\,\rho\, C_D\, A\; v_R^2$ (2.5)

The Lift and Drag Coefficients (C_L and C_D) are normally determined experimentally using a wind tunnel. But for some simple geometries, they can be determined mathematically. There are numbers used in aerodynamics to model all of the complex dependencies of shape, inclination and flow conditions on lift and drag. These complex dependencies include, for example, the downwash generated near the wingtips, which reduces the total lift coefficient of the wing. Both coefficients are dependent on the angle of attack, α, and the inclination of the blade β.

The projection of the lift and the drag force on the axis of movement (x axis on the figure) is so that:

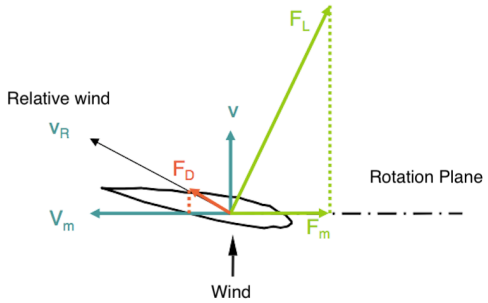

Figure 2.6: Lift (green) and Drag (orange) forces projection on x-axis[8]

$$\text{Lift force on x-axis: } F_m = \frac{1}{2}\,\rho\, C_L\, A\; v_R^2\, (v/v_R)$$
$$\text{Drag force on x-axis: } F_r = \frac{1}{2}\,\rho\, C_D\, A\; v_R^2\, (R\Omega/v_R)$$

Simplifying these expressions and considering the following equations, we can define the lift and drag forces acting on the axis of movement of the blade:

$$v_R = v\sqrt{1+\lambda} \text{ where, as seen above, } \lambda = \frac{R\Omega}{v}$$

Thus,

$$\text{Lift force on x-axis: } F_m = \frac{1}{2}\,\rho\, C_L\, A\; v^2\, \sqrt{1+\lambda^2} \qquad (2.6)$$
$$\text{Drag force on x-axis: } F_r = \frac{1}{2}\,\rho\, C_D\, A\; v^2\, \lambda\, \sqrt{1+\lambda^2} \qquad (2.7)$$

2.3.4 Mechanical power retrieved from incoming wind

The mechanical power retrieved from the blade and used in the movement of the rotor blades can now be calculated. Indeed, this power arises from the difference between the motor force (F_m) and the resistive force (F_r). That is:

$$P = R\,\Omega\,(F_m - F_r)$$

$$P = \frac{1}{2}\,\rho\,A\,\lambda\sqrt{1+\lambda^2}\;(C_L - \lambda C_D)v^3$$

Finally, we simplify this expression to reach the theoretical expression we set out to find. Since C_L and C_D depend on β, the mechanical power extracted is a function of β and λ

$$P = P(C_P) = P(\beta, \lambda)$$

$$P = \frac{1}{2}\,\rho\,AC_P v^3 \qquad (2.1)$$

2.3.5 Extrapolation to tidal turbines

As explained in the introduction, both the tidal and the wind turbine have the same working principle. We have illustrated the case for the wind turbine and would now like to draw a small comparison between the mechanical power extracted from the wind and from the marine currents.

In relation to density, water density is 800 times greater than air density. So the potential of power recovery in water is greater than in air, *ceteris paribus*. However, as we can see in the literature and will later demonstrate for our park, the power production of wind turbines is greater than that of tidal turbines. The reason behind this, is the fact that, firstly, the swept area of tidal turbines is smaller (shorter blades) due to environmental and technical constraints. Moreover, the speed of the incident fluid (air for wind turbines, water for tidal turbine) is greater for the case of the wind turbine. In fact, as we will see later, we will work with an average wind speed of 10m/s in comparison to an average current speed of 1,5m/s. This difference becomes a hugely limiting factor, since the mechanical power extracted is very sensible to the speed of the incoming fluid – speed is raised to the power 3 in the formula.

2.4 Power generation: transformation of mechanical energy into an electrical signal

In this section, we will examine the characteristics and working principles of the main elements that are involved in the process of energy transformation from mechanical energy into an electrical signal. The main elements of this process are induction machines: synchronous and asynchronous motors. We will detail their main differences, in order for us to establish evaluation criterion for the choice of our wind and marine current turbines. Hence, we will only study induction machines used as alternators to produce energy. We will also detail the operating principle of control systems and mechanical elements- key pieces for the optimisation of energy transformation.

2.4.1 Main components of energy transformation

We will now study the components that perform in the transformation of wind energy into an electrical signal. Firstly, we will enumerate them and detail their function in the energy transformation process. As explained before, the process of energy transformation from a the physical phenomenon (wind or current) into an electrical signal is equivalent. The main pieces of the process remain the same, as well as their working principle. What changes are their characteristics and capacities.

The incident wind on the blades enables a blade movement which causes a mechanical torque. This mechanical torque is transmitted to the rotor of the electrical motor through a gearbox. The gearbox adapts the value of the mechanical torque to the operating conditions of the electrical motor. An adapted mechanical torque is received by the rotor of the electrical motor. The electrical motor can either be an asynchronous or a synchronous motor. An electrical power output is created. This electrical power is filtered and controlled through a system of power electronics and transported to an electrical substation on the mainland.

Our main objective is to create a valid power output from an irregular incident wind. Indeed, the electrical network has constraints that have to be fulfilled. We have to feed the network with a power signal that has determined characteristics: constant frequency of 50Hz and voltage.

2.4.2 Electrical motor

Synchronous and asynchronous motors share the same components list and structure. Even though their working principle differ, they rely on the same physics law of induction.

The motor is composed of two main pieces: a rotor and a stator.
The stator is the stationary part of the rotary system of the machine. The stator is a ferromagnetic ring with notches, which host windings. The number of windings determine the number of poles of the rotor. 3 windings (one for each phase, as we are in a three-phase network) compose one pole. The Figure 2.7 draws its structure:

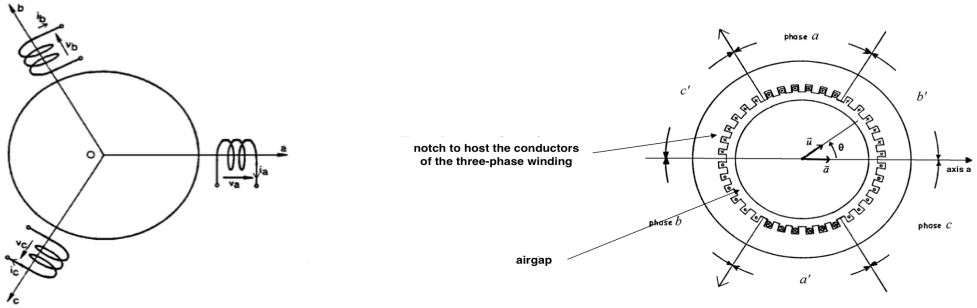

Figure 2.7: Constitution of a Stator [9]

The airgap of the stator helps reducing the losses due to hysteresis and Foucault currents.

The rotor is placed inside the stator. It is composed of an axis that support electrical coils. There are different types of rotors: winding rotors or magnet rotors.

The origin of the creation of power lies on the induction phenomenon. In the synchronous and asynchronous machines, working as alternators, an induced current is created in the windings of the stator. We will now study how this current is induced.

2.4.2.1 Synchronous Machines

The principle of functioning of synchronous machines lies on the interaction between a rotor (composed of magnetic and fixed poles) and a stator (composed of 3 windings).

The magnetic poles of the rotor can be created either by a coil flowed by a continuous current magnetizing the material, or by permanent magnet stuck to the rotor.

The rotor is connected to the transmission tree, moved by the incident wind on the blades. The movement of these magnetic poles create a moving magnetic field. The interaction of this moving magnetic field, with the windings of the stator, induce a current in the stator.

We can model the current induced in the windings of the stator:

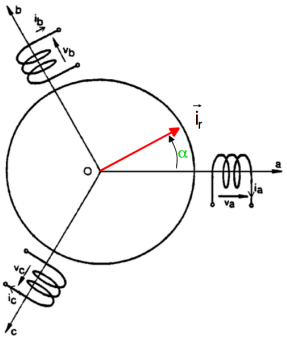

$$i_a = i_{max} \cos\alpha$$
$$i_b = i_{max} \cos(\alpha - \frac{2\pi}{3})$$
$$i_c = i_{max} \cos(\alpha - \frac{4\pi}{3})$$

Figure 2.8 : Induced current in the windings of the stator [9]

These induced currents in the stator windings create a magnetic field in the α direction. As the pulse of the induced currents is equal to ω, we have $\alpha = \omega t$. The magnetic field has therefore a rotational speed equal to: $\Omega = \frac{d\alpha}{dt} = \omega$.
The magnetic field created by the stator moves at the pulse of current.

We have then the interaction of two magnetic fields:

1. one which has a mechanical nature: the movement of the blades enable the rotation of the rotor and therefore the rotation of its magnetic poles
2. a second magnetic field created by the induced current in the windings of the stator.

It is the nature of this interaction that determines, if the synchronous machine is working as a motor, or as an alternator. In our case –alternator-, the poles of the magnetic field, created by the stator, are delayed compared to the poles of the rotor. This creates a resisting couple.

On the Figure 2.9, we can see in red the magnetic poles created by the field of the stator and in red the magnetic poles of the stator. In green, we can see the movement of the rotor.

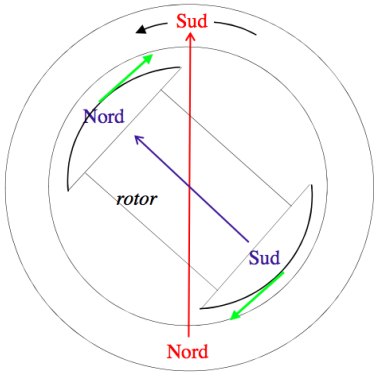

Figure 2.9: Interaction between the magnetic field of the rotor and the magnetic field of the stator [9]

In a synchronous generator, the speed of the rotor determines the speed of the moving magnetic field and therefore the frequency of the current and of the power generated. This implies the synchronism phenomenon: the rotational speed of the rotor is equal to the rotational speed of the stator.

Our wind turbine integrates a synchronous alternator. The reasons of this choice are detailed in the following sections *3.2 Choice of technology*.

2.4.2.2 Asynchronous Machines

The principle of functioning of asynchronous machines, also, lies on the interaction between a rotor (composed of magnetic and fixed poles) and a stator (composed of 3 windings).

However, the induction phenomenon is different. The rotor is also connected to the mechanical transmission tree, which is moved by the blades. The difference lies in the magnetization of the rotor: in the asynchronous machine, the rotor carries an alternative current, as it is connected to the network.

We distinguish: the speed of the rotor ω_m, that is given mechanically by the transmission tree, and the speed of the magnetic field, created by the rotor. Indeed, the rotor creates a magnetic field that moves at its pulse plus the pulse of the alternative current ω_r.

Therefore, the stator sees a moving magnetic field at ω_m+ω_r. This moving magnetic field induces a current in the windings of the stator. The induced current of the stator has a pulse $\omega_s = \omega_m + \omega_r$.

The current induced in the stator create, in turn, a magnetic field at ω_s.

In order for the asynchronous machine to work as an alternator, we need to have $\omega_m > \omega_s$. Therefore, the current feeding the rotor should have a pulse $\omega_r = \omega_s - \omega_m$.

In an asynchronous motor, we can define the slip: $s = \frac{\omega_s - \omega_m}{\omega_s}$, that represents the relative speed between the rotor and the movement of the magnetic field created by the stator.

Our marine current turbine integrates an asynchronous alternator. The reasons of this choice are detailed in the following sections *3.2 Choice of technology*.

2.4.3 Gearbox

The gearbox is composed of a low-speed tree, the gearbox and a high-speed tree. In the energy transformation process, the gearbox is found between the blades and the electrical motor.
The installation of a gearbox in the power transformation process is not compulsory. From the beginnings of wind turbine parks, gearboxes have always been part of the process. However, the actual tendency of new and modern wind turbines is the deletion of this component and the installation of "direct drive" turbines. Indeed, even though, gearboxes present undeniable advantages, it is the mechanical piece that has the most expensive maintenance cost and the shortest lifetime. This has encouraged industrial companies to further research on the deletion of this component.

Direct drive turbines present a reduced maintenance cost and have the largest power generation.

The initial necessity of gearboxes lied on the unadapted mechanical torque, created by the incident wind on the blades. The power formula is: $P_{mec} = Torque \times Speed$.
The wind creates a movement with a low speed and high torque. However, the electrical machines are not designed for these operating conditions.

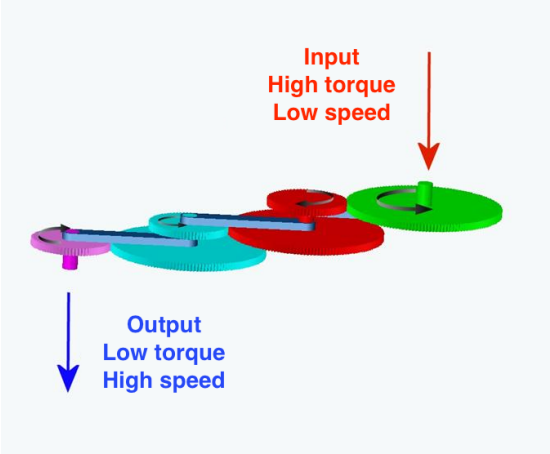

Figure 2.10: Gearbox [10]

A high mechanical torque implies a physically consequent machine (big in size). When the speed is low, in order for the machine to produce electricity, we need a high number of pair of poles. As seen in the point 2.4.2, a pair of pole on an electrical machine depends on the inductances installed on the machines. An elevated pair of poles implies an elevated number of inductances and therefore more space: a bigger and heavier machine.
However, it is not suitable to install such an electrical machine offshore, as it adds many inconveniences, such as the weight that the structure has to support. That is why gearboxes are useful.

We distinguish asynchronous and synchronous machines:

- Asynchronous machines need a gearbox because we are not capable of building asynchronous machines with such an elevated number of pairs of poles
- However, gearboxes are not compulsory with synchronous machine. We are able of reducing the size of synchronous machines. This is the case of direct drive turbines: usually they contain permanent magnet. Our wind turbine is therefore innovant. The new trends in the eolic sector is to install synchronous turbines, with permanent magnet and the direct drive turbines in order to reduce the nacel weight. Our park's wind turbine seems weightless compared to asynchronous wind turbines that demand a heavy gearbox.

2.4.4 Power electronics control system

Adjustable speed generator for wind turbines are necessary when output power becomes higher than 1MW. Variable speed implies variable frequency, which is incompatible with the grid's characteristics. A control system of power electronics has to be installed at the output of the electrical motor -either synchronous or asynchronous-, in order for the electrical power to be fed correctly into the network.

We have to feed a constant output with an irregular input (incident wind on the blades). The function of power electronics is to guarantee the characteristics of the power fed into the network. The importance of power electronics is even greater as the price of this component is very significant.

Again, here we distinguish asynchronous and synchronous machines. The main difference between both machines is the capacity of the power electronics system, and therefore the price. There are many possible connections of asynchronous and synchronous motor to the grid. We will study the most common and optimal cases used in offshore power generation: doubly-fed asynchronous generators (also called MADA machines) and direct drive synchronous generators.

2.4.4.1 Doubly-fed asynchronous generators

With asynchronous machines, the components of the power electronics system are two rectifier/inverter transistors.
Thanks to its parallel structure, we are able to guarantee a correct feeding power to the grid with less power electronics components. Indeed, only one third of the electrical power goes through the power electronics system. This enables to lower its capacity and therefore lower prices.

Doubly-fed asynchronous generator have the following advantages:

1. Reduced inverter cost: typically, inverter rating is 25% of the total power of the system, while the speed range of the asynchronous generator is $\pm 33\%$around synchronous speed *[11]*
2. Reduced inverter filter: filters only need to be rated at 0.25p.u of the total system power *[11]*

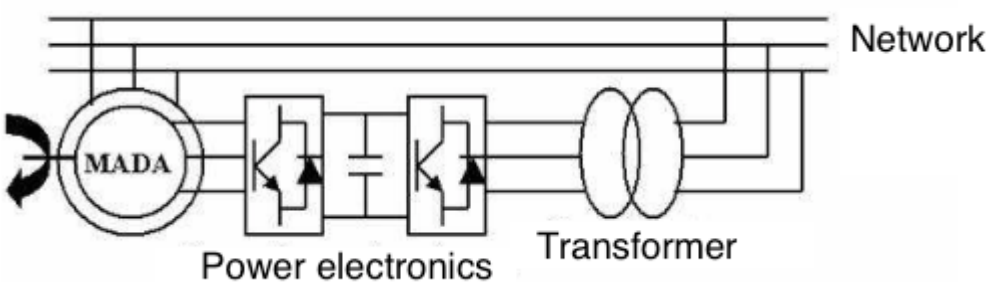

Figure 2.11 : Double-fed asynchronous generator power electronics[8]

2.4.4.2 Direct Drive synchronous generators

The synchronous machine produces a variable-frequency alternative power. The power converter is needed in order to implement a constant-frequency alternative power.

Because of its structure in series, the whole power output has to go through the power electronics system, this implies a larger capacity and therefore higher price: the power converter has to be rated at 1 pu of the total system power, as well as, the inverter output filter also rated for 1pu of output power. *[12]*
This makes the filter and power design difficult but above all costly.

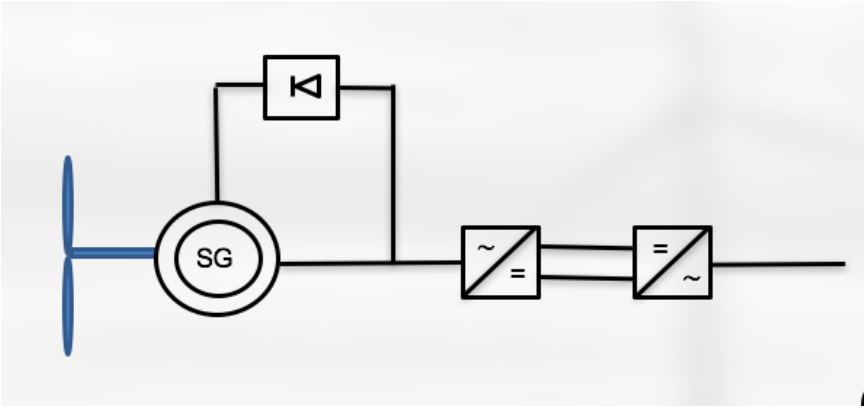

Figure 2.12: Synchronous generator power electronics [8]

2.4.4.3 Operating principle of the rectifier-inverter

The power electronics components used are switch converters (as explained above, they do not differ in the operating principle but only in their capacity and the way they are connected to the generator). The back-to-back arrangement of the converters, shown below, enables a mechanism of converting a variable voltage and variable frequency signal (output of the generator) into a fixed frequency and fixed voltage signal (compatible with the network).

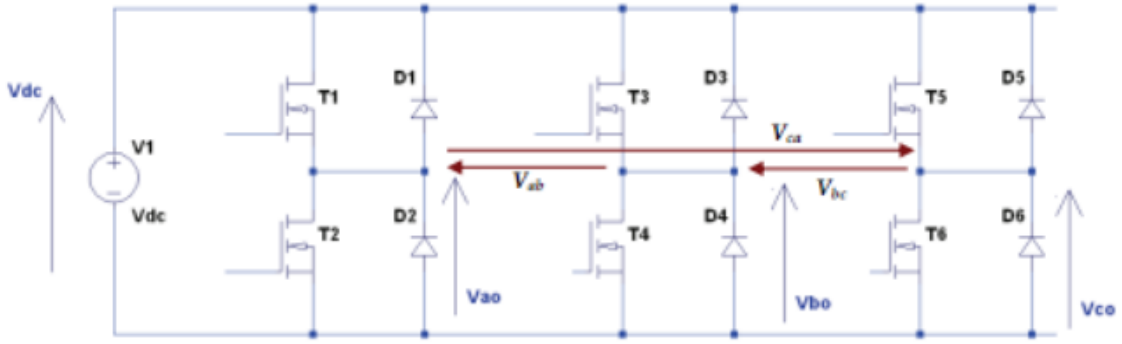

Figure 2.13: Six-switch voltage source inverter circuit [12]

There are many types of pulse width modulation (PWM) control system. The most adapted modulation for wind turbines is the Sinus Triangle. The PWM lies on the comparison between a carrier wave (sinus triangle waveform) and a modulating waveform (wave delivered by the generator). The instant of transistor commutation is determined by the intersection points between the carrier wave and the modulated wave. The frequency of the switch commutation and therefore the output-signal frequency depend on the fixed-frequency of the carrier wave.

The operating principle of PWM can be modelled simply:

$$If\ U_m > U_c, then\ S(t) = 1\ , else\ S(t) = 0$$

U_m *the voltage of the modulating waveform,* U_c *the voltage of the carrier waveform and* $S(t)$ *the output signal*

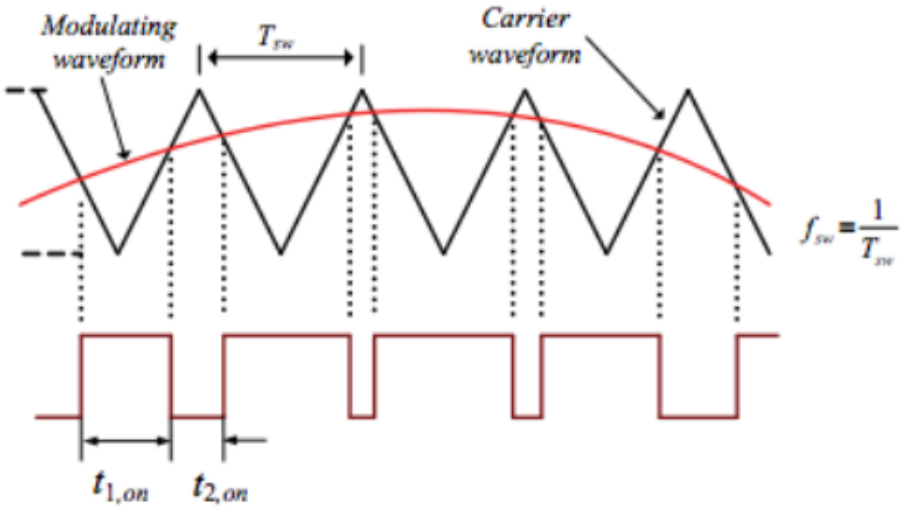

Figure 2.14: Example of carrier-based pulse-width modulated signal generation [12]

We can therefore define:

- the modulation index m: the relation between the frequency of the carrier and the modulating wave
- the modulation rate r: relation between the magnitude of voltages

The modulation index can be varied in time; therefore, any desired voltage and frequency can be generated at the output terminals.

In the three-phase balanced output line voltages, we can control the voltage magnitude with the value of m. The output frequency can be regulated by the frequency of the modulating waveform. The modulating waveform can be manipulated through microcontrollers or signal processors.

Here below you may find an example of input signal, and the corresponding output signal treated with PWM power electronics:

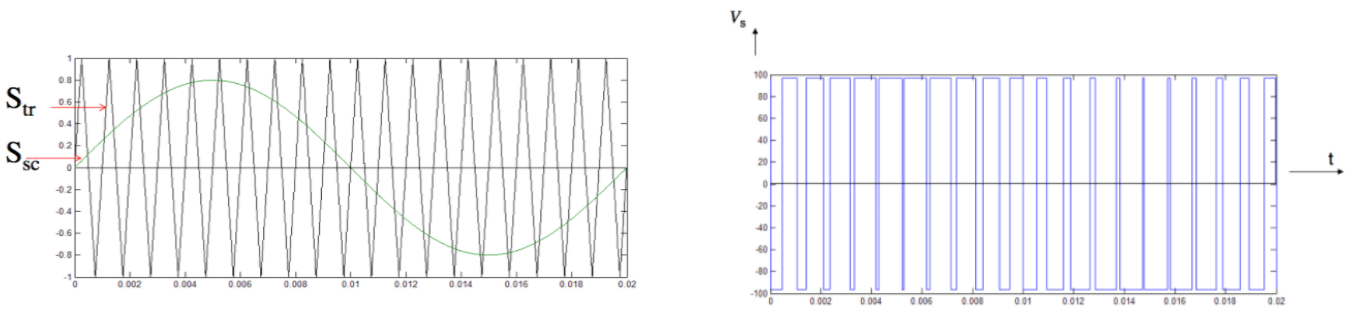

Figure 2.15 : Carrier and modulating waveform (left) and output wave (right) [13]

We note that the frequency of the output signal is different from the input signal.

2.4.5 Power transport

Once we have produced a fixed frequency and voltage power output, we must transport this energy from the offshore park to the mainland. In the case of our wind and hydraulic park, the energy production is consequent. The offshore park is connected to the high-voltage grid. We have to minimize the losses in the energy transport. The power consumed by the transport cables is proportional to the square of the current intensity: $P = RI^2$.

A step-up transformer will allow us to reduce this power losses. By elevating the voltage of the cables, we decrease the modulus of the intensity, and therefore the modulus of the active power consumed by the cables. A step-up transformer is installed at the output of the offshore park. The electrical power is transported with a low intensity and high voltage. A step-down transformer is installed at the mainland substation entry in order to adapt the voltage to the grid's voltage.

Also, electrical power is transported as a continuous signal and not sinusoidal signal. The signal has to be transformed. It is more convenient to transport electricity as a continuous signal: the occupied area of a cable by an alternative current is larger than the occupied area of a continuous signal.

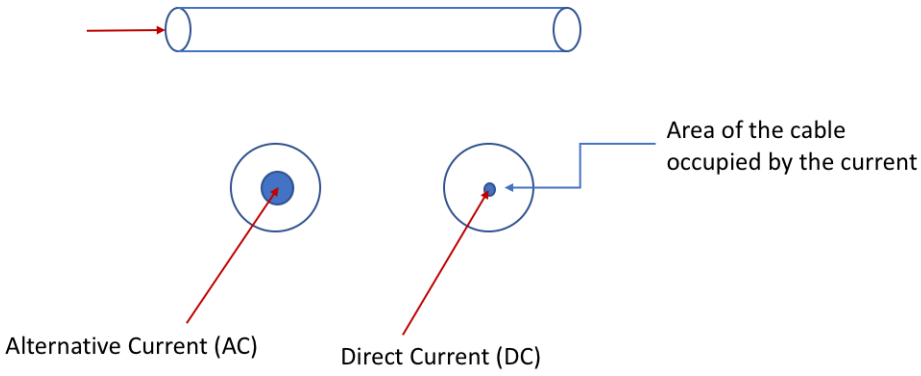

Figure 2.16 : Area occupied by the current in the transport cable

2 different structures are needed in order to limit the losses in the energy transport: a step- up and a step-down transformer in order to elevate and lower the voltage, and an AC-DC rectifier bridge.

2.4.5.1 Transformers

A transformer is characterised by its transformation rate *m,* which is calculated as the relation between the number coils of the secondary inductance and the number of coils of the primary inductance. The equivalent scheme of a transformer is:

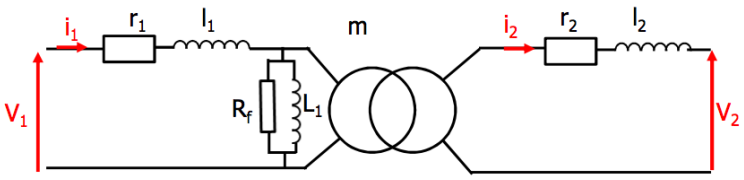

Figure 2.17: Equivalent scheme of a transformer [14]

2.4.5.2 AC-DC Rectifier Bridge

An AC-DC rectifier bridge is an element of power electronics that enables the transformation of an alternative signal into a direct signal (and vice-versa for an DC-AC rectifier bridge). It is composed of six thyristors, connected this way:

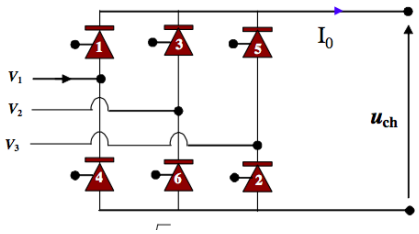

Figure 2.18: AC-DC rectifier bridge [13]

The operating principle of the rectifier bridge depends on the pulse current. This pulse current is given with an α delay compared to the three-phase voltage V. The delay angle α of the pulse current marks the form of the output voltage signal U. We will have to choose α in order for the output signal U to be a continuous signal. We obtain this condition for $0 < \alpha < \frac{\Pi}{2}$.

Thanks to the alternative opening and closing of the thyristors, the output voltage measured is continuous as shown in the Figure 2.19:

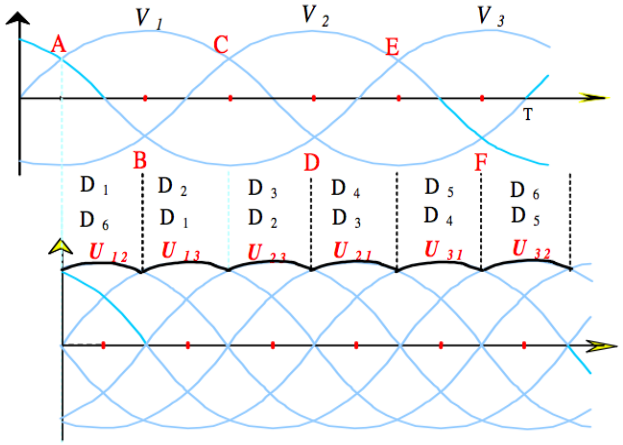

Figure 2.19: Output voltage of the AC-DC rectifier bridge [13]

However, in the last years, new methods of energy transport are being explored. Although, the final desired result is reached -we do obtain a continuous signal from a sinusoidal signal-, this method introduces a lot of perturbative harmonics in the signal. It is necessary to install IFA2000 filters in order to purify the signal. The inverters -we currently work with- cannot support elevated voltages (above 400 kV used for electricity transport). For 6 years, industrials have been studying a new multi-level structure for energy transport (MMC: Modular Multi-Level Converter*). [45]*

2.5 Innovation Review

In this section, we go over the state of the art with regards to the combined use of ocean energy - wave, offshore wind, currents, offshore solar, biomass - for power production. In doing so, we hope to underline to the pertinence of our project, which is inscribed in a very active research axe of renewable energy solutions.

Indeed, the relevance of the cost reduction potential of a joint installation offshore has been fully comprehend by the Spanish company Iberdrola, who launched in 2010 the CENIT-E OCEAN LÍDER project (Ocean Renewable Energy Leaders) *[15]*. It is an ambitious technology initiative promoted by a consortium of companies, with a strong capacity in researching, which addresses the challenge of generating and creating the knowledge and technologies necessaries for an efficient and sustainable renewable ocean energy generation. OCEAN LIDER projects' main target is to design integrated facilities for the use of renewable ocean energy.

To further empathise the will to combine ocean energy recuperation methods in combined platforms, we can take the example of how NTNU AMOS centre in Norway is working on addressing fluid-dynamic loads/motions and structural response in severe waves, wind and

current. They contribute with integrated mathematical modelling as a basis for design, analysis, control and optimization of wind turbines and wave energy converter parks. *[16]* Their outcomes want to propose new concepts for integrated wind and wave energy parks with fish farms, new strategies for autonomous optimization-based predictive control of offshore wind and wave energy converters and parks, and demonstration and case studies based on simulations and laboratory experiments.

Finally, we can illustrate a commercial case that goes in the same direction as our project: The Able Marine Energy Park (AMEP), a fully consented project that offers 1389m of new heavy duty deep water quays and 366.7 hectares of developable land. It is designed for the marine renewables sector providing a multi-user facility for the manufacture, storage, assembly and deployment of marine energies, especially next generation offshore wind turbines and their associated supply chains. It is indeed a platform that validates to a certain extent our initial cost reduction hypothesis. *[17]*

All in all, we have established through this review that there is a research gap in the design of joint facilities for marine energy recuperation, that some initiatives (OCEAN LIDER) are trying to explore. Furthermore, we have gone through some commercial examples that show that the industries involved in marine energies are ready, and willing to design systems in accordance with a joint recuperation of energy from the sea (NTNU AMOS). They approve of building larger, taking into account the economies of scale, such clustering brings about.

3. OFFSHORE ENERGY PARK DESIGN

3.1 Site Selection

In this section, we will go through the steps and criteria we followed to select the area, in which to deploy our proposed offshore energy recuperation facility. To start with, the decision was taken to locate the facility in French waters, due to France's technical possibilities, its Atlantic coast's potential for offshore wind energy recuperation and its political willingness to explore and extract energy from the sea. *[18]*

Having established this, we took the informed decision to locate our park in Normand waters, guided partly by the observation of available maps by France Energie Éolienne *[19]* and SHOM's empiric database *[20]* of mean wind (Figure 3.1a) and marine current speeds offshore in French waters (Figure 3.1b). For the average wind velocities, maps are created from isobars and the availability of averaged information offshore is scarce, therefore we illustrate instantaneous information in our (Figure 3.1a).

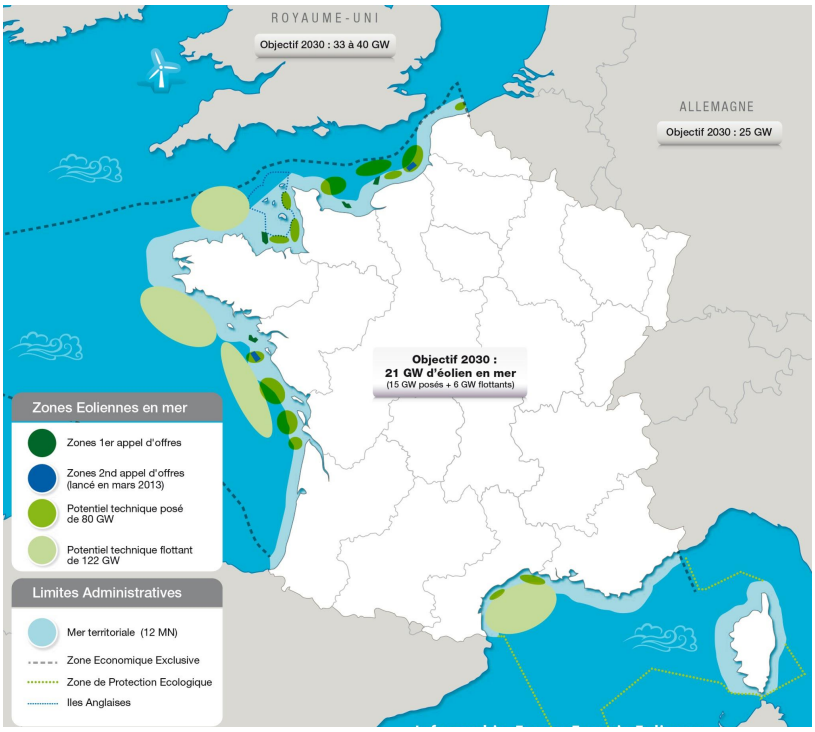

Figure 3.1a: Favourable zones for offshore wind, France Energie Éolienne

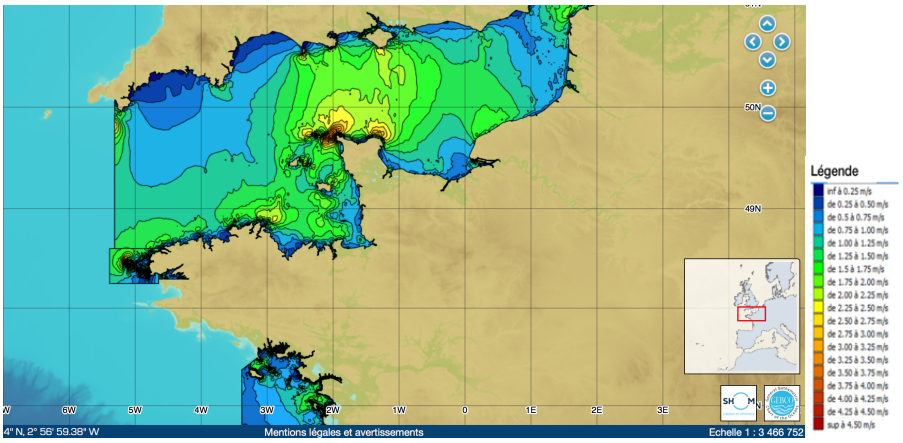

Figure 3.1b: 3D marine current database, SHOM

However, this choice was also validated by the academics and industries' interests in Brittany and Normandy's waters for marine energy recuperation. Indeed, there are currently six projects in offshore wind energy farms along the coast of the English Channel – one at the Gulf of Saint-Malo, another in front of Cherbourg, for example. *[21]*. With regards to tidal energy, RTE accompanies the development of sea energy, after its 2012 study on how to best adapt and connect to the French electrical system, the potential of power generation that marine energy supposes. On the basis of this study, an AMI (Appel à Manifestations d'Intérêts) was published in 2013, for the construction of pilot hydraulic parks, on two highlighted zones ideal for hydraulic energy recuperation: le passage du Fromveur and le Raz Blanchard. *[18]*

We hence studied these two areas of interest for academics, politicians and the energy industry, in order to determine which one would prove more efficient and effective for our proposition of jointly recovering marine current energy and offshore wind energy park. Due to the smaller size of the area in le passage du Fromveur, with high current and wind energy potential, and to its excessive proximity to land, we finally decided to choose le Raz Blanchard as the perfect setting for our park.

We will now examine how the exact area we allocated to the park was decided upon. We had to optimise both the wind energy potential (maximum wind velocities) and the current energy potential (maximum current velocities) under certain restrictions. The following criteria summarises the steps we followed.

3.1.1 Meteorology

The most important criteria to be met, by our selected location, was for it to have high wind speeds and high marine current speeds, over the period of one year, in order to maximise the energy recuperation of the park. It is crucial to understand the importance of having annual data, for both wind and current power generation calculations, due to the fluctuations of these resources - daily and seasonally for wind, and in phase with the moon for the tides. Needless

to say, in order to estimate the annual power production of our park (see section 4), we need to take all hourly fluctuations into account, since average speeds would be too simplistic and unrealistic.

We initially explored the empirical data offered by French Government's tools and databases such as SHOM *[20]* (marine current speeds, Figure 3.2) and MéteoFrance (offshore wind speeds) *[22]*. However, we soon realised that some of the data incomplete or that the point where the data was taken lacked in accuracy. Moreover, we were unable to find hourly data, which is the optimal option to take to reflect the daily fluctuations in wind (although not as necessary for the more consistent current speeds).

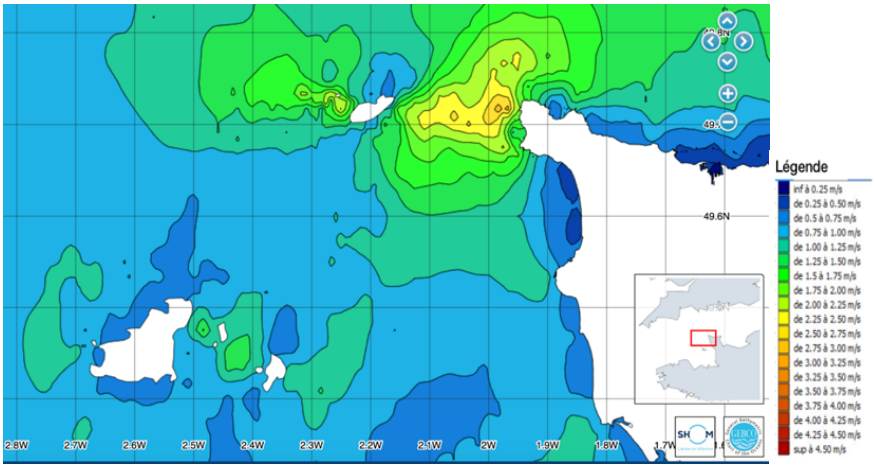

Figure 3.2: Marine currents maximum speed, by SHOM.

We hence searched for simulated, rather than empirical data, in order to have a complete and broad database that would better reproduce the meteorological conditions of the area under study. We contacted Open Ocean Energy *[23]* a company that provides on-demand access to metocean data, statistics and reports through essential analytics and display tools to be used for site characterization, during the planning and development of offshore projects and facilities.

With their Metocean Analytics tool, they provided us with hourly wind and marine current speeds and directions for the year 2015.

More precisely, Openocean offered to us data from their following databases:

A. The wind database over the French west and north coasts was performed by VORTEX using the computer code Weather Research and Forecasting (WRF). It is a mesoscale numerical weather prediction system, with scales from tens of meters to thousands of kilometres.

This proved very profitable with regards to the location accuracy of the data we use. The wind data was given at 100m above the mean sea level, which is pertinent since the hub height of our wind turbines is 96m (the choice of the wind turbine is detailed in 3.2.1). The

angles of incidence of the wind were also provided, on an hourly basis and will be used in the park design with regards to turbine orientation (section 3.3).

Examples of maximum and mean wind magnitudes from this database can be seen in Figures 3.3 and 3.4.

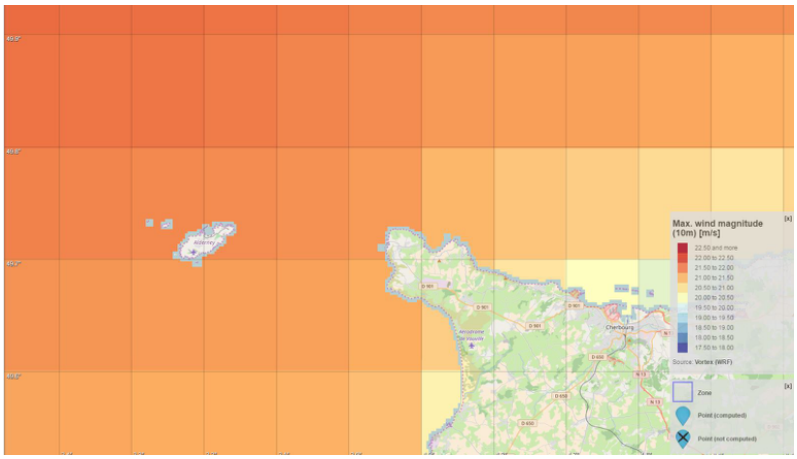

Figure 3.3: Maximum wind magnitude, OpenOcean.

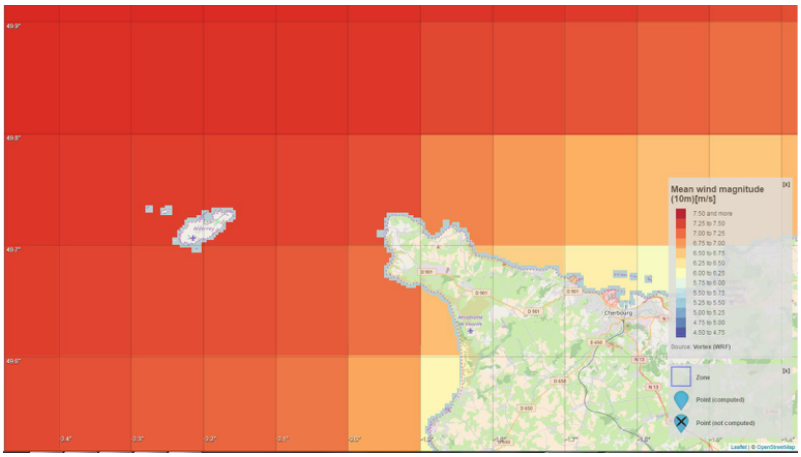

Figure 3.4: Mean wind magnitude, OpenOcean.

B. The wind database, from which the pertinent data was extracted, was MANW250. This is a 2D database, depth-averaged numerical simulation, performed by Ifremer, using the numerical hydrodynamical model MARS2D (Model for Applications at Regional Scale, [Lazure, 2008]). The simulation has a spatial resolution of 250m.

Since the marine current recuperation technology chosen (see section 3.2) is moveable along the vertical pole of the turbines they are mounted upon, a depth-averaged data is ideal for our study.

Examples of maximum and mean current magnitudes from this database can be seen in Figures 3.5 and 3.6.

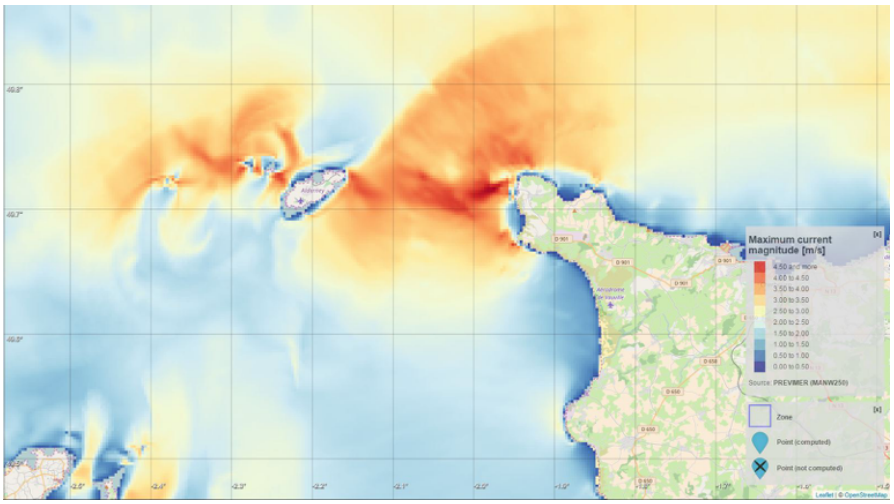

Figure 3.5: Maximum current magnitude, OpenOcean.

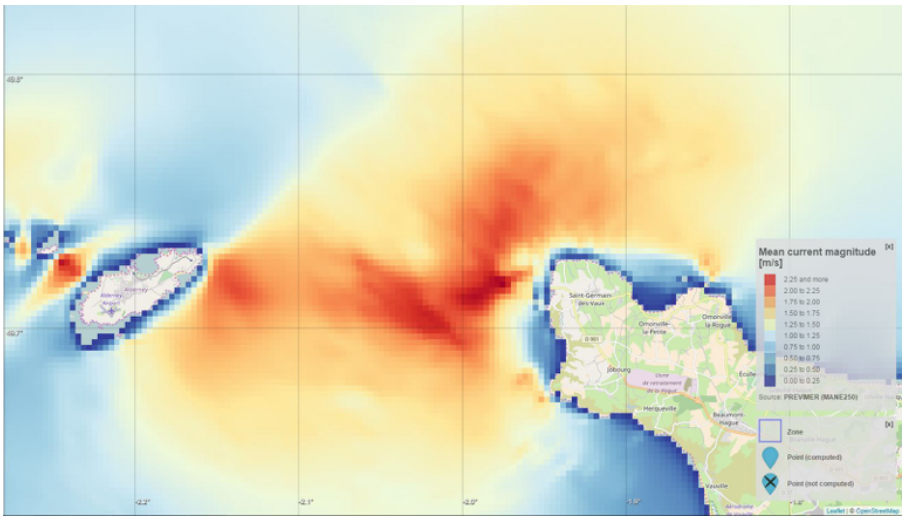

Figure 3.6: Mean current magnitude, OpenOcean.

3.1.2 Bathymetry and bed sediments

A second parameter, that has to be taken into account for our installation, is the seabed depth. Indeed, a site's seabed morphology and sediment regime are important features that influence the selection and design of:

1) foundations and moorings used for technology deployment,
2) electric cables used for interconnection between devices and electricity transfer to shore,
3) potential environmental impacts to the sediment regime, bed morphology, and benthic organisms. Bed sediments were not assessed for our reference resource site.

However, the bathymetry is a crucial consideration for foundations installation and a

parameter that can easily multiply the costs of a facility, or render it unfeasible technically. Indeed, for the current technological advancements, at about 50m of depth, the use of a monopole structure to support wind turbines is not possible, and a more complex jacket structure has to be used. *[24]*

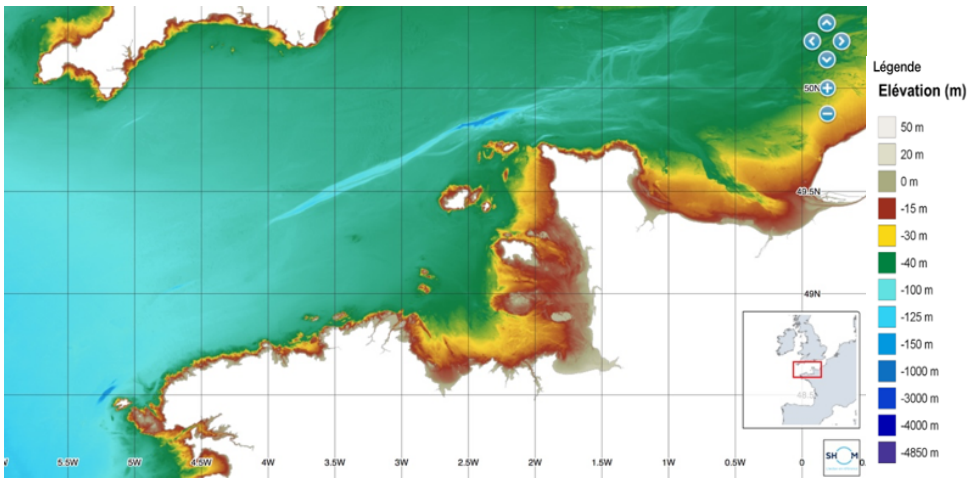

Figure 3.7: Barometry English Channel, SHOM

When examining le Raz Blanchard, we realise that most of the area sufficiently away from coast has a depth of less than 50m, mostly that of 40m (in green). However, we can see the existence of underwater cliff (100m, in blue) that is found within the area of our chosen site. Indeed, no units will be installed in this area to avoid challenging and expensive foundation installation.

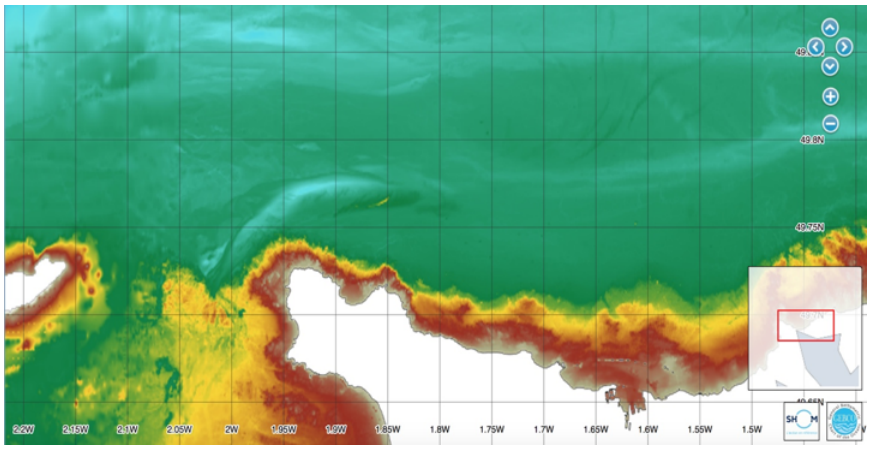

Figure 3.8: Barometry le Raz Blanchard, SHOM

3.1.3 Commercial Routes and Cabling

Restrictions regarding commercial shipping routes and underwater power cabling are important, if we want to give our project a pertinent and realistic approach. We used the following maps, concerning these two restrictions, to further delimit the useful area for the

deployment of our joint energy recuperation facility.

Figure 3.9: Commercial shipping routes, Google maps

Figure 3.10: Submarine power cables [25]

3.1.4 Geopolitics and Legal dimension

Final important considerations, that had to be taken into account, were the political and social risks of deploying our park in a given area.

With regards to geopolitics, we risked entering in international waters. Indeed, as Figure 3.11 shows, there are areas of sea around the Island of St Anne, that pertain to the United Kingdom. For administrative and bureaucratic reasons, it is preferable for the proposed park not to belong to two different countries.

We have hence decided to stay within France's exclusive economic zone (thick red line on Figure 3.11).

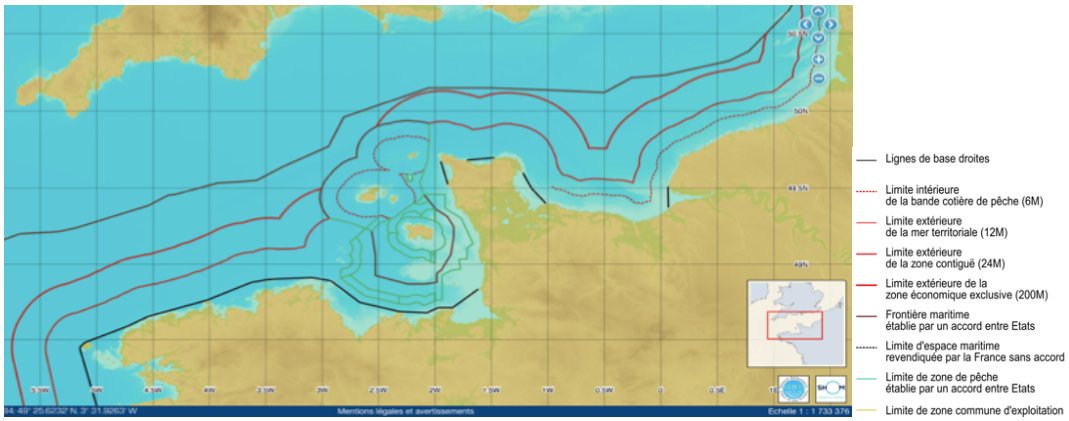

Figure 3.11: Power cables, SHOM [25]

As for social risks, the public acceptance of the proposed project largely depends on its visual impact for the coast. Although it could be argued, that the potential for job creation and investment in the area could counter such drawback.

In any case, the visibility of a windfarm is of course affected by topography. The concept of the ZVI (Zone of Visual Impact), in professional landscape, has been used by academics to determine the necessary spacing of offshore wind energy farms from the coast. In this sense, the International Energy Agency states that "Visual impacts are only normally important for residents and tourists up to a distance of about 10 km, with the main effects on amenity being concentrated within a few kilometres of the wind farm". Said distance will be kept in mind in determining the specific where the plan is to be set.

3.1.5 Final Location

In order to take an educated decision, all the aforementioned restrictions and parameters were cross-analysed. The available maps which showed the geographical constraints mentioned above were hence superposed, resulting in the following selected area:

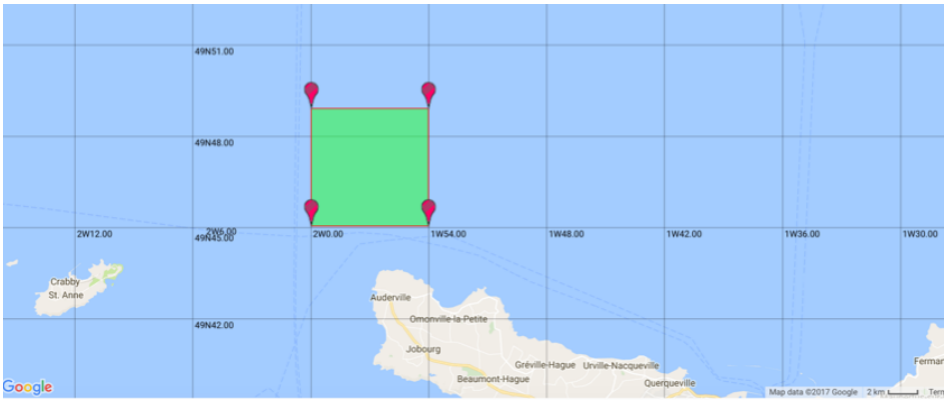

Figure 3.12: Area selected for joint energy recuperation facility

This area corresponds to 52.25km^2 of ocean in le Raz Blanchard. More precisely, the coordinate points in latitude, longitude are as follows:

-1.999833583831787, 49.75058547173751
-1.999833583831787, 49.81498323527079
-1.8999481201171875, 49.814948620925826
-1.8999481201171875, 49.7506617244979

All aforementioned restrictions have been taken into account. However, with regards to distance from the coast, the threshold for visual impact is not respected. The closest point to the coast in our area is at 3 km to the coast (3.139 km to Pointe de Grouins) and the furthest point to the coast in our area is at 10 km to the coast (10.786 km to Nez Bayard).

Experts agree that a distance of over 10km and preferably 15km from the coast should be respected in order to reduce the Zone of Visual Impact (ZVI) *[26]*. However, since there are no legal restrictions imposed on this matter, this condition will remain unresolved, especially since it is near the coast that the greatest current speeds are to be found. We will however consider this in the design of our park. That is, we will strive to settle a smaller density of wind turbines in the area closer to the coast, than in the area furthest from the coast, and inversely, so for the less visible marine current turbines.

Thus, having established our selected area, we can now show the raw data to be used for our power generation model. That is, the hourly wind and current speed and their angles of incidence, over the period of one year (2015), retrieved from the midpoint of the selected area. The data used for the calculation of our annual power production is hence shown in Figure 3.13 and 3.14.

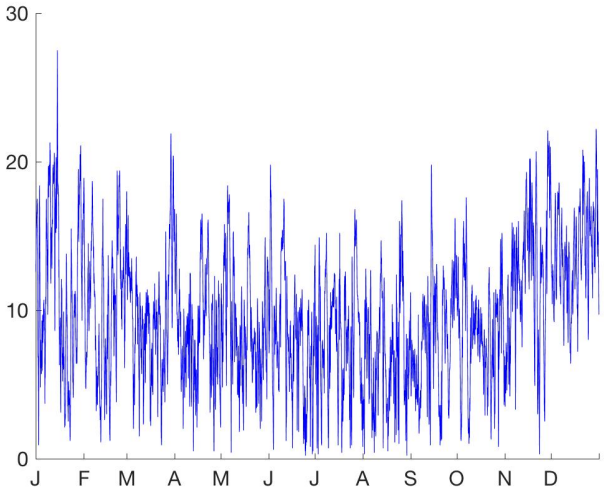

Figure 3.13: Seasonal wind magnitude flutuation, 2015, OpenOcean.

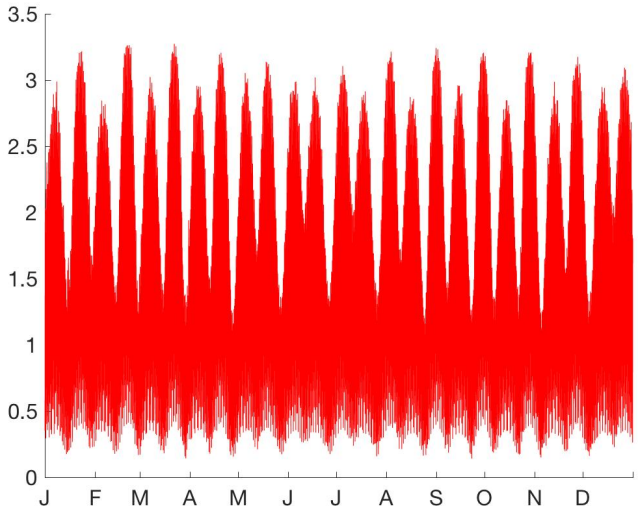

Figure 3.14: Stable current magnitude with 15-day fluctuations, 2015, OpenOcean.

3.2 Choice of Technology

In order to design our combined wind and current turbine farm, we had to select a wind and a current turbine respectively. Our choice was based on four criteria; Supply Chain, Cost Reduction, Cutting Edge Technology and Mechanical Compatibility, as well as availability of information. These elements will be further detailed in section *3.2.3 Advantages*.

Regarding the wind turbine technology, investment in green and renewable energy, over the last couple of years, has made it possible to produce more efficient and affordable wind turbines. Power output from wind turbines has increased considerably (see Figure 3.15). Now 8MW turbines are being developed, especially offshore, where the implementation costs account for a very large percentage of the total cost. So it tends to be economically more profitable to build bigger offshore turbines (detailed explanation of the economic breakdown in section 4. Economic Modeling)

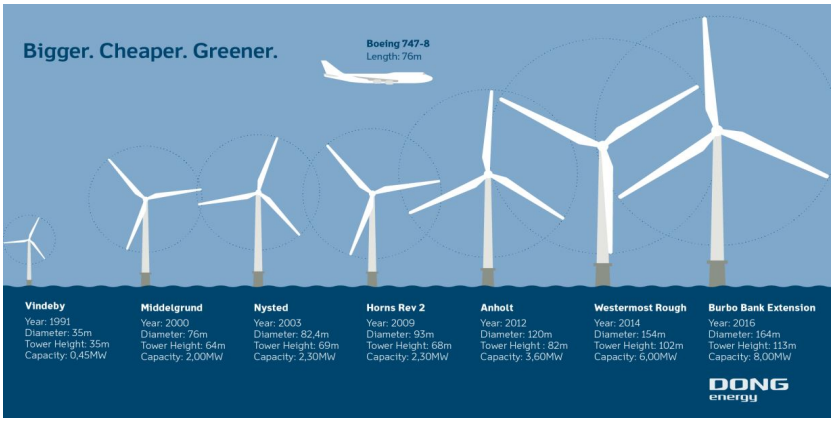

Figure 3.15 Evolution of Offshore Wind Turbines from Dong Energy [27]

Due to the lack of information and confidentiality policies from wind turbine manufacturers, only three turbines were taken into consideration, all of them 3-blades horizontal axis turbines (Figure 3.16):

- NH Vestas 8MW: with a 164m rotor diameter, this wind turbine is currently the among largest offshore wind turbine producing up to 8-9 Mega Watts. Produced by Vestas, its first prototype unit was operated in 2011 in Osterild, northern Denmark. The first initial industrial units were dispatched in 2016. *[28]*

- Adwen-AD180: This turbine came as a result from a joint venture from Gamesa and Areva. It has the biggest blade in the market, with a total length of 88 meters, and a total power output of 8MW. It is estimated that by 2018 serial production will be achieved. *[29]*

- Siemens Sapiens: This 6.0MW turbine uses direct drive technology (instead of a gearbox, see the detail of this technology in the section 2.4.3 Gearbox). It boasts to have less moving parts and a tower head, which is 360 tons lighter than its competitors. As a consequence of this, installation, infrastructure, installation and service cost are considerably reduced. *[30]*

The biggest single contribution to cost reduction has been the offshore wind industry's early adoption of larger turbines. Turbines such as MHI Vestas Offshore Wind's 8MW model, the upcoming Adwen (Areva and Gamesa JV) 8MW, and Siemens' and Alstom's 6MW machines, are sure to push costs down even further for the upcoming rounds of offshore wind projects.

Figure 3.16: the NH Vestas 8 MW (left), the Adwen AD 180 (center) and the Siemens Sapiens (right) [31]

Contrary to Wind turbines, tidal stream generators have not evolved as much, and the number of business, which develop and produce tidal stream turbines, is largely lower than wind turbines. Even though, wind turbines produce more energy than tidal stream generators, these do have a significant advantage. This is that marine currents are much more predictable and constant than wind, giving this form of energy generation a big potential.

Only two marine current turbines (horizontal axis) were taken into consideration for our mutualised farm which were (see Figure 3.17):

- Sabella D10: This bidimensional tidal stream turbine can produce up to 1.2 MW of energy, depending on the current. With a rotor diameter of 10m and a gravity based foundation, this turbine could be used in a tidal energy farm in the Fromveur Passage (currently under development).

- SeaGen: First deployed in 2008, this tidal stream turbine appears to be the leader in its sector. Thanks to the two generators connected to a cross arm, which can move up and down, maintenance operations become easier and cheaper.

Figure 3.17 Sabella D10 (left) and the Seagen (right)

Our final choice for the wind turbine was the Siemens Sapiens 6.0 MW and the Sabella D10 for the tidal stream turbine.

3.2.1 Siemens 6.0 MW Offshore Wind Turbine

With more than 20 years of experience in the field, Siemens is considered as the leading turbine suppliers when it comes to offshore wind power, with a combined market share of 63% of European offshore wind turbines *[32]*. In 1981, the first offshore wind warm was built using one of Siemens wind turbines.

What makes the Siemens Sapiens 6.0 MW so unique, is that, it is based on direct drive technology (absence of gearbox to change the rotor speed). As a consequence of this, the Siemens Sapiens has less moving parts, in comparison to geared machines, and a tower head which is comparatively lighter. Equally, the generator uses a permanent magnet, which eliminates excitation losses from induction generators. These features have, as a result, an improvement in efficiency whilst increasing simplicity.

This technology has been designed to exploit a broad range of offshore environmental conditions, ranging from inland waters with moderate wind speeds, to most offshore sites. Standard Wind Turbines are normally programmed to shut down, when the mean wind speed exceeds a certain threshold. In the Siemens Sapiens case, the high wind shutdown is replaced with an intelligent, load-based reduction in output power at high wind speeds. This system is named “High Wind Ride Through System”.

With a rotor diameter of 154m and 75m-blades, the Siemens Sapiens produces a nominal power of 6.0 MW. The power can be regulated through the pitching of the blades and the variation of the rotor speed. The blades are produced in one piece, in order to eliminate weaker areas at glue joints. This way reliability is increased for greater safety.

Equally, the Siemens Sapiens is equipped with a diagnostics service, which enables the early detection of anomalies and prevents potential failures. In order to avoid and prevent serious damages, a service planning is optimised, based on the analysis of vibration patterns.

3.2.2 2.0 MW SeaGen tidal turbine

Our initial idea was to study, and develop the venturi axis turbine, as there are currently not so many tidal turbines which use this technology. Yet the large number of horizontal axis turbines changed our mind. Our final choice was the SeaGen turbine, which also is the largest tidal turbine nowadays.

The SeaGen has become the world’s largest scale commercial tidal stream generator. It was a considerable evolution, from its predecessor the 300kW SeaFlow (see Figure 3.18), which had only one rotor. The SeaFlow was used as a prototype, for the SeaGen and was never connected to the grid.

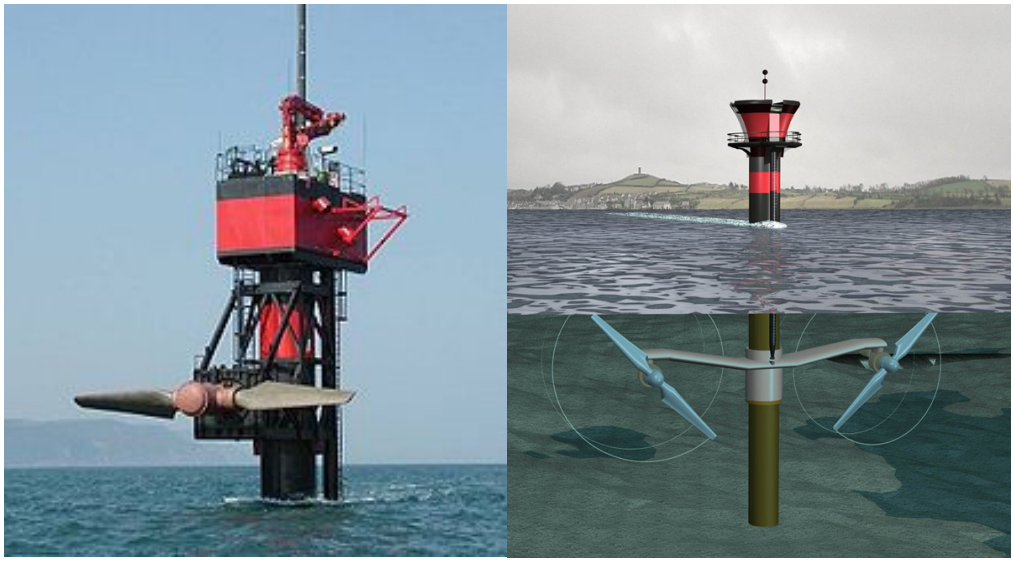

Figure 3.18 Seagen Flow, North Coast of Devon (left) and Seagen (right) [33]

Contrary to its predecessor, the SeaGen has two 2-bladed horizontal-axis rotors, each with 16 meters of diameter, mounted on at the end of a cross beam. The speed of the generator is increased thanks to gear boxes attached to the rotors. The orientations of the rotor are fixed. A preliminary tidal study is necessary to ensure optimal conditions. Nonetheless, the blades can be pitched 180º, so they can be used for currents coming from both directions.

The cross arm is mounted onto the steel body tube, which is fixed to seabed. A motor allows the cross to move up and down, to obtain the optimal conditions, and to raise the cross arm above the sea water level for maintenance purposes (as shown in Figure 3.19).

The cross-arm assembly is nearly neutrally buoyant. The attached rotors can be recovered and redeployed, with a minimal amount of lifting crane capacity. Therefore, the design minimizes the handling requirements during deployment and recovery, which reduces overall cost in all O&M activities including access to the power conversion chain (PCC).

Figure 3.19 : SeaGen under maintenance [33]

At the top of the steel body tube, there is a "control room", in which all systems and power trains are found. This ensures, that the electrical components are kept in a controlled and dry environment. The main structural element is the tubular steel pipe which carries all the weight of the components, as well as the operational force on the rotors. The detailed technical specifications of the SeaGen are found in the Annexe 1.

Since 2008, a SeaGen is plugged into the national grid. Currently, a project to build the first entire tidal farm, in its early stage, is taking place in Brough Ness, Ireland. The farm would be composed of 66 SeaGen tubines. *[34]*

3.3 Park Design

Once the technology to be employed and the exact site location have been chosen, it is crucial to analyse the different limiting parameters that impact our park design. The main limiting parameter is, in our case, the wake effect created by the turbines in the wind and in the water flow. These wakes are going to create instabilities and are going to impact negatively on the energy production. Therefore, a sufficient spacing is necessary to ensure that neighbouring turbines can produce as efficient and optimal as possible. Nonetheless, the bigger the spacing the more cable is needed to connect these, so it is vital to find the optimal equilibrium.

As previously mentioned, obstructions (the wind and tidal turbines) are going to create a region with a disturbed flow downstream. In our case, we find ourselves confronted with two different fluids (air and water) and solids (wind and tidal turbines) with different parameters and conditions.

There are 4 limiting factors to take into consideration:

- In the Air:
  - Wake created by the Wind Turbine
- In the Water:
  - Wake created by the Tidal Turbine's Rotors
  - Wake created by the Tidal Turbine's Body
  - Wake created by the Wind Turbine's Body

3.3.1 Wind Turbine Wake

The wake is a structure which emanates from the rotor blades, and creates downstream whirlwinds. This turbulence is created by a deficit of speed. The level of turbulence affects the behaviour and the performance of a wind turbine : the generated power is reduced and the loads on rotors are increased. The whirling effects begin in the edges and develop towards the

centre, as we can observe in figure 3.20:

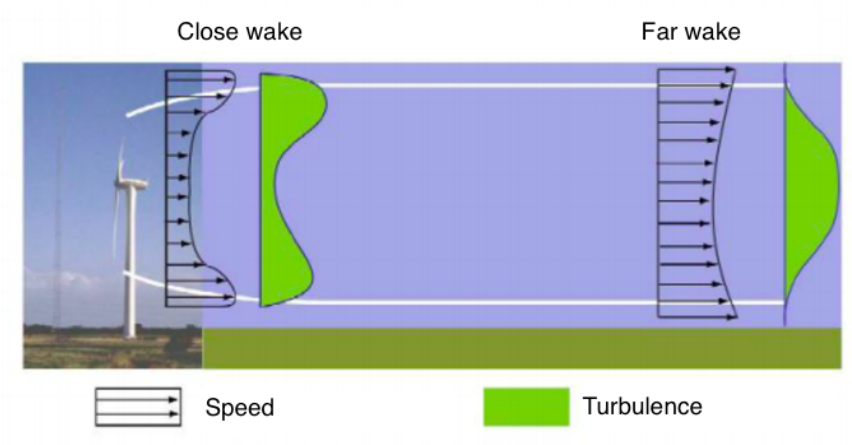

Figure 3.20: Close and Distant Wake Effect

In order to display and calculate empirically the wake effect, the use of smoke is pretty common. In Figure 3.21, the testing of wind turbine models is shown. We can appreciate the turbulence created by these in wind tunnels. Most of the wake effect is caused by the rotor (unlike the case in the water which the wake effect from the cylindrical body does play an important role).

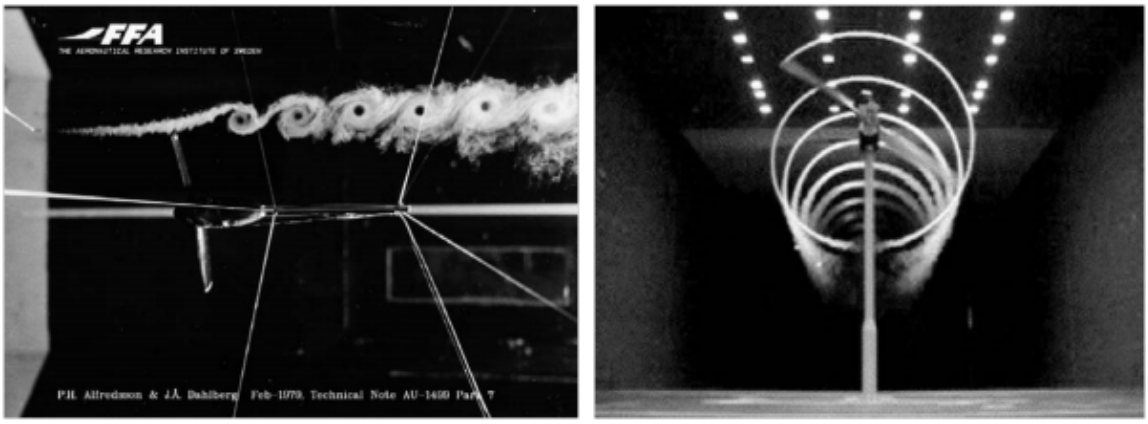

Marginal whirlwind of a rotor tested by the FFA *[35]*

Wake of a wind turbine tested by the NREL *[36]*

Figure 3.21 : Wind Turbine Model Tests

Currently, the average separation, between wind turbines in existing offshore parks, is about 7 rotor diameters in the windward direction and 4 diameters of rotor in crosswind direction. The optimality of this distribution has to be studied.

When it comes to efficiency, this distribution might not be the optimal. Until now, wind turbines were placed at 7 diameters of rotors between two consecutive wind turbines. Nevertheless, this separation is not sufficient to completely overcome the wake effect. That is

what Meneveau and Meyer found in their study. Instead, they found that 15 diameters of rotor were needed to ensure an optimal flow for the following wind turbine. Nevertheless, for our project the results of this study have to be mated. Indeed, their study aims to maximise the efficiency, without considering economic or optimality arguments- such as the cable needed to connect these turbines. *[37]*

Having contacted researchers and engineers, we found that most of the current wind turbines spacing used between 6-7 rotor distance, up to 9 or 10 for more recent parks *[38]*. Due to the lack of resources and the staggering organisation of the park (Section 3.3), we have decided to implement a spacing of 10 rotor diameters, to follow the more actual trend in wind park designs. Further studies concerning this decision, could still be made.

3.3.2 Downstream Water Wake

In the water, as previously mentioned, the presence of obstacles – here the rotors, the tidal turbine body, and wind turbine body - disturb the water flow, and consequently, energy production. The effect of these three elements will be studied separately in the following sections.

3.3.2.1 Wake created by the marine current turbine

As a consequence of the water flow through the SeaGen rotor turbines, the water flow's structure is modified and becomes very turbulent. There is a high dissipation rate and the turbulence can be considered as "destructive". This results in the turbulence dissipating fast, *[39]*. We will see that this parameter is not the limiting one, so there has been no quantitative study of it. *[40]*

3.3.2.2 Wake created by the marine current tower

The Marine current generator tower is the most responsible for the wake effect in the water. Its cylindrical body acts as an obstruction to the flow, creating velocity fluctuations and a more turbulent flow. In the *SeaGen Environmental Monitoring Programme* from 2011, empirical studies of the tidal turbine conclude (for a flow of 4m/s) that: "The data [...] that a discernible wake is only apparent a maximum of 300m downstream of the installation, which is caused largely by the tower. Beyond 300m, there is little or no evidence of wake sub-surface. No evidence was found of a downstream wake generated by the turbine rotors. [..]". *[40]*

Although purely based on bibliography, this parameter of 300 meters of spacing will be considered for the calculations of the design of the park.

3.3.2.3 Wake created by the wind tower

The Wind Turbine body also disturbs the water flow and is subject to the wake effect. Unfortunately, and unlike for the SeaGen, there is very little data of the wake effect in the water created by the wind turbine body. Indeed, currently, offshore parks that are being constructed are "only" wind turbine parks or "only" tidal current turbine parks. However, in our jointed park, we need to study the interactions and the effects between both structures. This study is not found in the literature as such jointed park has never been constructed. We need to fulfil this study as this parameter is crucial to the design of our park, and to install a correct spacing between wind turbines and marine current turbines. To obtain this parameter, a fluid mechanics simulation was carried.

We assumed that the considered problem could be treated as a classical flow of an inviscid - incompressible fluid around a cylinder that is transverse to the flow (see Figure 3.22). This phenomenon, called "Flow Past Cylinder", has been widely studied, providing us a theoretical background, that will be used to validate (at least qualitatively) our simulation.

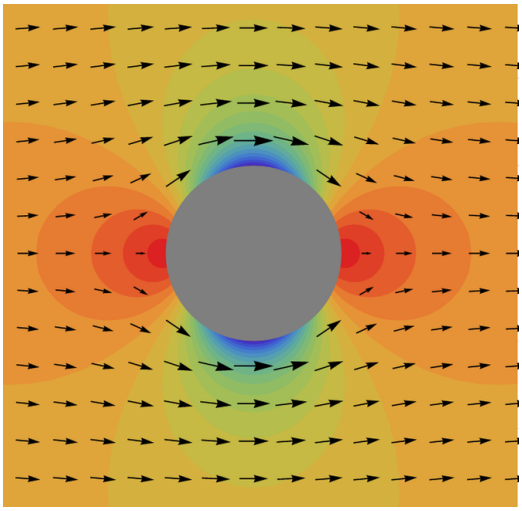

Figure 3.22: Flow Past Cylinder Diagram [41]

The operation principle of the simulation is relatively simple. In order to make the calculation by means of a computer, the definition of a meshing is needed for the discretisation of the Navier-Stokes equation. Indeed, a compromise has to be found between the lack of continuity of the numeral calculation in finite time, and the precision of the result. The computing power is one of the major problems of IT modelling. The Simulation software chosen for the fluid mechanics simulation is Fluent.

Among the configuration parameters of the simulation model, a choice had to be made between three different types of simulations format proposed by Fluent. These are presented below, in decreasing order of computational power needed, and thus, in decreasing order of the results' precision.

The DNS (Direct Numerical Simulation), shown in Figure 3.23, is the most complex and calculation demanding simulation. Indeed, the Navier-Stokes equations are numerically solved, without any turbulence model. In other words, the entire range of spatial and temporal scales of turbulence must be resolved. The computational resources needed for this calculation method exceed the most powerful computers currently available –moreover, the calculation time is increased for high Reynolds, which is the simulation case in study.

The LES (Large Eddy Simulation) is another computational fluid simulation, based on a mathematical model. Unlike the DNS, this method ignores the small length scales, as they are, computationally speaking, quite expensive to resolve. Therefore, the computed result is not as precise as in the DNS. Yet, it also uses less computational power. This simulation is broadly used in many engineering applications.

Finally, the RANS simulation (Reynolds Average Navier Stokes) is the most affordable simulation, when it comes to computational power, for turbulent models. Its downside lies on the calculation precision (see Figure 3.23). The operating principle of this method is the instantaneous decomposition of the Navier-Stokes equation (using the Reynolds decomposition). The decomposition separates flow variables -such as the velocity- into a mean (time-average) component and a fluctuating component (as shown in Equation 3.1):

$$u(x,t) = \bar{u}(x) + u'(x,t) \tag{3.1}$$

In the RANS simulation, the fluctuation term, also called Reynolds Stress, is obtained using a series of models. Indeed, a wide range of models are offered by the simulation program (Fluent). Below, you may find a list of models, ordered in increasing complexity. Note that the first models are used for laminar flows.

- Inviscid
- Laminar
- Spalart-Allmaras (1 Equation)
- K-epsilon model (2 Equation)
- K-omega model (2 Equation)
- Transition K-kl-omega (3 Equation)
- Transition SST (4 Equation)
- Reynolds (7 Equation)
- Scale-Adaptive Simulation

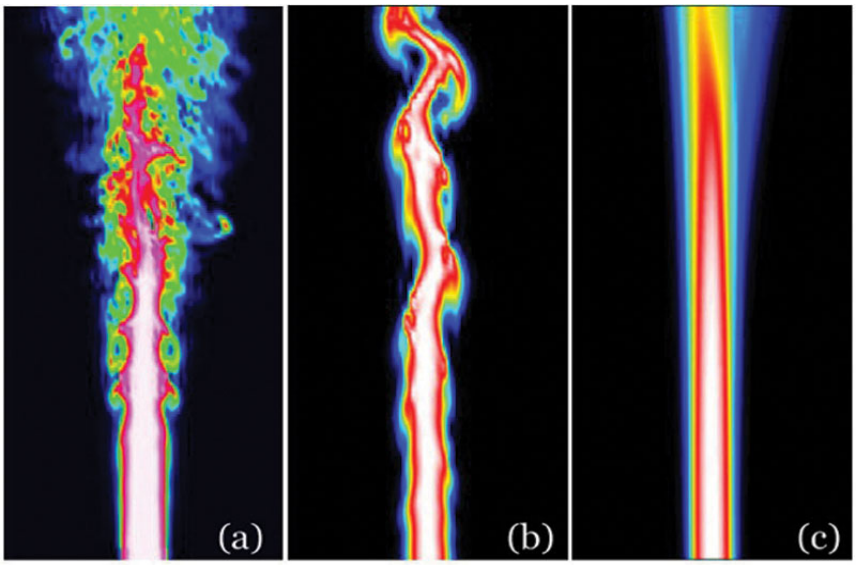

Figure 3.23: Simulation results obtained with (a) DNS , (b) LES, (c) RANS calculation method

For the studied case, with the limited computational resources and the required precision, the RANS turbulent model will be computed in the Computation Fluid Dynamics Software tool-Fluent. Indeed, we are calculating the distance, where the water flow is still turbulent, after meeting a wind turbine body. This distance is required in order to place our tidal turbines. A low precision is yet satisfactory, with an order of magnitude of a meter.

3.3.2.3.1 Fluent Simulation methodology

The simulation's objective is to calculate the impact of the tower body in the water, and the minimum distance needed to ensure an undisturbed incident flow on the tidal current turbines This maximisation parameters will determine the structure of the park design and maximise the efficiency of the tidal turbines.

Firstly, the regime of the water flow had to be established (boundary conditions). To do this, the calculation of the Reynolds number was necessary, as showed in the following Equation 3.2. The Reynolds number obtained is $26{,}24 \times 10^6$.

$$Re = \frac{\rho u L}{\mu} \qquad (3.2)$$

Simulation parameters had to be established in the following order: geometry building, mesh definition, choice of the model and the finally running the numerical analysis.

The geometry chosen was a 2D section (see Figure 3.24). Although turbulence is a 3D phenomenon, a 2D surface can be used. Indeed, the average flow variables, in each cross-section, are equal (except for the boundaries: seabed and water surface). Thanks to this 2D selection, computational power can be saved.
The 2D section has a dimension of 500×100 meters, that represents the water flow. Inside,

a circle of 6,9 m diameter is placed at $50m$ from the inlet. This circle represents the Siemens Sapiens body in the water; 6,9 m corresponding to its tower diameter.

The mesh chosen had to ensure a precision of the nearest meter. The uniform mesh was build, including approximately 13000 knots.

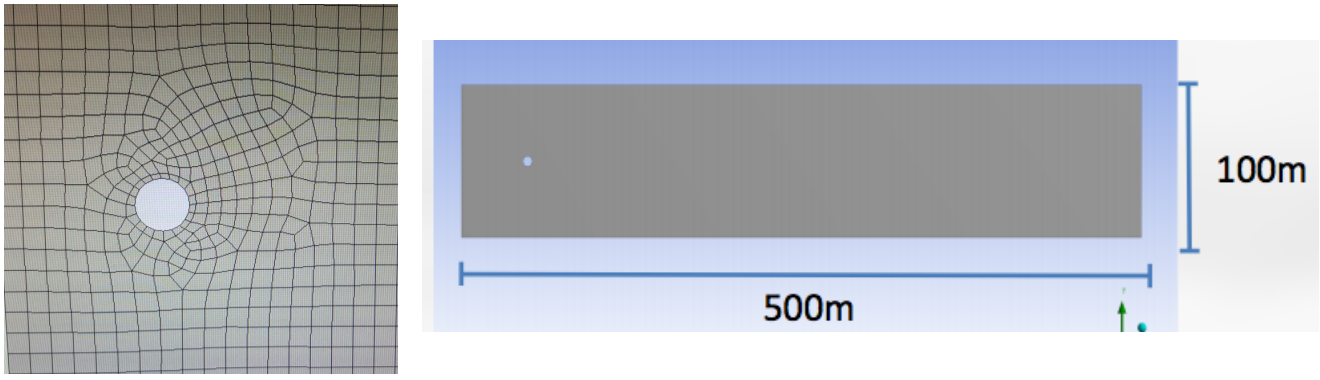

Figure 3.24: Geometry (right) and zoom in of the inner circle mesh (left)

Regarding the RANS turbulent models available, we computed the $K-\epsilon$ model *[42]*. It is the most commonly used model to simulate mean flow characteristics, for turbulent flow conditions. There are two transport variables in this model:

- The K determines the energy of the flow. It represents the turbulent kinetic energy.
- The ϵ represents the rate of turbulent dissipation

The numerical analysis order considered was 2nd degree. As a first approach, we can consider this calculation level sufficient. *[42]*

Nonetheless, before validating our model, a theoretical analysis applies. In our case, the Flow Past Cylinder problem has been widely studied. The results of the simulation can be predicted theoretically. *[43]* In the Figure 3.25, we can compare, qualitatively, the simulation results with the theory.
Indeed, we had to test our model. We do not own an approximated value of the simulation result expected. There is no possible way of testing this result (a physical experimental test could be carried in a lab for instance). However, we do know the expected results of this model for non-turbulent flows. That is why we have, first, imputed the cases, whose results was previously known, in order to check if the meshing and calculation were correctly made and executed by the program.

The test-cases carried are shown below in the Figure 3.25. You may find on the left the results of the simulation and on the right the theoretical result expected. Three tests were conducted for different values of the Reynolds number: $Re = 1\,; Re = 300\,; Re = 28{,}24\times10^{6}$. That is to say, a laminar flow, a middle value (Karman vortex street appear) and a completely turbulent flow have been tested.

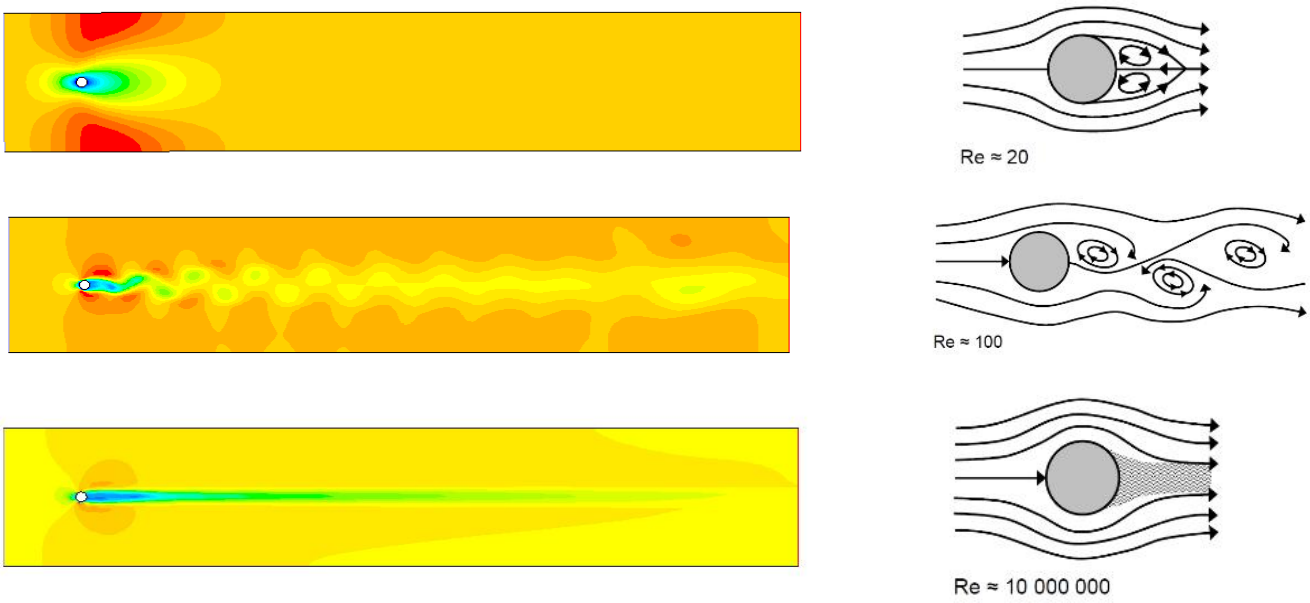

Figure 3.25: Simulation against theory; Simulated Re=1 (top), Re=300 (middle) and Re=28,24×10⁶ (bottom)

The simulated results validate the computed model. We may proceed with the real case scenario.

3.3.2.3.2 Results and Conclusions

As a first approach, two flow variables were considered: velocity and turbulent kinetic energy. The following tidal current turbine can be placed once the downstream flow repossesses the same characteristics as before meeting the wind turbine's body. In other words, the fluid has recovered the same velocity and turbulent kinetic energy as the initial incidental flow. In the Figure 3.26 are shown the simulation results obtained using the $K-\epsilon$ model.

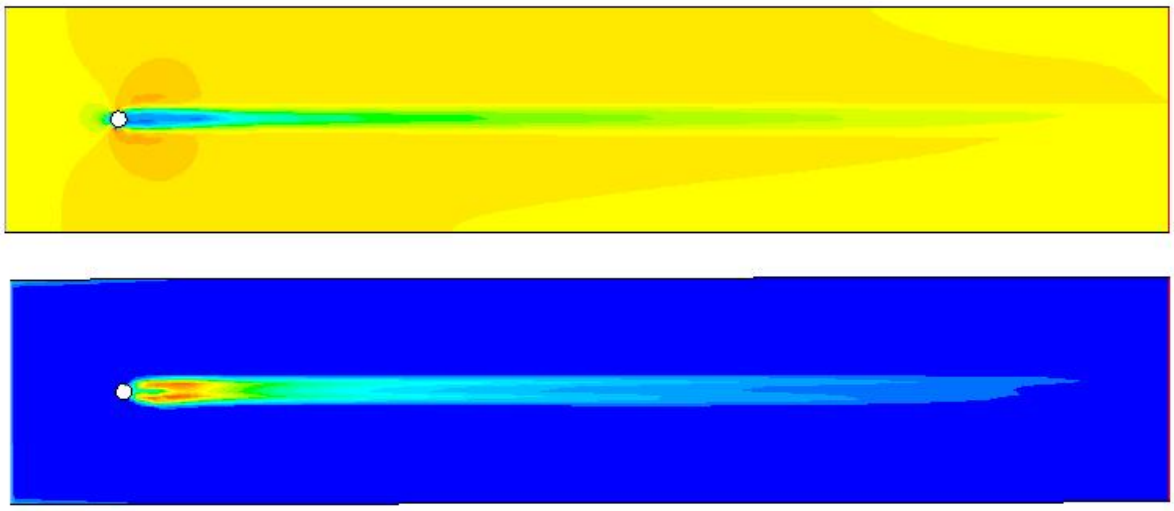

Figure 3.26: Graph simulation results: velocity (top) and turbulent kinetic energy (bottom) obtained with Fluent

As preliminary conclusions, it is noticeable that, the velocity and the turbulent kinetic energy reach their initial values at 395m. Nonetheless, a safety margin should be left. The final parameter for the needed spacing between wind turbines and tidal current turbines is 400m.

In addition to this, the fluid's velocity magnitude along the midline evolve as follows (see. Figure 3.27).

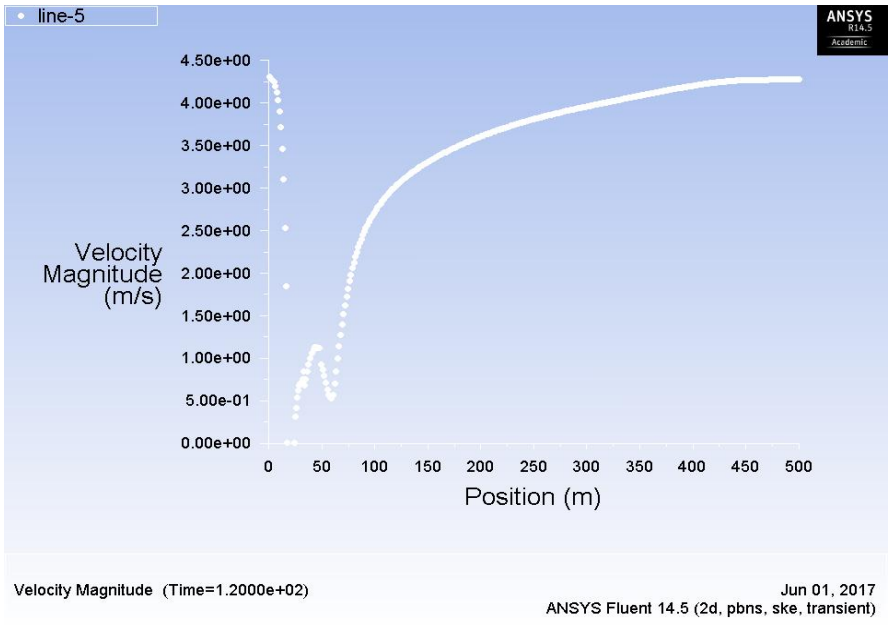

Figure 3.27: Evolution of the velocity value along the mid-line crossing the tower.

The graph of the Figure 3.27 validates the chosen parameter. 400m after meeting the wind turbine's body, the fluids' velocity has reached its initial velocity value of 4,3m/s.

Also, in order to validate qualitatively the obtained results, other turbulent models were computed: the Spalart-Allmaras and the $K-\omega$ (K-omega) model. as shown in Figure 3.27. We can notice that the Spalart-Allmaras model calculated a bigger wake that the other models. However, the $K-\omega$ model results are significantly similar the $K-\epsilon$ model results.

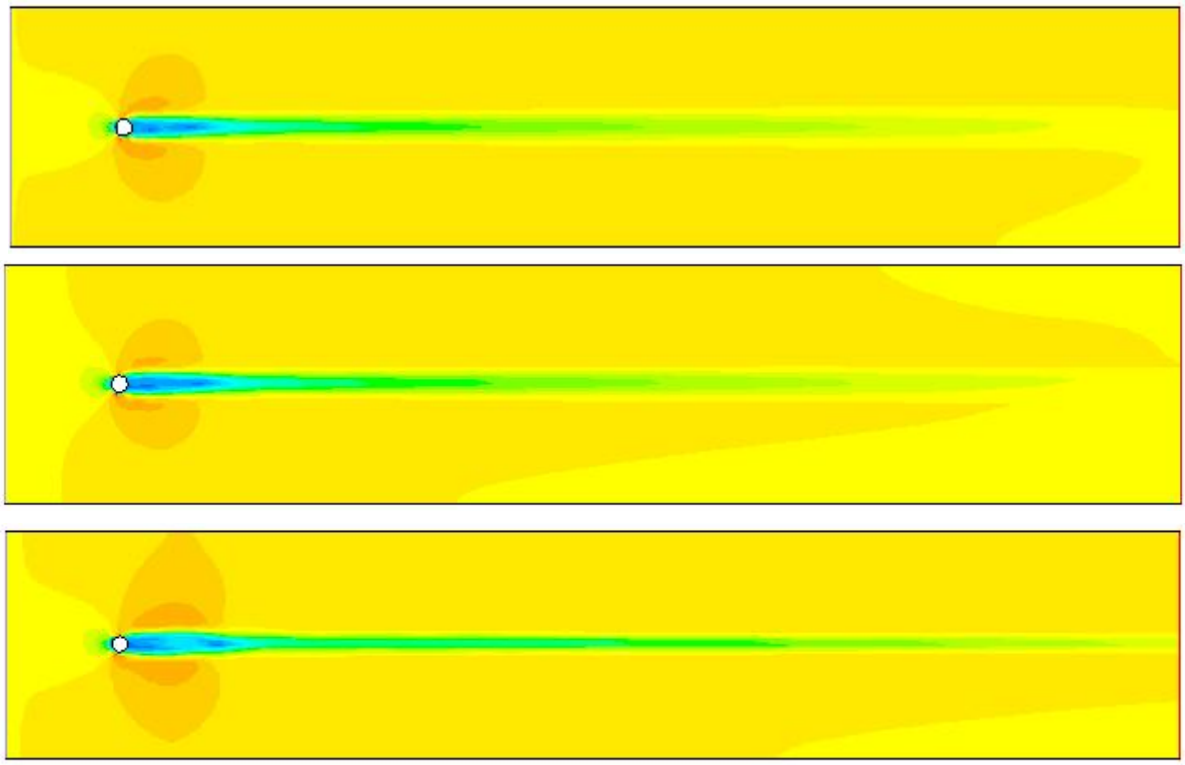

Figure 3.28 Graph simulation results: implementation of the Spalart-Allmaras *model (top),* $K-\omega$ *(middle) and* $K-\epsilon$ *(bottom)*

It is important to keep in mind that this result remain a first and initial approach. As a very precise result is not necessary to the resolution of our park design, no further time will be inverted in improving the precision of the model and to simulate in further depth. Amongst the further steps, the verification of other models, the computation of more precise meshes (with more knots) and empirical experiments could be done to further the validation and the pertinence of the obtained value of the parameter.

3.3.3 Wind and Tidal Current Park Configuration

3.3.3.1 Recuperation units

We have now established the spacing limitations between our energy recuperation units.
The key parameters are as follow:

- 400m in the direction of current flow between a wind turbine and a tidal current turbine, as calculated in the *3.3.2.3 Wake created by the wind tower.*
- 300m in the direction of current flow between two tidal current turbines (explained in *3.3.2.2 Wake created by the marine current tower*).
- 10 rotors diameters ($10\times154=1540m$) in the direction of current flow between two wind turbines (the value of the parameter is explained in the *3.3.1 Wind Turbine Wake*).
- 3 rotor diameters ($3\times154=462m$) in the perpendicular direction of current flow

between wind turbines (the value of the parameter is explained in the *3.3.1 Wind Turbine Wake*).

What must be noticed is that the values of the spacing of wind turbines is greater that the spacing between tidal current turbines. Also, the capacity of tidal current turbines (2MW each SeaGen turbine) is littler than the wind turbines' capacity (6 MW each).

Tidal current turbines will have to cohabit with wind turbines. In the park, tidal current turbines will be found at the foundations of the wind turbines. In order to further the joint and to reduce costs, we have decided to implement two different types of energy recuperation units:

- a jointed wind and tidal current recuperation unit (see the Figure 3.29 below). Indeed, the SeaGen tidal current turbine is also made by Siemens. This is the main reason why, it has been thought that the production of this two recuperation units could also be jointed.
  The SeaGen structure (see Figure 3.18) has a body that goes up above sea level. At this point, would start the body of the wind turbine. On the same body structure would be found a Siemen Sapiens 6.0MW wind turbine at the top, and at the bottom, a SeaGen 2.0MW tidal current turbine.
  We could reduce foundations cost, but also electrical components costs such as cabling. This structure has also been proposed as the main changes in the production supply chain would not be elevated.

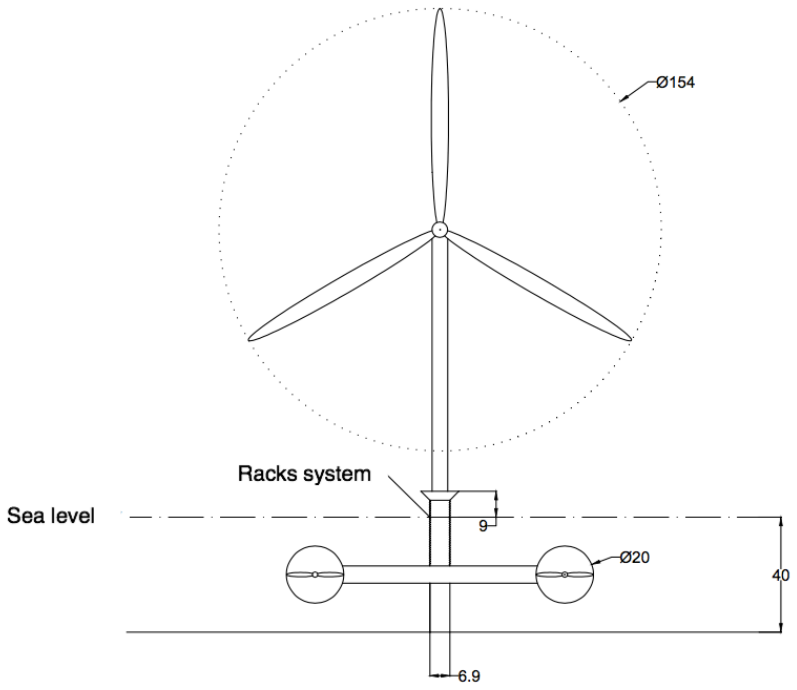

Figure 3.29: Sketch of the jointed recuperation unit: 6.0MW wind turbine and 2.0MW tidal current turbine (measures given in m)

- tidal current turbines and wind turbines can also be found separated in the park, as shown in the Figure 3.30.

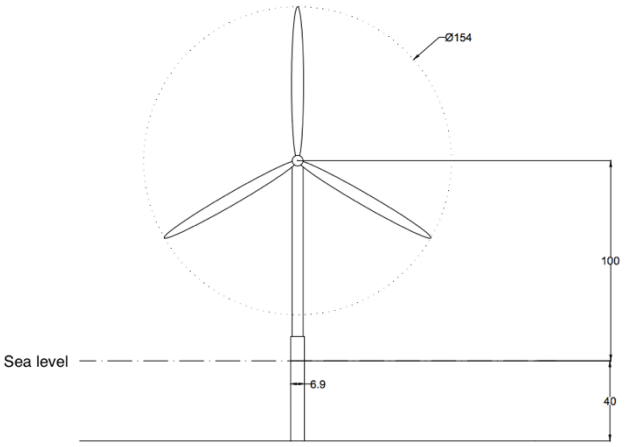

Figure 3.30: Sketch of the wind turbine (measures given in m)

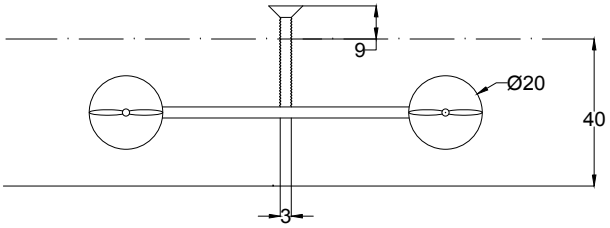

Figure 3.31 Sketch of the tidal current turbine (measures given in m)

3.3.3.2 Marine current turbines configuration

The key parameters for the configuration design of the marine current turbines are the following spacings:

- 400m in the direction of the current flow between a jointed recuperation unit (wind turbine + marine current turbine unit, sketched on the Figure 3.29) or a wind turbine unit (sketched on the Figure 3.30) and marine current turbine unit (sketched on the Figure 3.31).
- 300m in the direction of the current flow between two marine current turbines.

Both values of spacing are very close. Because wind turbines are found all throughout the park, we will compute the tidal current turbine configuration with a spacing of 400m. A grid pattern of this spacing is computed on the Figure 3.32. In our chosen location, the prevailing current flow direction is bearing of 149 degrees (Direction convention: current going towards). Finally, we obtain a map of the possible location for marine current turbines:

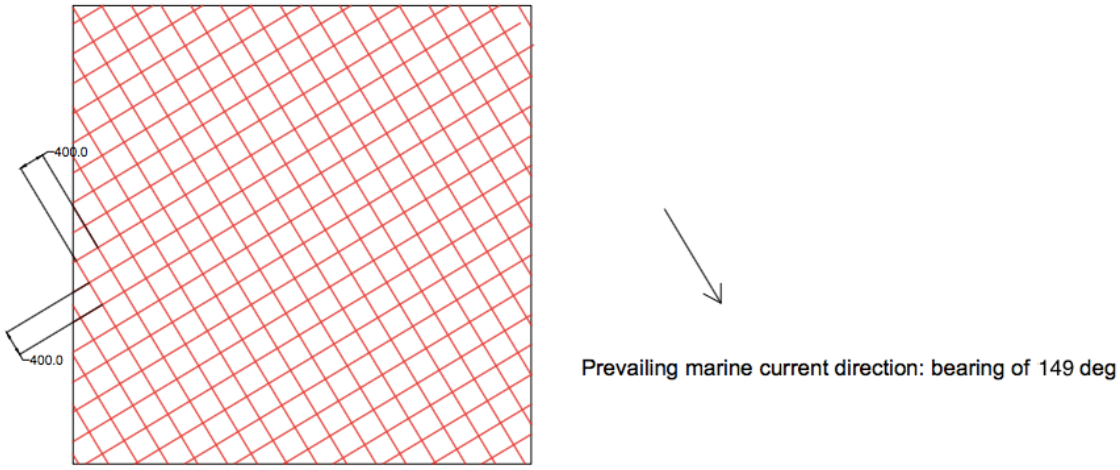

Figure 3.32: Grid pattern computed with AutoCAD for the spacing of tidal current turbines

3.3.3.3 Wind turbines configuration

The key parameters for the configuration design of the marine current turbines are the following spacings:

- 10 rotor diameters (1540m) in the direction of wind flow between two wind turbines.
- 3 rotor diameters (462m) in the perpendicular direction of wind flow between two wind turbines.

In our chosen location, the prevailing wind direction is bearing of 20 degrees (Direction convention: wind going towards).

According to the literature, there are 3 different ways of spacing, presented below. We will study their different advantages and calculation methods related to the available space for our park. The spacing methods are:

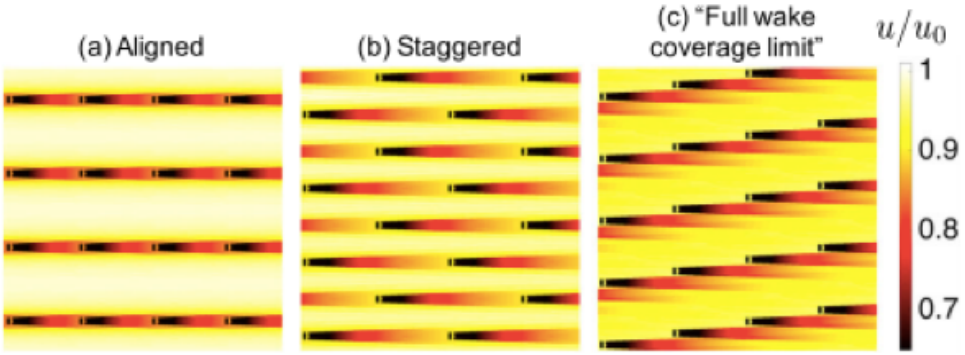

Figure 3.33: Different types of wind turbine spacing [44]

Figure 3.33 shows the different wind farm layouts, the key problematic of the spacing is that wake of each turbine should be correctly calculated in order for this wake not to affect the following energy recuperation unit.

We define w_f, the wake coverage area, defined as the percentage of the area, in fully

developed regime, of the wind farm where $u < 0.95\, u_0 - u$ being the velocity of the wind and $u_o$the initial wind speed. Here, $w_f = 0.35$ (aligned), $w_f = 0.60$ (staggered) and $w_f = 1$ (full wake coverage limit).

In the full wake coverage limit layout, the performance of the wind farm is better than in aligned or staggered wind farms. By performance is understood the most optimal spacing: in a given area, the Full wake coverage limit is the layout that includes the larger number of energy recuperation units, with no interactions between the different units. Indeed, the distance between directly upstream turbines is larger, this allows turbines on the next downstream row, to be placed with a little deviation so that they remain just outside the wake. We define *s,* the spacing between turbines in the incident wind current direction. For *s* < 7D, the staggered wind farm layout still has a wake area coverage, and therefore, the full wake coverage limit only outperforms the staggered layout for s > 7D. However, many other factors should be taken into account while deciding the type of park layout, such as:

- Ψ , the alignment angle with respect to the incoming flow
- it is not compulsory to input a constant stream wise spacing between the wind turbines

The data indicate, that the highest power output for the entire wind farm, is obtained for the smallest alignment angle Ψ, for which wake effects from turbines in the first few upstream rows are minimal. We need to compute the minimum angle that ensures that the power output of the second row is close to the power output of the first row. *[44]*

Our park area is large enough for the total installed power. There is no such need of computing the maximum optimal spacing, as the geographical and locations restrictions are not so strong. That is why we have decided to compute a staggered layout for our wind farm.Finally, we obtain a map of the possible location for wind turbines, using the staggering location method:

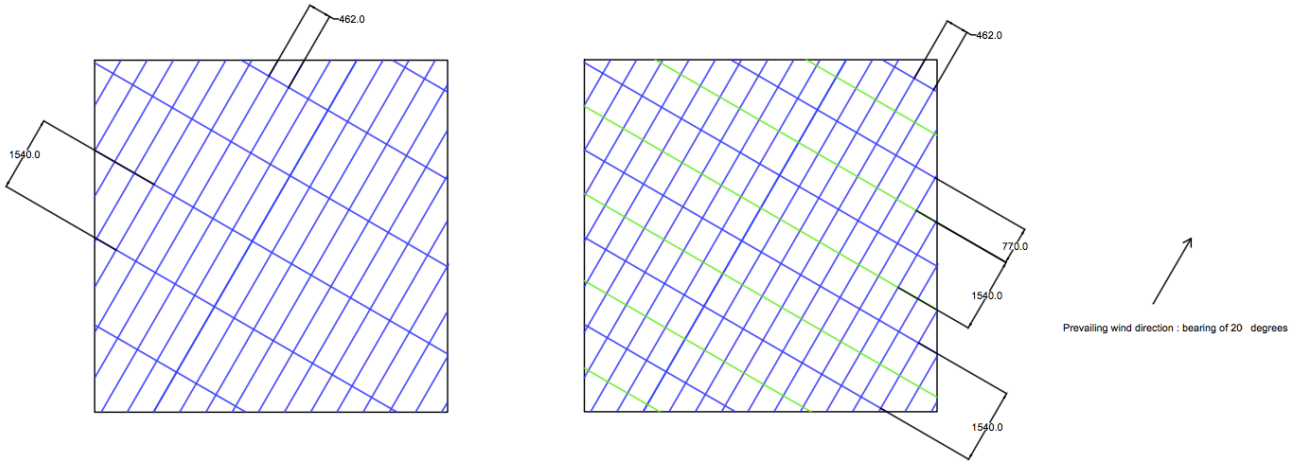

Figure 3.34: Grid pattern computed with AutoCAD for the spacing of wind turbines: aligned (left), and staggered (right)

3.3.3.4 Final configuration of the park

These turbulent effects downstream are determinant parameters in the next step of the park design: the assembled geographical distribution of the energy recuperation units in the chosen area of 51,25km^2. Indeed, the trend nowadays lies on the construction of bigger capacity parks, because of the evolution of technology and the reduction of park costs. In 1991, the average nominal production of parks was 6MW, whereas in 2015 the mean nominal power production stands at 350 MW.

Considering the area of our chosen location, the spacing constraints for our park and the current trends in wind park size, we have decided to a design park with a capacity of 500MW. That is:

- Wind power recuperation units: 50 x 6MW = 300 MW
- Current power recuperation units: 100 x 2MW = 200 MW (50 units as jointed wind and current recuperation units and 50 units in the current recuperation units).

As shown before, in the park design key parameters, the meteorological information of our site should also be considered. Turbines should be correctly orientated to maximise the energy recuperation. To start with, the angle of incidence of the marine current and of the wind is crucial in determining the direction, at which, the aforementioned turbulence parameters are applied. The hourly direction of these currents was also provided by Open Ocean for the year 2015. From this data, we have retrieved the prevailing current and wind directions:

- Prevailing wind direction: Bearing of 20 degrees. Coming from a SW direction. See Figure 3.34, blue line orientation.
- Prevailing current direction: Bearing of 329 degrees. Coming from a NW direction. See Figure 3.32, red line orientation.

By superposing the two possible location maps of both marine current and wind turbines, we have obtained the final turbine location map for our park:

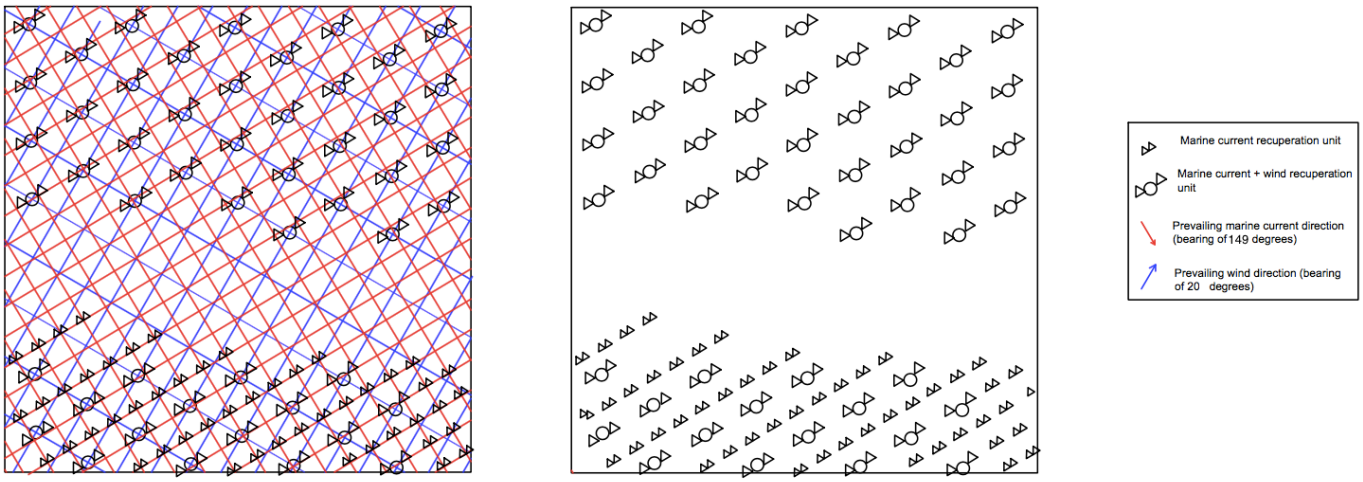

Figure 3.35: Marine current and wind turbine location map
Please note that triangles and circles are not drawn on scale

The unoccupied space crossing Figure 3.35 divides the figure into a northern part and a southern part. This space allocation was necessary to avoid the underwater cliff, that is found at this point of our chosen site. Indeed, no units are installed in this area, since the cliff has a depth of 100m, which would make elevate the costs of the foundation and installation of the units, up to a level where profitability would be jeopardised. Indeed, currently, there are no offshore parks placed at such depths. This would not only be a challenge in terms of economy but also in terms of technology. Avoiding this cliff seems the best option. What is more, we suggest that this space could be used for major access routes for Operation and Maintenance vessel communication of the park.

The analysis of Figures 3.5 and 3.6 reveal that the tidal current speed is greater in the southern part of our location. This explains our choice of inputting a greater density of tidal current units in the southern part of our chosen area than in the northern part. Indeed, we have:

- In the northern part: 34 tidal current energy units are placed. All are found as a jointed wind and tidal current recuperation unit.
- In the southern part: 16 current energy units are placed in the form of as a jointed wind and tidal current recuperation unit and 50 units are placed as standalone current recuperation units.

Contrary to this, for the jointed wind and tidal current recuperation units, there is a higher number of units in the northern part of our area than in the southern part. This is due to the fact that, although there is no apparent French legislation on the minimum distance to the coast for offshore technology – this distance is determined personally for every project - we wanted to minimise the visual impact of the park from the coast. Indeed, from a distance of 10km offshore wind turbines of our rotor diameter (154m) are barely visible (as explained in the section *3.1.4 Geopolitics and Legal dimension*).

This makes:

- 34 jointed wind and tidal current recuperation units in the northern part. These are at about 10km from the coast, hence invisible.
- 16 wind and currents recuperation units in the southern part. These are at about 4km from the coast, hence visible.

In the following map, we can see our park in its geographical position:

Figure 3.36: Location map of the tidal current and wind turbines

3.4 Annual Energy Production

Once we the park has been designed, we know precisely the number of wind turbines and tidal current turbines installed, as well as their exact location. With the turbines characteristics, and the meteorological data of the chosen location provided by Open Ocean, we can compute an hourly production of our site for a year long. The calculation of the annual production is needed in order to then study of the economic viability of our park.

An important parameter to consider that is crucial in our simulation is the capacity factor C_p (the calculation of this coefficient has been explained in the section *2.3.1 Power Coefficient: an introduction*). The Capacity Factor of a power plant is the ratio of its actual output over a period, to its potential output, if it were possible for it to operate at full nameplate capacity continuously over the same period of time. The Capacity Factor is calculated by dividing the total amount of energy produced by the plant during a period of time; divided by the amount of energy, the plant would have produced, at full capacity.

The capacity factor of a wind turbine lies between: $C_p \in [0.35\ ;\ 0.42]$

3.4.1 Simulation Methodology

To simulate our park, we need to compute separately the energy produced by the wind, and the energy produced by marine currents. Indeed, previously (see Section *2.3.5 Extrapolation to tidal turbines*), we had demonstrated that the calculation methods of the power output of a wind turbine could be extrapolated for tidal current turbines. The only parameter that had to be change was the density of the fluid. However, with this simulation, we are aiming at a more precise and realistic value of the power production of the park. The wind turbine integrates a synchronous generator with a permanent magnet and the marine current turbines work with an asynchronous generator; that is why two different simulations are required.

To simulate both productions, we have decided to work with the program Simulink. Two options have been considered:

- we could either start the block diagrams programming from the beginning, or,
- study the pre-existing models on Simulink and understand their key parameters, in order to adapt and modify these models. Modifications are necessary for the program to fit the characteristics of our park and simulate it correctly.

Because our project pretends to be innovative, we have decided to take our decisions according this characteristic. If we had started the model from the beginning, because of the complexity of the transcription of the physical model to a block diagram problem, we would not have been able to compute many of our park properties. Besides, the model would have remained too naive, in order for us to obtain the precision of results we are aiming for.

3.4.1.1 Simulink Wind Model

The decision, taken with our project manager teacher, Amir Arzandé (teacher at CentraleSupélec), was then to adapt a pre-existing Simulink model in order for it to fit our park's characteristics.

The first step was to find the Simulink function that would best fit our park.
After doing some research and comparing different models, we have decided to compute the function: `power_wind_type_4_det`.

This function computes a 10 MW wind farm, consisting of 5 wind turbines, of 2MW each, connected to a 25kV distribution system. The system exports power to a 120 kV grid through a 30 km cable, 25 kV feeder. The wind turbine contains a synchronous generator. The function of this model was to observe the steady state operation of the wind turbine, and its dynamic response to a voltage sag, resulting from a remote fault on the 120-kV system.

If we run directly the initial program, the farm produces 10 MW. The corresponding turbine speed is 1 pu of generator synchronous speed. During the voltage sag, the control systems try to regulate DC voltage and reactive power at their set points. The system recovers, after fault

elimination.

Many parameters had to be changed. Our first approach was to adapt the characteristic of the synchronous generator to our Siemens 6MW wind turbine, and maintain the computation of the grid and the control system. However, we have met serious problems reaching coherent solutions. Indeed, there were a lot of parameters that were dependent and concatenated. Because of the complexity of the code, many parameters were out of our reach. What is more, it sometimes reveals complex to know the value of these parameters for our own park, as the data available of our technology (Siemens wind turbines) are not fully accessible, and some remain trade secret.

After several meetings with two expert teachers in electrical grid from CentraleSupélec: Amir Arzandé and Jean Claude Vannier, it was decided to lower our simulation expectations, following their advice. They advised to simplify the model by deleting block diagrams, that would only compute optimization functions, and we would not consider as essential in the energy transformation process.
Finally, our simulation will compute only the power generated by the wind turbine with an input wind. The transport of the electrical power to the grid was considered as secondary, and is left aside for a further study. The control system has also been simplified: the pitch angle control system has been deleted. However, the cut-in and cut-off speed, as well as the production power function, have been computed directly on the excel data, rather than in the Simulink program.

In brief, the Simulink program receives a wind speed input. The first block diagram computes the mechanical torque produced by the given wind input. This mechanical torque is then given to a second block diagram, that models a synchronous generator. Finally, the program displays on the scope the values of the Active Power (P in MW), Reactive Power (Q in Mvar) and the rotor speed (w_r in pu).

3.4.1.1.1 Adaptation of the control system

A part of the function we had to simplify and compute was the mechanical torque.
Following our guideline, it was decided to delete the pitch control angle system. These element removals are thoughtful. Yet, undoubtedly the deletion of these blocks remains a loss of information, but it was estimated that the simplification can be considered as minor in the calculus of the power produced.

As we have deleted the pitch angle control, and computed the cut-in and cut-off directly on the input data, we need to input a substitute. Again, we have assumed that those control systems could be integrated in the value of the C_p. Based on our wind characteristics and turbulence, we have chosen a C_p= 0.36. According to theoretical values, the C_p of wind turbines lies between 0.35 and 0.42. Our value is therefore coherent, with values found in the literature.

We have decided to apply the cut-in and cut-off with excel on the Input Data, provided by Open Ocean. The program applied is based on the characteristic power generation curve of the wind turbine:

- if the wind speed magnitude < cut-in speed (= 4m/s), then the wind-speed magnitude = 0 m/s.
- if wind speed magnitude > cut-off speed (= 25 m/s), then the wind speed magnitude = 0 m/s.
- if wind speed magnitude is > nominal speed (= 13 m/s) and < cut-off speed, then wind speed magnitude = nominal speed (=13 m/s).

3.4.1.1.2 Adaptation of the mechanical system

Based on all these hypothesis, we have managed to compute a turbine and drive train block diagram. The program receives a wind speed. With the incident wind speed on the blade, the program calculates the mechanical power produced. This mechanical power is then transformed into a mechanical torque. The mechanical torque is given, as an input, to the electrical block diagram. Indeed, the mechanical torque allows the rotor movement and is the cause of electricity production.

On the Figure 3.37, appears the mechanical block diagram.

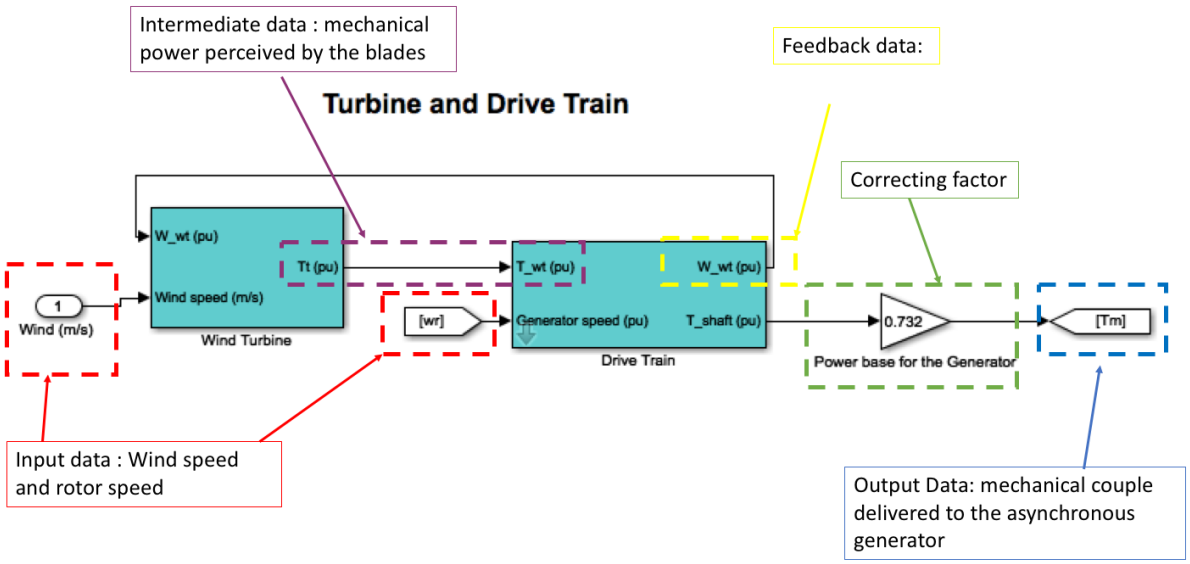

Figure 3.37: Turbine and Drive Train block diagram

On the Figure 3.38, you may find a zoom on the Wind Turbine Mask shown in the Figure 3.37. Notice that the mechanical power extracted by the blades is in this program modelled by the theoretical equation explained in the section *2.3.*

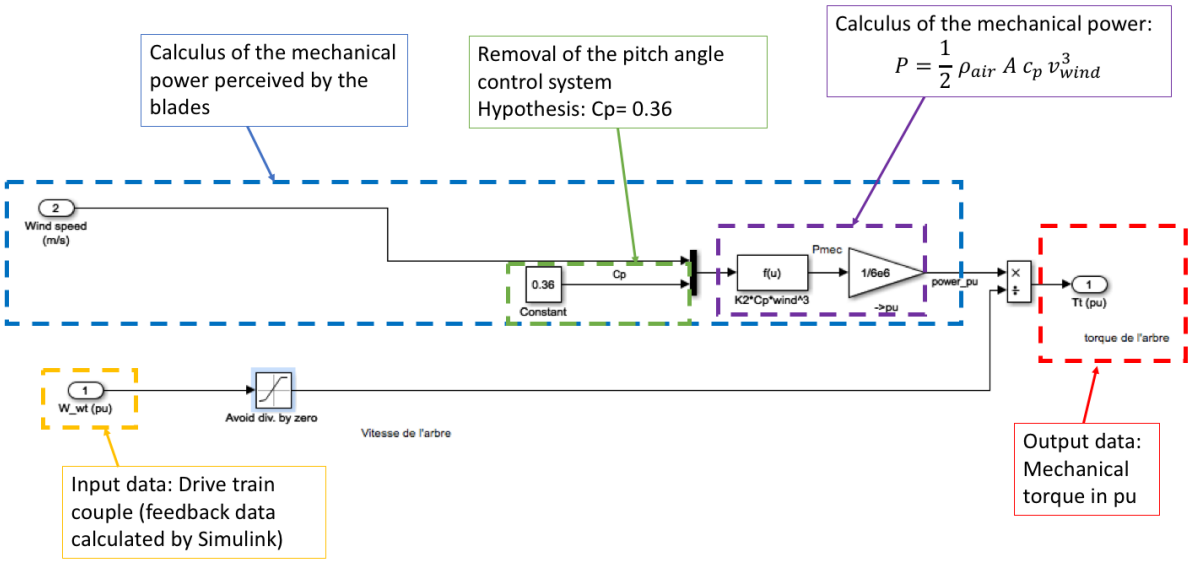

Figure 3.38: Calculation of the mechanical torque

3.4.1.1.3 Adaptation of the synchronous generator key parameter

The problem, faced for the adaptation of wind generator data, is that Siemens does not provide such detailed information about the generator of the wind turbine (value of resistances, pairs of poles…). However, all the generator data in the program is computed in pu units. This allows, through a factor, to adapt the value of our turbine.

Indeed, for the initial turbine, the value of the parameters in pu units are calculated using, as a base, the nominal power $Pn = 2e6\ VA$ and the voltage $Vn = 730V$.

The values of resistances in pu units are then computed through the method:

$$S_n = 3\, V_n\, I_n$$

$$V_n = \frac{U_n}{\sqrt{3}}$$

$$Z_n = \frac{V_n}{I_n}$$

The value of the resistances (Z in Ω) are converted to pu units (r in pu): $r = \frac{Z}{Z_n}$

For the pre-existing turbines, the initial programmers had calculated the value Z_{n1} to convert the value of their resistances to pu units. Alike them, we need to calculate the value Z_{n2}.

Let r_1 be the values, in pu units, of the pre-programmed resistances, and r_2 the value of our wind turbines resistances in pu units.

$$Z_{n1} \times r_1 = Z_{n2} \times r_2$$

$$\Leftrightarrow r_2 = \frac{Z_{n1}}{Z_{n2}} \times r_1$$

We only need to compute the ratio $\frac{Z_{n1}}{Z_{n2}}$ to obtain the value of our resistances, knowing that $Z_{n1} = \frac{V_n}{I_n} = \frac{V_n^2}{S_n}$.

We consider:

Pre-existing model	New model
$Sn = 2MW$ $f = 60\ Hz$ $Vn = 730\ V$ $Z_{n1} = (\frac{730}{\sqrt{3}})^2 \times \frac{1}{2e6} = 0.0888$	$Sn = 6MW$ $f = 50\ Hz$ $Vn = 690\ V$ $Z_{n2} = (\frac{690}{\sqrt{3}})^2 \times \frac{1}{6e6} = 0.02645$

Table 3.1: Reference values for the pu units calculation

We obtain $\frac{Z_{n1}}{Z_{n2}} = 3.3579$. We multiply all the values of the programmed resistances by this constant to adaptate them to our model.

The value of the time constant of the rotor do not need to be modified. *[45]*

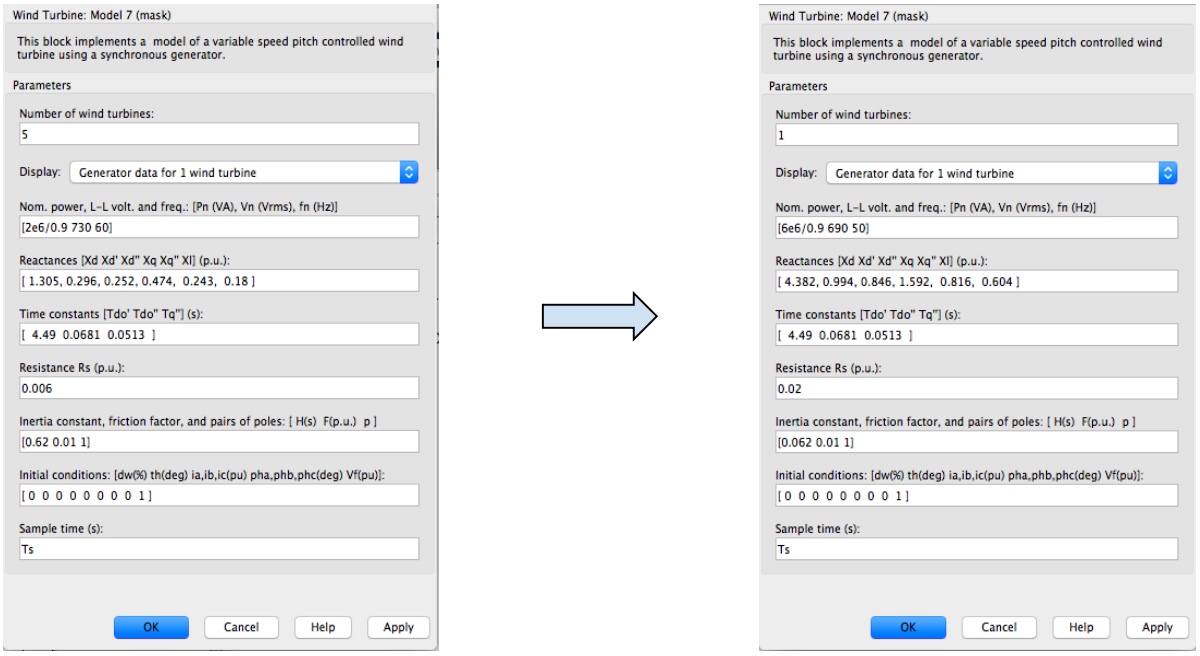

Figure 3.39 : Initial generator data (left) and adapted generator data (right)

The model generator, that was programmed on the model, is a synchronous generator connected to a voltage. As we can see on the Figure 3.40, below, the synchronous turbine receives as an input a voltage V_f.

Indeed, this type of motor does not correspond identically to the one of our chosen wind turbine (which has a permanent magnet and not an input voltage). We have chosen, in compliance with our expert teacher (M. Amir Arzandé) to maintain the programming of the block diagram responsible for the input voltage V_f rather than changing it into a permanent magnet. *[45]*
The adaptation of this input (from Voltage input into Permanent Magnet) would have brought a lot of changes, and difficulties in the adaptation, compared to the variations in the results of the simulations. We have therefore made the assumption that, the power generated, by these two types of synchronous generators, was significantly identical.

3.4.1.1.3 Adaptation of the grid

Finally, it was decided to delete the grid. The data of the electrical cables and the transformers, used to simulate the energy transport from the offshore park to the grid, did not anymore fit the model (as we have changed the data of the motor). Maintaining the grid simulation would have brought a considering amount of work, and is not essential to our project. We have left this part for a further study.

However, the removal of the grid needs a substitute. We have added a consuming resistance and connected it to the ground. We have also computed a scope at the terminals of the resistance. On the Figure 3.40, you have an overview of all the electrical block diagrams computed.

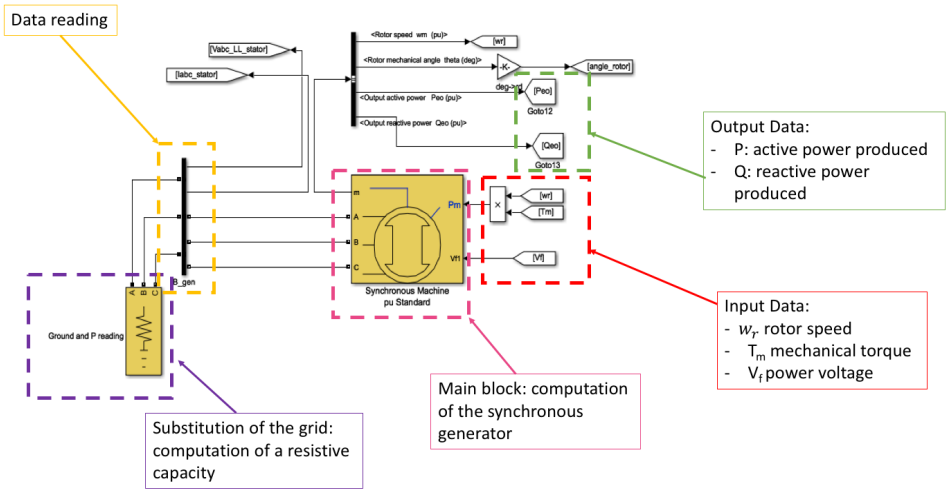

Figure 3.40: Electrical and mechanical Block Diagram

3.4.1.1.4 Simulation Results

We have obtained a Simulink Block Diagram that enables us to calculate the power produced by our Siemens 6MW wind turbine for an incident wind speed. You may find on the Annexe

5, the final overview of the Simulink blocks. The initial program was used to study the steady state of a wind farm, so it manages to reach steady state in a reasonable lapse of time: in around 12s.

Below, on the Figure 3.41, you may find the scope reading for an input wind of 13 m/s (nominal wind speed):

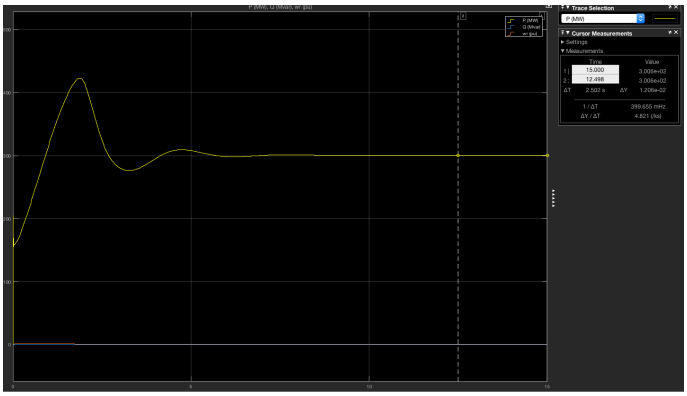

Figure 3.41: Power generated by the wind turbine park for an input wind of 13 m/s (Simulink Scope reading)

Because of the considerable amount of data we handle (hourly wind speed magnitude for a whole year), it was necessary to compute a MATLAB function, that would feed in the input data and save the simulated output. This function reads the wind speed from a `.txt` file and stores the information in a vector. This information is, one by one, read by MATLAB and ran by the Simulink Program. The final value of the Power generated (P in MW), computed by Simulink, is stored in another vector in MATLAB. The time of program running is non-negligible (around 9 hours).

The generated power during a year is finally:

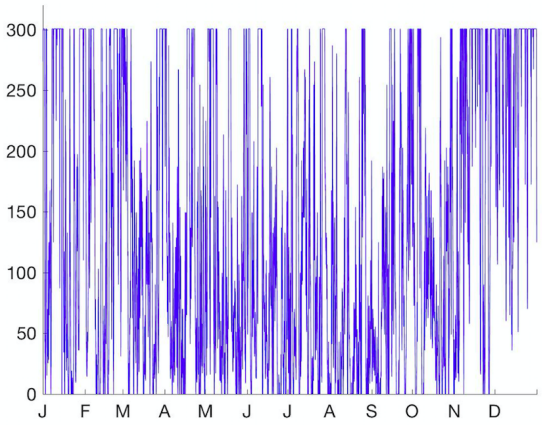

Figure 3.42: Power generated by the wind turbine park (in MW) during a year (MATLAB graph)

The curve is yet variable. We cannot really observe any type of symmetry or seasonality.

22,61% of the time, the wind turbine park works at its nominal speed. The efficiency of the park can be then considered as is high.

3.4.1.2 Marine Current Model

Our goal remains to model the power production of our entire innovative park: wind energy (as done in the previous section) and tidal current energy with Simulink. This section will detail the tidal current park simulation. However, the Simulink model used for wind turbines is not transposable to marine current turbines as the SeaGen turbines use an asynchronous motor.

3.4.1.2.1 Function selection and adaptability

Alike the wind turbine's model, we have chosen a pre-existent Simulink model of an asynchronous generator, programmed by the function: `power_windgen`. This function computes a wind turbine with an asynchronous generator in an isolated network. We have made the hypothesis, that the principle of converting marine current energy to electrical power, is comparable to the conversion of wind power to electrical power. Their mechanical and electrical components remain the same. The extraction of energy depends on the mechanical power captured by the blades of the machine, modelled by the formula:

$$P_{mec} = \frac{1}{2}\rho_{fluid}\, A\, v^3 C_p$$

The important difference in power that can be extracted from this both sources is caused by the fluid's density. Water is indeed 800 times heavier than air. If tidal current speeds were of the same order of magnitude than wind speeds, the power generated by marine currents would be greater. However, marine current speeds are significantly inferior to wind speeds. As the velocity is elevated to the cube, this causes such an important difference between the power generated by both sources. However, the principle remains the same and is modelled by the same function.
That is why a Simulink model of wind turbine can be adapted to a Simulink model for marine current. *[45]*

Our final Simulink problem is modelled:

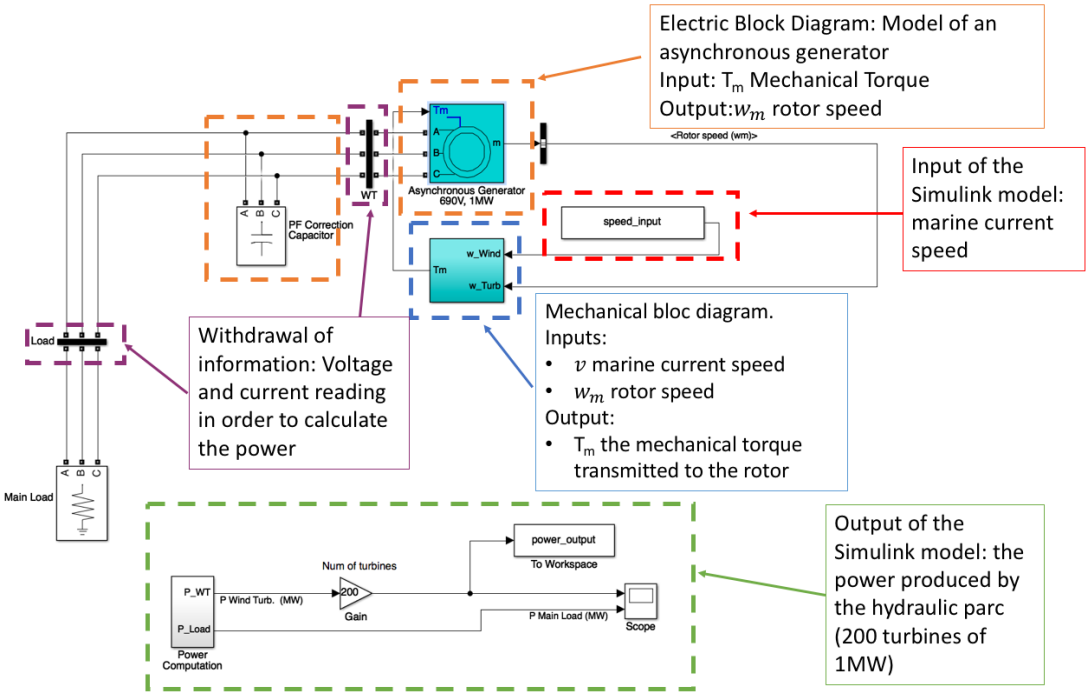

Figure 3.43: Simulink Model of conversion of marine current energy to electrical power

In the following sections, we will detail the programming of each block diagram.

3.4.1.2.2 Deletion of Blocks in the pre-existing model "power_windgen"

To adapt our model, we have inputted the same method as the one used for the wind turbine model. We have simplified the process of energy conversion by the removal of blocks that did not contribute to the system of conversion. However, these deleted blocks were replaced, to counter the loss of information.

Initially, in the pre-existing model, a complex load was computed (series of loads in parallel, controlled by a frequency regulator). We have, instead, programmed a simple consumer load, this simple loaf is used to represent the final use of the electricity generation distributed through the grid. A mire integrated model could include the line transformations of the electricity through its transport and distribution.
Also, the initial program represented a wind turbine in an isolated network. That is why, it also had computed a Synchronous Condenser Motor, to supply the isolated system with electricity, when no wind was available. Indeed, in the original model, when the power produced by the wind turbines was not sufficient to supply the consumer load, this condenser motor would be turned on. However, our offshore park does not have such a system, as it is connected to the network. We simply delete this block. The control system was also deleted for the same reasons as in the wind turbine model – since, our study does not focus on this matter and this block is not critical for the simulation.

3.4.1.2.3 Adaptation of the mechanical block diagrams

You may find below, on the Figure 3.44, the detail of the programming of the Mechanical Block Diagram (blue block on the Figure 3.43):

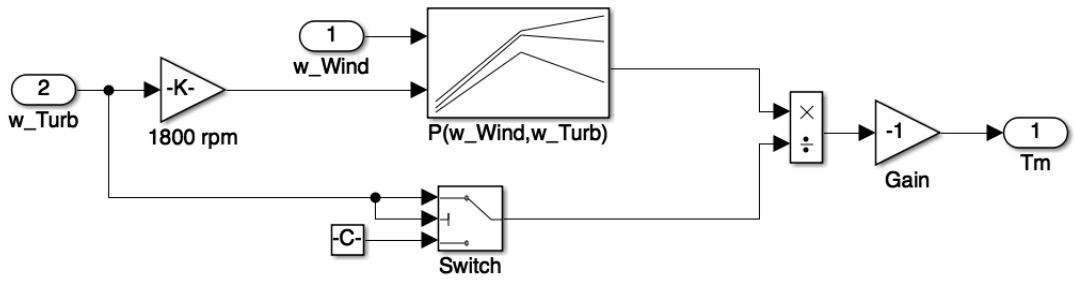

Figure 3.44: Simulink Model of calculation of the mechanical torque

This block diagram implements the mechanical torque transmitted to the rotor of the turbine and created by the incident tidal current. The inputs are the tidal current speed and the rotation speed of the rotor of the asynchronous generator.

The rotor speed is given in pu units, we convert it to rad/s, by multiplying it by its nominal speed (1800 rpm) – constant block K on the Figure 3.44.

In the next block (above) on the Figure 3.44, were implemented a series of power curves. For a given tidal current speed and rotor speed, the program reads on the curves the mechanical power generated. Yet, this block differs from the one implemented for the wind model. Indeed, as seen on the previous Section *3.4.1.1.2*, the turbine drive train computed a mechanical torque, by using a theoretical function. However, here we use power curves. These power curves also consider performance parameters, like the C_p.

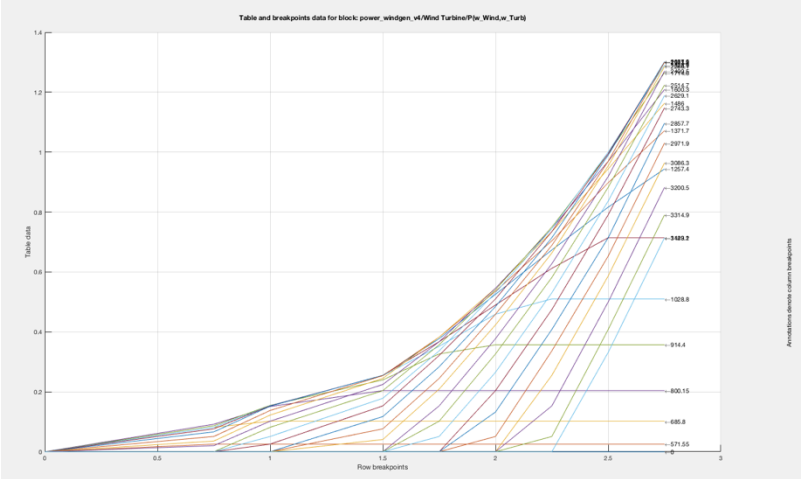

Figure 3.45: Tidal current power curves
X axis: marine current speed (m/s) ; Y left axis: power output (pu); Y right axis: rotor speed (rpm)

As you can see on the Figure 3.45, at the nominal tidal current speed (2.5 m/s) and nominal rotor speed (1800 rpm), we obtain a power output of 1 pu. Notice that the power output implemented here, can go beyond the nominal power, or, that for low tidal current speeds, power is produced. However, this does not represent the real situation as the asynchronous generator is piloted by a cut-in and cut off control system.

To avoid this problem and alike the wind speed model, we have programmed the cut-in and

cut-off speed on Excel too:

- if the current speed magnitude < cut-in speed (= 1m/s), then the marine current speed magnitude = 0 m/s
- if wind speed magnitude is > nominal speed (= 2.5 m/s), then wind speed magnitude = nominal speed (=2.5 m/s)

This way the power generated is equal to zero, for marine current speeds below zero. It is equal to the nominal power (1MW per turbine) for speeds beyond the nominal speed, so 2.5m/s. Between 1m/s (cut in speed) and 2.5m/s (nominal speed), the program computes the magnitude of the power generated by the park.

After the computation of the output power in pu, the program compares this power with the rotor speed to calculate the torque (computed as a division block on the Figure 3.44), indeed: $P = C \times w$

The couple is afterwards inverted (multiplied by -1). We have reached a driver mechanical torque. We need to compute a resisting couple, that is why the negative gain is necessary.
We have finally reached a value for the mechanical torque

3.4.1.2.4 Adaptation of the asynchronous generator

Alike the adaptation of the synchronous generator, we need here to compute new value of the motor resistances in pu.

The initial programmed motor had a nominal power $S_{n1} = 250\ kW$, a voltage $V_{n1} = 480\ V$ and frequency $f_1 = 60Hz$. We have changed these parameters to the values of the asynchronous motor of the Seagen Turbine: $S_{n2} = 1\ MW, V_{n2} = 690\ V\ ;\ f_2 = 50Hz$.

As explained before in the Section *3.4.1.1.3*, we only need to calculate the value of the ratio: $r = \frac{Z_{n1}}{Z_{n2}}$, knowing that $Z_{n1} = \frac{U_{n1}^2}{S_{n1}}$.

For this case we have: $r = 1.76$. We can finally calculate: $r_2 = \frac{Z_{n1}}{Z_{n2}} \times r_1$, the value of the resistances in pu. You may find below, on the Figures 3.46, the adaptation of these values:

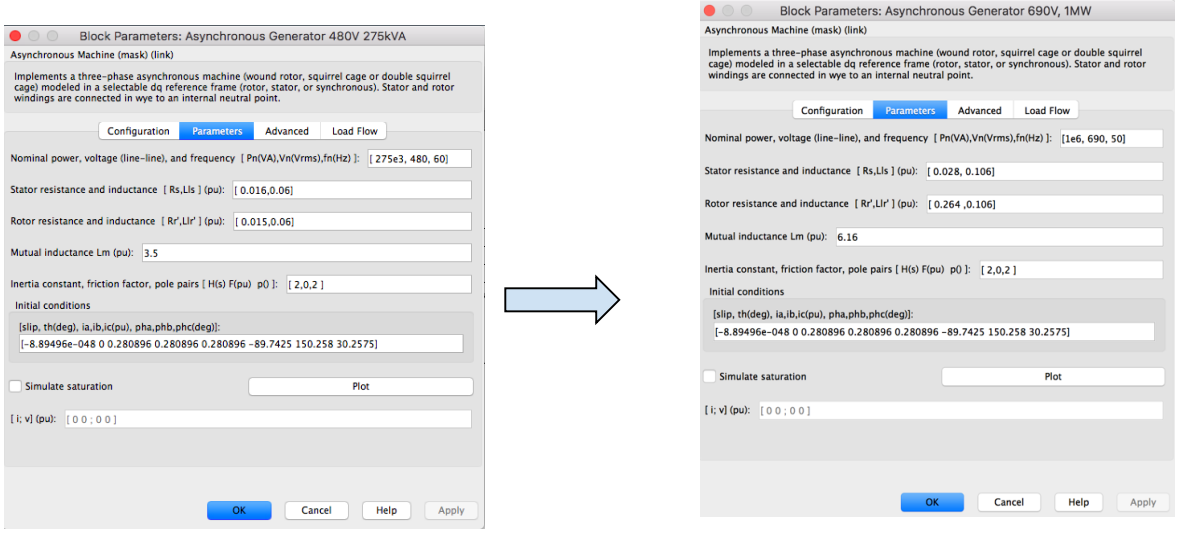

Figure 3.46.A: Motor's initial values

Figure 3.46.B: Motor's adapted value

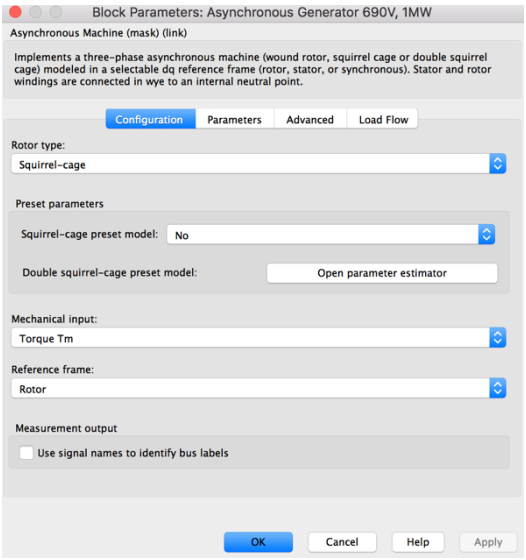

Figure 3.46.C: Type of asynchronous motor chosen

3.4.1.2.5 Adaptation of the consumer load and capacitor bank

At the output of the asynchronous generator, we need to connect a bank of capacitors. As explained in the Section *2.4.2.2*, the functioning of an asynchronous generator consumes reactive power. This reactive power is, however, not found naturally on the network. We need to install a bank of capacitor to generate this reactive power needed.

Also, in series with the capacitor bank, is found a resistance that models the consumer load. It was decided not to compute the whole system of cable tray to the ground. However, the power generated by the asynchronous generator must be consumed by an electric component on the grid: that is the function of the resistance.

The power output generated, by one turbine of 1MW, is read at two nodes: after the asynchronous generator and after the bank of capacitor. The active power read at both nodes is the same as the capacitor bank only generates reactive power, and does not consume or generate active power. We read the voltage and the current intensity to calculate the instantaneous power generated.

The result obtained is the active power generated by one wind turbine. We have to multiply this result by 200 to obtain the power generated by our whole SeaGen turbines of our park.

3.4.1.2.6 Analysis and validation of the simulation Results

We have the hourly marine current speed data given by OpenOcean, so 8760 data points. Again, alike the wind model, we have prepared a MATLAB program in order to run the Simulink model for each value of tidal current speed. This way we obtain the hourly production of our hydraulic park during one year.

The marine current simulation was longer than the wind speed current. The wind model simulation reached steady state in 12s. Because of the asynchronous generator, the marine current model takes a longer time to reach steady state. For speeds close to the nominal

speed, steady state is reached around 25s. For speeds, close to the cut-in speed, steady state is reached around 50s. This increases consequently the time of calculation

For instance, for an input equal to the nominal current speed (2.5 m/s), we obtain the following curves:

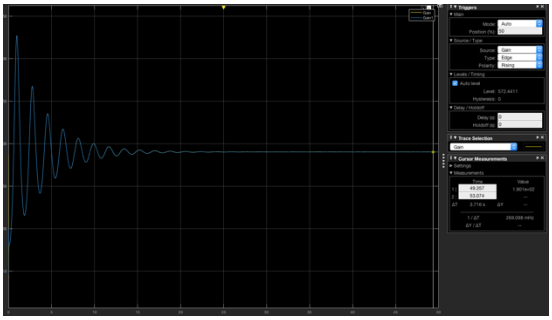

Figure 3.47.A: Power output for nominal current speed

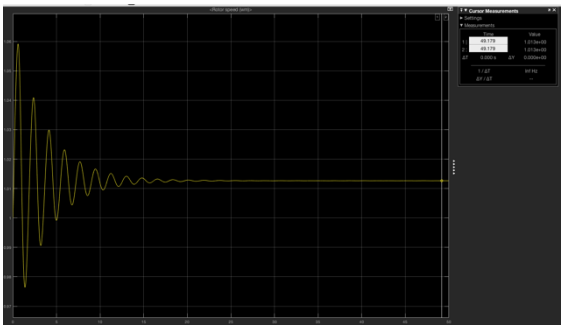

Figure 3.47.B: Rotor speed for nominal current speed

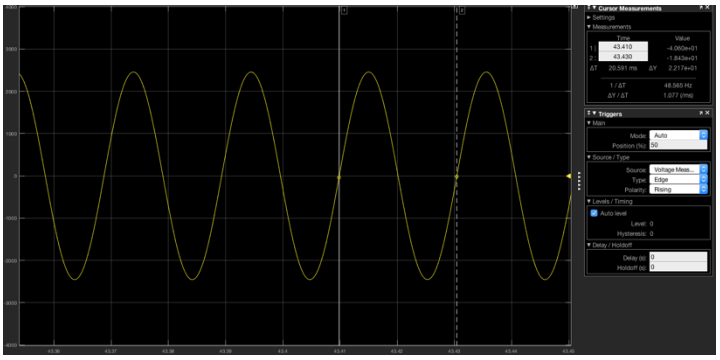

Figure 3.47.C: Voltage (phase to phase) and frequency measurement at the consumer load

On the Figure 3.47.A, we can see that steady state is reached rapidly from t = 25s. The power output, for nominal current speed, is not exactly equal to nominal power. We could have expected a power steady state value at P = 200MW. However, we can read P = 190,1 MW. This is due to the asynchronous machines losses.
On the Figure 3.47.B, we can analyse the variation of the rotor speed. The rotor speed reaches a steady state value of 1,013 pu. This also justifies that our machine is working correctly. As the asynchronous machine operates in the generator mode, its speed is slightly above the synchronous speed.

On the Figure 3.47.C, we have measured the voltage between phases at the consumer load. We can see that the voltage delivered to the consumer has a frequency of 48.57Hz, which is very close to the frequency of the network (50Hz). However, this value should be corrected to a more precise range [49.5 Hz ; 50 Hz] thanks to system control. This way, we are producing a power that can be exploited.

For an input current speed close to the cut-in current speed (1.5 m/s), we obtain:

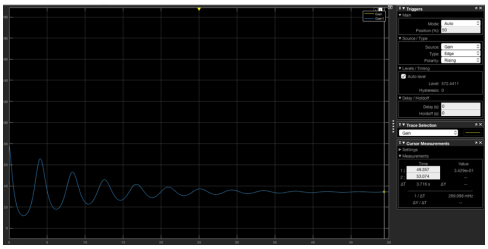

Figure 3.48: Power output for low current speeds

We can see, on the Figure 3.48, that the power output is much lower than the nominal power. At steady state for an input wind of 1.5m/s, we produce an output power of 34,29MW << 200MW. Also, we can remark that the time taken by the simulation to reach steady state is considerably longer (around 45s).

3.4.1.2.7 Marine current power output for the park

Finally, we obtain the annual production of our hydraulic park (see Figure 3.49). The analysis of this graph is found further on the section 3.4.3 .

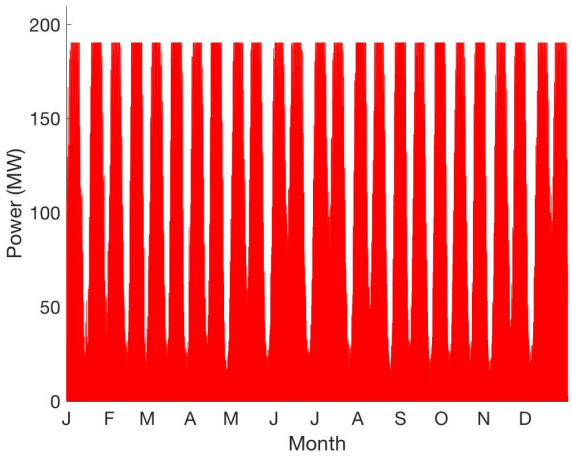

Figure 3.49: Marine current power produced by the park (Simulink Model)

3.4.2 Simulation Methodology on Excel

We have decided to compare the results of this simulation with the theoretical power extracted, that can be calculated with an Excel Program. Indeed, this Excel model leads us to results faster and easier than the Simulink model. However, these results remain very approximatively. They will only be used as a comparing point.

3.4.2.1 Marine Current Model on Excel

We have computed the theoretical mechanical power for the marine current:

$$P = \frac{1}{2}\,\rho_{seawater} C_p\, A\, v_{current}^3$$

$$with\ \rho_{water} = 1024{,}9\ \frac{kg}{m^3}\ [46]; A = \pi R^2 = 314{,}15\ m^2\ ;\ Cp = 0.398$$

The value of the C_p coefficient has been input so that, for a marine current input of 2.5m/s (nominal speed), the power generated should be equal to its nominal power 200 MW. To satisfy this equation, we need C_p= 0.398.

We contrast this value with the ones found in the literature. According to Bloomberg New Energy Finance report of 2013, the value of the C_p for tidal energy lies between [0.25 ; 0.45] *[47]*. Our calculated value is therefore coherent.

For this new model on excel, we obtain the power generated curve of our park:

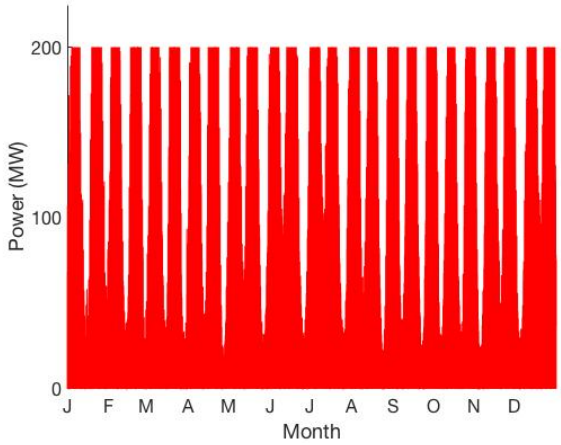

Figure 3.50: Power generated by the marine current turbine park (Excel Model)

3.4.2.2 Wind Model on Excel

For the wind model, we have computed the power output, with the same formula as the water:

$$P = \frac{1}{2}\,\rho_{air} C_p\, A\, v_{wind}^3$$

$$with\ \rho_{air} = 1{,}204\ \frac{kg}{m^3}\,[48];\ A = \pi R^2 = 18626{,}503\ m^2\ ;\ Cp = 0.245$$

The value of the C_p coefficient has also been input, so that for a wind speed of 13 m/s (nominal speed), the power generated should be equal to its nominal power 6 MW. To satisfy this equation, we need C_p= 0.245.

According to the Bloomberg New Energy Finance Report of 2013, the value of the C_p for wind energy lies between [0.32 ; 0.42] *[47]*. The C_p value, we have used in our Simulink model, is therefore correct and adapted to real-life parks. However, the value of the C_p obtained with the simplified Excel model seems low.

The reasons, that justifies this value, are that the C_p, found in the literature, often only refers to the losses in the mechanical transformation of energy (from the incident wind on the blade to the mechanical torque obtained on the transmission tree). We are not considering the electrical losses, in the process of transformation of the mechanical torque to an electrical signal. However, Simulink does consider and model these losses.

The efficiency along the process of energy transformation can be modelled numerically with these values:

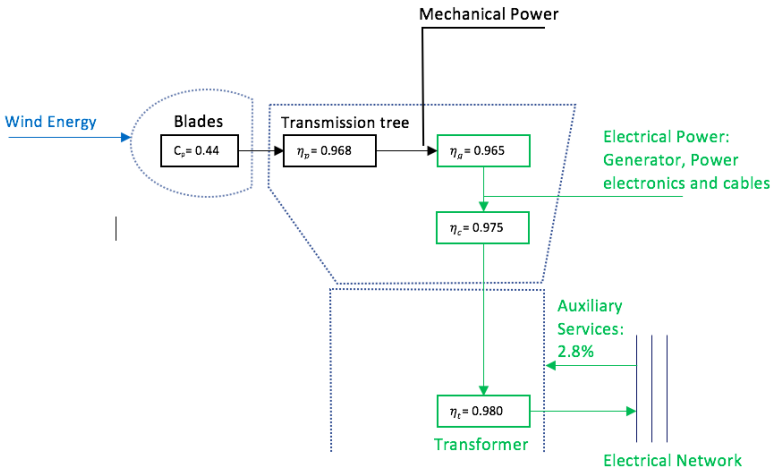

Figure 3.51: Efficiency of the process of energy conversion

According to the Figure 3.51, the losses, in the electrical process of energy transformation and the transmission tree, have an efficiency of $0.968 \times 0.965 \times 0.975 \times 0.98 = 0.8925$.

For the value of the C_p input in our Simulink model: C_p= 0.36, we can calculate the efficiency of the whole energy transformation process to input it on our Excel Model. However: $0.36 \times 0.8925 = 0.321$ does not correspond with the efficiency of 0.24 found on Excel.

It is coherent that the value of the Excel model is lower than the Simulink model. Excel only refers to mechanical losses. However, we are forcing, for a nominal speed, to obtain nominal power without considering electrical losses. Excel is a very simplified version of the process. Simulink describes the transformation more precisely.

For this new model on excel, we obtain the power generated curve of our wind turbine park:

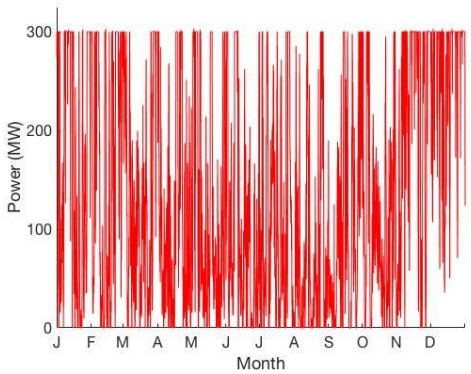

Figure 3.52: Power generated by the wind turbine park (Excel Model)

3.4.3 Results and conclusions

By adding the power generated by wind and marine current, we can obtain the power curve of our park using both models:

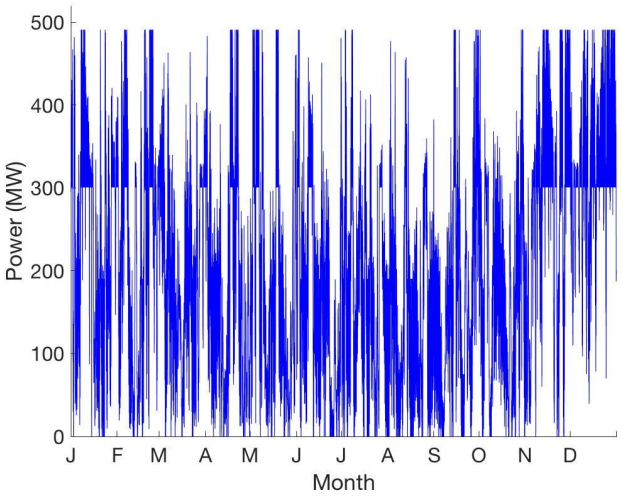

Figure 3.53.A: Power generated by the park (Simulink Model)

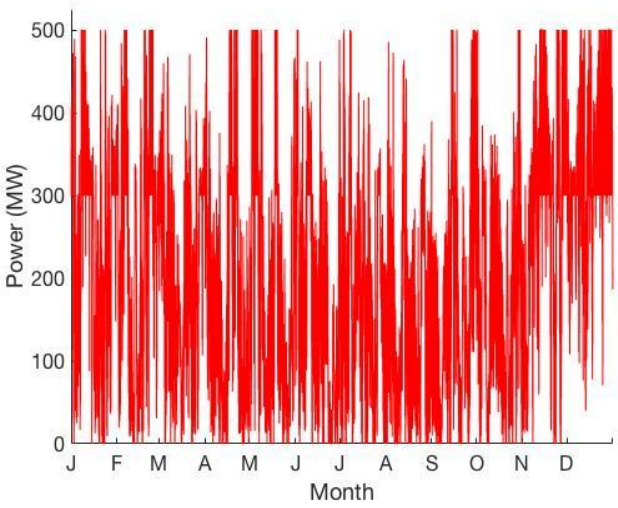

Figure 3.53.B: Power generated by the park (Excel Model)

For the rest of our project, we will study the values obtained with the Simulink model, as it is a much more precise model, than the one input on Excel.

We obtain an annual power production of our park: 1.763.030,334 MWh.
22% of the time, the wind turbines work at its nominal rate and 10% of the time the hydraulic turbines work at nominal rate. This justifies the optimality of the site selection.

From these graphs (Figures 3.53.A and 3.53.B), we can observe the complementarity of both sources of energy. Indeed, marine current is much more predictable than wind. Tide is less fluctuating. The production of our combined park is more stable than wind parks. This presents economic advantages. An advantage of fossil energies or nuclear energy is the reliability of its energy production. Here, we are getting closer to this result with the combination of two renewable energies.

4. ECONOMIC MODELLING

Now that we have completely defined our park design, as well as, computed its production. It is necessary to calculate its economic sustainability. Indeed, an economic comparison between actual wind offshore parks and our jointed park is needed, in order to justify its construction. Throughout this section, we will examine the different existing economic tools, used to evaluate the value of a park and afterwards apply them to the designed park.

4.1 Existing Economic Models and Tools

This section will examine the use of economic models and tools available to assess, analyse, and optimise renewable energy and energy efficiency technologies for our project. Many of these tools can be applied on a global, regional, local, or project basis.

Throughout the online Wind Energy MOOC course available at Coursera *[49]*, delivered by the Wind Energy department, at the Danish Technical University (DTU), some of these methods were presented. In order to choose from the main economic indicators, it is crucial to first understand what they represent, and how they are constructed.

4.1.1 Payback time

The Payback time method indicates how many production years are needed for the original investment to be paid back. It is a straightforward tool, that gives a rather simplistic calculation ignoring at any time the value of the money. In other words, 100 Euros next year are worth the same as 100 Euros this year, which is not true in the real world. However, for the purpose of this calculation, this is assumed.

Payback time is calculated by estimating the annual production of a facility and its subsequent annual revenue - that is, the annual production, times, the estimated sale price of the electricity. Moreover, we need the annual operating cost of the facility; usually calculated from the operating cost per turbine in the examined facility.

Payback time is calculated as follows:

$$t = \frac{Capital\ investment}{Annual\ revenue - Annual\ costs} \tag{4.1}$$

4.1.2 Net Present Value

The net present value gives us an idea of whether a proposed project is profitable or not. This indicator helps in the decision, as to whether to go ahead with a project, or not.

The definition of the Net Present Value is that, it is the sum of the cash flows (revenue minus the costs), with the monetary actualisation. This means we need to translate money in the future, back to today's money. To do so, the discount rate is used. This rate considers not only the time value of money, but also, the risk or uncertainty of the future cash flows. The greater the uncertainty of future cash flows is, the higher the discount rate will be.

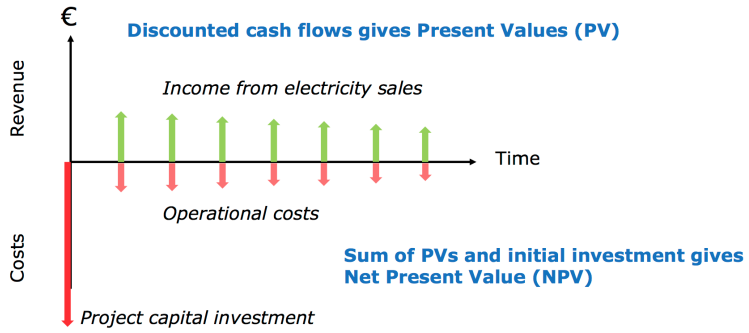

Figure 4.1: Cash flows and Capital Investment before actualisation, DTU Wind Energy MOOC

Having calculated the actualised cash flows, the initial capital investment must be subtracted to obtain a "net" value. The result is interpreted as the measure of the attractiveness of this investment.

If the NPV is greater than zero, then the project will be profitable, and should be furthered. If it is less than zero, then it is likely that the project is not going to be profitable.

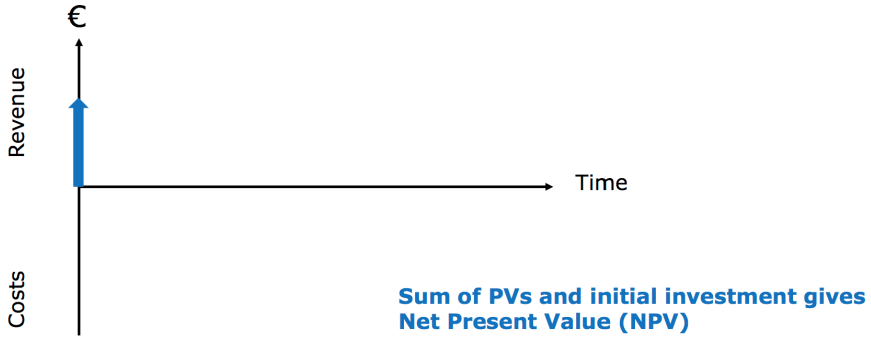

Figure 4.2: Net Present Value example, after actualisation DTU Wind Energy MOOC

4.1.3 Levelised Cost of Energy (LCoE)

The levelised cost of energy method helps in the comparison of projects, via contrasting the cost of generation from different projects. The aim of this tool is to find a cost per Megawatt hour, that can be used for this comparison.

The data needed is: the capital investment (hereof, Capex, in monetary units), the operational costs (hereof, Opex, in m.u), and the decommissioning costs (in m.u) and the annual energy production. We do not use, however, the revenue at any moment, since we are calculating and comparing generation costs among projects.

As for the NPV, we firstly discount all annual costs back to today's money, through the discount rate, and add investments and actualised decommission costs.

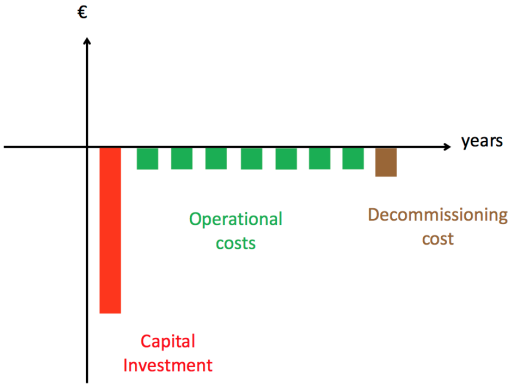

Figure 4.3: Costs throughout facility's lifetime, DTU Wind Energy MOOC

Secondly, we use the accounting technique of amortisation to get an equal amount of the costs, for each year of the facility operation. This is called "levelling" costs out over the lifetime of the park.

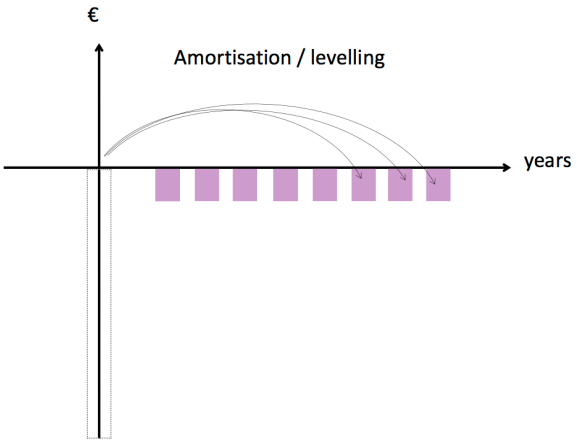

Figure 4.4: Levelling of costs, DTU Wind Energy MOOC

If we divide the annual levelised cost by the Annual Energy Production (AEP), then we get to the levelised cost of energy for our project.

$$LCoE = \frac{Levelised\ cost}{Annual\ Energy\ Production} \quad (4.2)$$

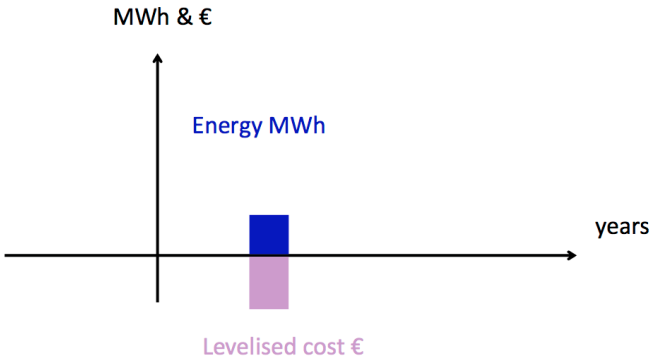

Figure 4.5: LCoE example, DTU Wind Energy MOOC

4.1.4 Discussion

The chosen tool, for the economic justification of our park, is the Levelised Cost of Energy method. This decision was taken for three main reasons.

Firstly, the LCoE model is the appropriate tool for project comparisons. Our joint facility proposition should respond to the following question: how do the benefits of recuperating wind and current energy, in one site, outweigh that of recuperating the same energy in different locations? In order to answer this question, we need to compare the economics of our joint proposal, to that of the separate production of energy. The LCoE indicator is hence the optimal tool to use.

Secondly, our economic profitability hypothesis is that of cost mutualisation possibilities in our joint park, bringing about overall cost reductions. We are hence only working on the cost structure of offshore facilities, not on their revenue. The LCoE is the only tool, from the ones presented above, that only takes into account cost - and not revenue. So, it represents a mean of comparing costs of our joint project, to two separate facilities (wind and marine current), or one type of joint generation with another type of separated generation.

Thirdly, and following on from the latter point, omitting the revenue, from our economic tool calculation, supposes a huge opportunity in terms of transparency and extrapolation possibilities. Indeed, if we were to include revenue in our calculations (if we were to choose Payback time or Net Present Value as indicators), we would be obliged to index our calculation to electricity's sale price previsions over 20 years. This would, on the one hand, trump our values, by introducing the fluctuations of the money market, rendering them less legible and transparent for comparison. Moreover, on the other hand, electricity prices vary from one country to another, so that our proposed methodology could only be valuable in

France. Indeed, working only from a cost perspective avoids limiting our study, due to harmonisation impediments. It is surely for this reason that the overwhelming majority of the literature available uses the LCoE, when studying the economics of renewable energies. *[50], [51], [52].*

In order to realise the boundaries of this model, we should mention that, despite its widespread use, the levelised costs of energy metric has several key limitations. Truly, by simplifying costs into one single number, it blurs the distinction between capital and operating costs, obscures the importance of interest rates, and implies only one optimal economic outcome. Other operating, economic, and policy assumptions, that are critical in forming the metric, can significantly impact its outcome. All in all, LCOE should not be the only metric used to compare the economic attractiveness of different energy sources – more holistic approaches are needed.

4.2 LCOE of offshore wind energy and tidal energy Models

This section covers the construction of the Levelised Cost of Energy method, for our proposed joint energy recuperation facility.

Three steps will be followed:

- LCOE calculation for a 50x6MW offshore wind farm
- LCOE calculation for a 100x2MW marine current facility
- LCOE calculation for our joint facility and its cost reduction opportunities

The third point of this study will be examined in Section *4.3. LCoE of proposed facility: Sensitivity Analysis.*

We will indeed perform a Life Cycle Cost Analysis (LCC) for each technology, defined as: "Life cycle cost is all the costs generated during the life cycle of an item" (Swedish Standard Institute). To do so, we need to examine the cost portfolio of each technology. The methodology, used for the latter LCoE calculation, was performed following the steps outlined in the DTU's Wind Energy MOOC online, and using the according excel functions *[49].*

The facilities lifetime has been settled to 20 years, according to the literature found in this sense.

4.2.1 LCOE calculation for a 50x6MW offshore wind farm

Attention must be drawn to the difficulty endured, in order to gain insight into the cost portfolio of wind farms form industrial sources, due to data confidentiality. The use of data created by institutes and research organisations largely helped in this sense.

4.2.1.1 Calculation of the LCoE indicator

The document "Cost of Wind Energy Review, 2014" by the National Renewable Energy Laboratory *[51]* finally provided us with the required information to model economically our offshore, fixed-bottom (monopile) 300MW reference model. However, limitations include the use of a unit turbine of 3.39 MW in their per unit cost structure, that had to be proportionally arranged to fit in our case.

The detailed cost portfolio over the wind farm's lifetime can be found in *Annex 3,* but the summarised cost structure of the Capex can be commented and be depicted as follows:

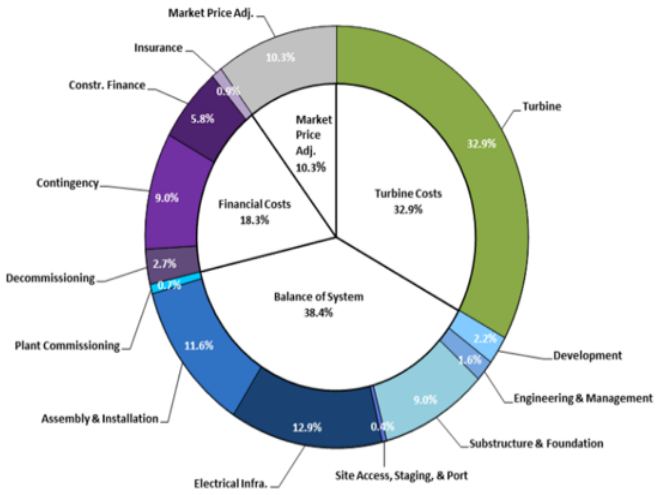

Figure 4.6: Capex cost structure for offshore reference wind plant model, NREL

As we can see in the Figure 4.6, currently, the most important component of cost is indeed the wind turbine. Our joint park proposition does not propose cost reductions in this parameter. However, other big cost components, such as Assembly and Installation (11,8%), Electrical Infrastructure (12,9%), and Substructure and Foundations (9%) are areas in which a joint installation, such as the one proposed, sharing electrical infrastructures and common foundations, could suppose a big difference. Moreover, a joint organisation of Operations and Maintenance operations could reduce the Opex costs.

A summary of the calculations and results of our LCoE indicator are thus performed in Table 4.1.

Capex	170014558,10 €
Decommissioning cost	17001455,81 €
Opex	34,82 €/MWh
Discount Rate	9,8%
LCoE	52,57 €/MWh

Table 4.1 Summary of the 50x6MW offshore wind farm LCoE

The Opex, Capex and discount rate were also chosen following the NREL's 2014 report *[51]*. The decommissioning cost was established at 10% of the Capex value.

4.2.1.2 Discussion

To validate our LCoE results, we have searched, in literature, to compare our results to that, of current offshore wind farm proposals of similar characteristics in terms of capacity.

We can highlight two examples that show, how the new high capacity offshore wind farms, have LCoE indicators similar to the one calculated above (52,57 €/MWh).

Firstly, the Kriegers Flak in Denmark *[53]:* it is a 600MW offshore farm, that will supply power to the Danish grid under a fixed price contract from 2019 to 2032 and based on 50,000 full load hours, according to documents published by the Danish energy ministry. Vattenfall's record-low offshore is such that : "We estimate that actually over the lifetime of the project, the average revenue is around $40/MWh [37.6 euros/MWh]".

Secondly, Dong Energy won a contract in 2016 to develop a 700MW Dutch offshore array at 72.70 euros per MWh.

Other projects, such as those in deep UK waters, are going ahead at higher cost. This explains why the global benchmark, while falling rapidly, is well above these recent figures from Denmark and the Netherlands. Since our project is set to be deployed in shallow waters, the [37 € ; 72 €] range proves that our LCoE calculation is acceptable and realistic for our given park.

4.2.2 LCOE calculation for a 100x2MW marine current facility

4.2.2.1 Calculation of the LCoE indicator for the marine current park

In this case, there is little commercial deployment of marine current facilities –although many trials exist around the world. Moreover, multiple technological propositions for marine current recuperation turbines exist: different mechanical assemblies, different physical phenomena involved in the energy recuperation process etc. - as underlined in the *3.2 Choice of technology* section of this report. This means that there is less of a rich literature regarding the economics of SeaGen's marine current turbine.

However, thorough research brought us to the document "Methodology for Design and Economic Analysis of Marine Energy Conversion (MEC) Technologies" by the Sandia National Laboratories *[55]* which examined, among others, SeaGen's proposition (RM1 in the document) for a 100-unit facility, which is exactly our case. Limitations for this dataset include the use of a unit turbine of 1 MW in their per unit cost structure, that had to be proportionally arranged for in our case.

This Reference Model Project (RMP) by Sandia National Laboratories *[55],* sponsored by the U.S. Department of Energy (DOE), was a partnered effort to develop open-source marine hydrokinetic (MHK) point designs as reference models (RMs) to benchmark MHK technology performance and costs, and an open-source methodology for design and analysis of MHK technologies.

The detailed cost portfolio over the current recuperation facility's lifetime can be found in *Annex 4*, but the summarised cost structure of the Capex can be commented and be depicted as follows:

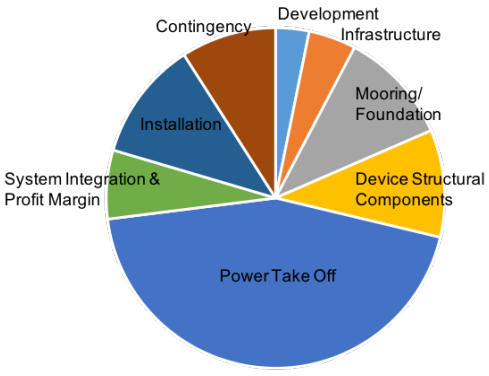

Figure 4.7: Capex cost structure for offshore reference marine current plant model, 100-unit array, Self -produced

As we can see in the Figure 4.7, currently the most important component of cost is Power Take Off. This component includes (as shown in the *Annex 4*) all the elements in the Power

Conversion Chain (Gearbox, Generator, etc.). Structural components and elements of the power conversion chain (PCC) are clear cost drivers, for all of the RMs and device components. For these, future R&D efforts should be methodically applied to reduce its costs and LCoE indicators. Our joint park proposition does not propose cost reductions in the PPC parameter. While there are some cost savings to be expected, simply by increasing the manufacturing and fabrication volume from one to 100. Also, major per-unit cost savings are expected to be realised within the installation cost category and the infrastructure cost category. Indeed, other big cost component, such as Device Structural Components (10,2%), System Integration and Profit Margin (6,5%), and Installation (11,4%) are areas in which a joint installation, sharing electrical infrastructures and common foundations, could suppose a big difference. Moreover, a joint organisation of Operations and Maintenance operations could reduce the Opex costs.

A summary of the calculations and results of our LCoE indicator are, thus, performed in Table 4.2. The detailed steps are retrieved in *[49],* with the dataset of the detailed cost breakdown in the spreadsheet developed by ReVision, entitled "Reference Model 1 CBS.xlsx" *[56],* for report *[55].*

Capex	634000000 €
Decommissioning cost	63400000 €
Opex	1000 €/MWh
Discount Rate	9,8%
LCoE	1025,86 €/MWh

Table 4.2 Summary of the 50x6MW marine current facility LCoE

The Opex, Capex and discount rate were also chosen following the Sandia National Laboratories report *[55]* and spreadsheet *[56].* The decommissioning cost was established at 10% of the Capex value.

4.2.2.2 Discussion

To validate the calculated LCoE results, we have searched, in literature, other examples of tidal energy recuperation, to compare our results to. This task will only provide an approximate order of magnitude of the value of LCoE we are looking for, since these can vary massively depending on the technology in use.

We have, however, retrieved values the document "World Energy Perspective: Cost of Energy Technologies" by the World Energy Council and Bloomberg New Energy Finance *[52],* in order to better comprehend our results.

Geography	CAPEX (USDm/MW)	OPEX (USD/MW/yr)	Capacity factor (%)	LCOE (USD/MWh)
High cost	16.05	~130,000	25	1,049
Central	9.28	~130,000	35	451
Low cost	6.73	~130,000	45	263

Table 4.3: Levelised cost of tidal energy per region, Bloomberg energy Finance

We can see that our value for LCoE corresponds to that of a high cost tidal energy recuperation facility.

4.3 LCoE of proposed facility: Sensitivity Analysis

In order to perform an LCoE calculation for our joint facility, we will perform cost reduction educated hypothesis and observe the sensibility of the LCoE's indicator, involved in our park, to these quantitative cost reductions.

Figures 4.8 and 4.9, found below, will show these cost reductions, if all the cost mutualisation hypothesis for Capex were applied for equal reductions from 10% to 50%, in each highlighted component.

Figures 4.10 and 4.11, found below, will show the Opex cost mutualisation hypothesis with cost reductions from 10% to 50%.

4.3.1 Calculation of the LCoE indicator for the joint park

The hypothesis in cost reduction due to cost mutualisation opportunities are as follows: Foundations and structure component, Installation, Electrical System, Operation and Maintenance.

- *Foundations and structure components*

This first cost reduction scenario refers to the reduction in monopole structures, designed for our park, due to the possible mechanical coupling of the technologies. Indeed, since the monopile body of the 50 wind turbines will be shared with that of 50 tidal turbines, the cost of the foundations and the monopile for marine current turbines will decrease.

For tidal technology, we have seen that the monopile, laying in Mooring and Foundation, represents 10,8% (*Annex 4*) of the marine current Capex. Whereas, this respective component, for wind turbines, is included in the Balance of system component (*Annex 3*), under Substructure and Foundation, representing 9% of the wind offshore Capex.

In order to perform the sensibility analysis, we will suppose a maximum cost reduction of 50% for the Mooring and Foundation component of the tidal LCoE, which is the maximum possible reduction, knowing there will be half the number of monopoles and foundations. We will, as well, suppose a maximum cost reduction of 50% for the wind LCoE Substructure and Foundation. Results are shown in Figure 4.8 and Figure 4.9.

- *Installation*

Here, we refer to the possibility of mutualising the installation processes, resources and logistics of the marine and the offshore wind turbines.

For the tidal technology, the Installation costs represent 11,4% (*Annex 4*) of the marine current Capex. Whereas, this respective component for wind turbines is included in the Assembly Installation Component section (*Annex 3*), representing 11,6% of the wind offshore Capex.

Indeed, we will suppose a maximum cost reduction of 50%, due to the potential reduction in the number of vessels needed, the cost of labour and the logistics potential reductions. Results can be seen in Figure 4.8 and Figure 4.9.

- *Electrical System*

When evaluating the electrical synergies, we refer to the possibility of mutualising structures such as the underwater cabling, the marine and on-land substations, as well as, facility transformations or other independent electrical equipment that could be pooled to serve both technologies.

For the tidal technology, the System Integration and Profit Margin costs represent 6,5% (*Annex 4*) of the marine current Capex. Whereas, this respective component for wind turbines is the Electrical Infrastructure, representing 12,9% *(Annex 3*), of the wind offshore Capex.

The power synergies are supposed to entail a maximum reduction of 50%. We recommend a further study of the electrical coupling possibilities of the two technologies, in order to further the cost reduction of the power conversion chain. Results can be seen in Figure 4.8 and Figure 4.9.

- *Operation and Maintenance*

Throughout the lifetime of the park, costs can also be reduced. That is the case of O&M costs. By jointly recuperating energy, many processes can be mutualised such as, vessels accessing the site for repair, or scrutiny and environmental monitoring. Therefore, efficient logistics will result in overall reduction of O&M costs, in comparison to the separate parks.

Indeed, our park allows the lowering of delivered costs for components, by dramatically reducing the number of supply chain interventions (lifts and moves), and the reduction of the components 'journey' and overall 'industry carbon footprint'.

The overall O&M cost reduction for both marine current and offshore wind technologies is supposed to be at a maximum of 50%. Results can be seen in Figure 4.10 and Figure 4.11.

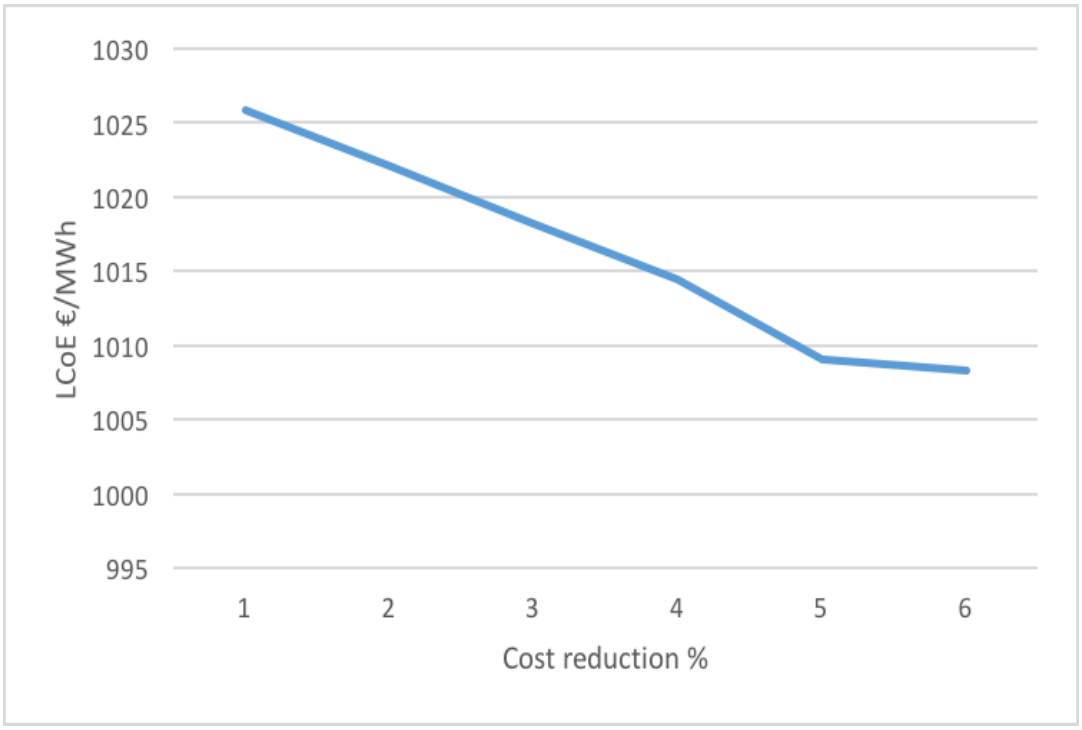

Figure 4.8: Sensibility Analysis of LCoE tidal energy for cost mutualisation in Foundations and structure components, Installation and Electrical System, self- produced.

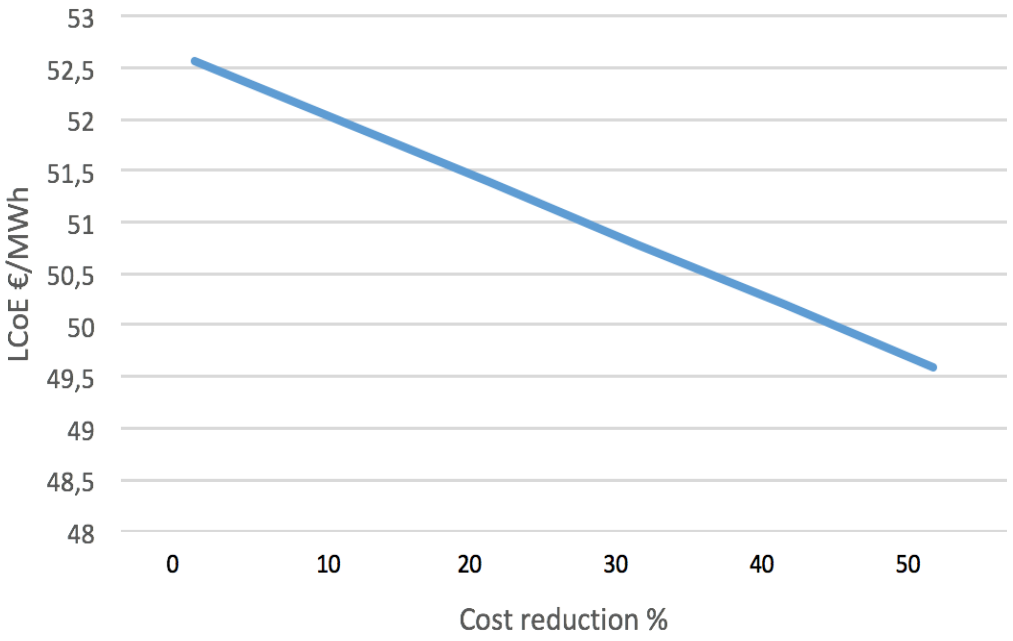

Figure 4.9: Sensibility Analysis of LCoE wind energy for cost mutualisation in Foundations and structure components, Installation and Electrical System, self-produced.

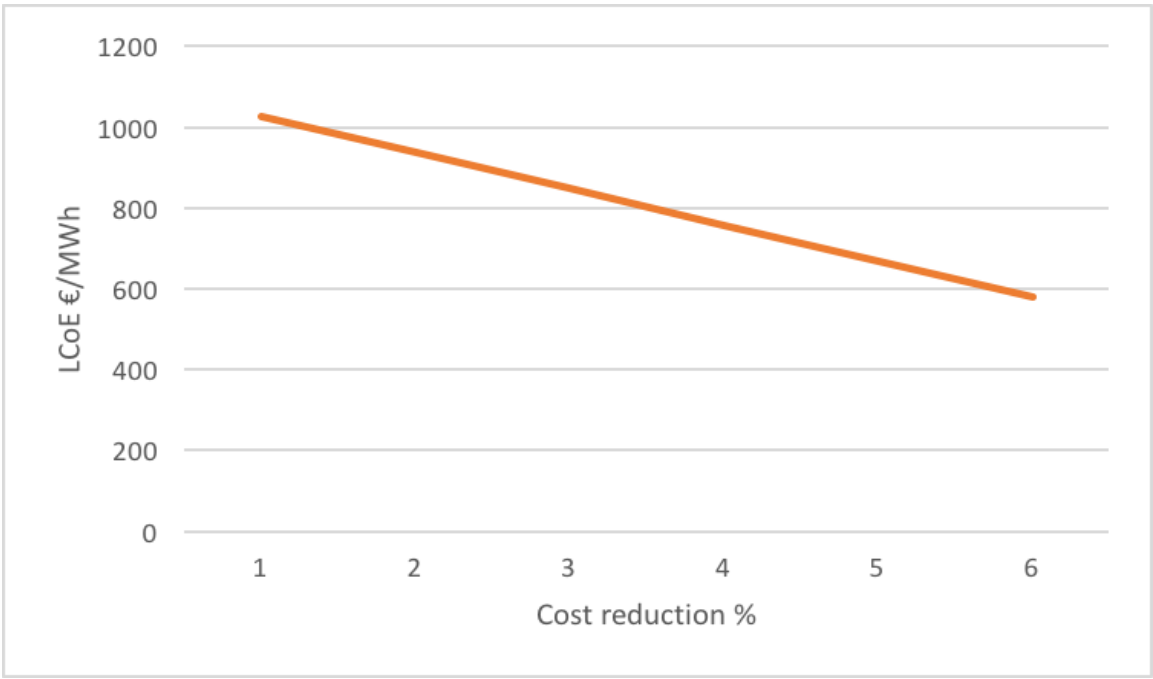

Figure 4.10: Sensibility Analysis of LCoE tidal energy for cost mutualisation in Operation and Maintenance, self- produced.

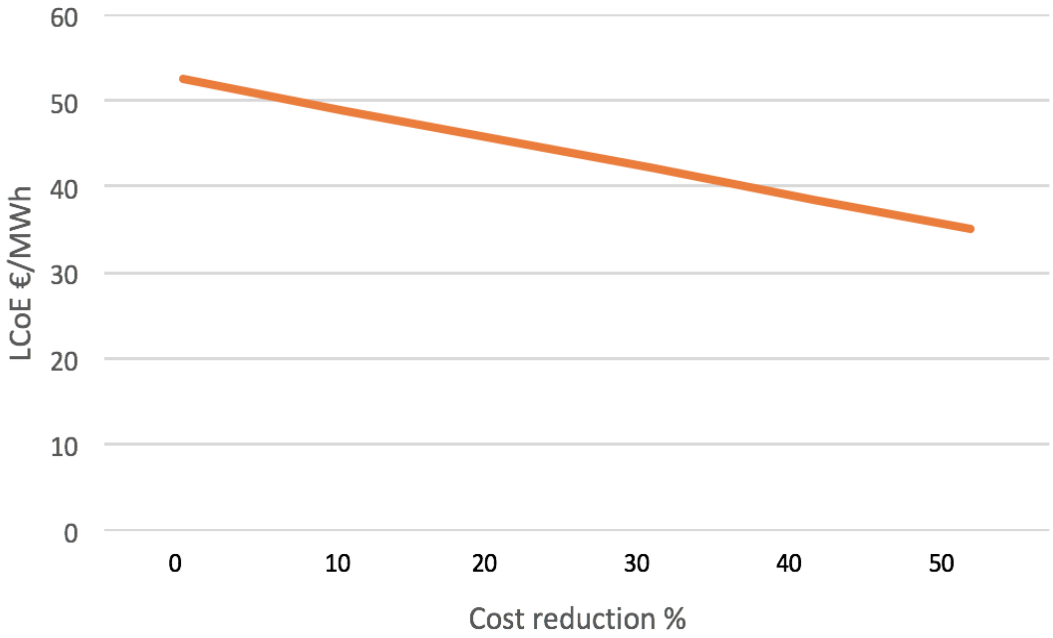

Figure 4.11: Sensibility Analysis of LCoE wind energy for cost mutualisation in Operation and Maintenance, self-produced.

4.3.2 Discussion

The combination of all the aforementioned strategies shows the cost mutualisation from the worst-case scenario – scenario where, all cost mutualisation entail a 10% cost reduction - to the best-case scenario -scenario where, all cost mutualisation entail a 50% cost reduction.

All in all, the combination of the 'big space in the right place' brings cost advantages on a major scale. Some key advantages of our joint facility, in terms of cost and other, should also be mentioned. Indeed, a truly integrated cluster would bring additional benefits, and have a profound impact on wider business behaviours towards the sector. That is, an integrated cluster will enable deeper relationships between manufacturers and key suppliers to be enhanced. Moreover, having a critical mass of activity, in one geographic area, will accelerate innovation and shorten 'time to market'.

As the results show qualitatively and argumentatively, cost reductions can be achieved through cost mutualisation opportunities. However, we have been unable to further quantify the cost reductions that these would entail, due to the inexistent previous examples and databases, of such technological and logistic combinations. Furthermore, a combination of cost mutualisation that entail cost reductions in different degrees (i.e 10% for installation + 50% for O&M) can be examined with our dataset and method. A simplistic example has been given in this report's sensitivity analysis – equal amounts of cost reductions for every cost mutualisation, since it was deemed to bring about enough information on our method and to illustrate its potential qualitatively.

Nonetheless, our results can be highly beneficial, if the "reverse engineering" approach is to be used. That is, having calculated the percentage reduction of a certain mechanical/electrical/logistics synergy to a given park – in an academic context or for commercial reasons – our graphs easily show the variation in LCoE that said mutualisation would suppose for the facility as a whole.

5.CONCLUSION AND FURTHER STEPS

5.1 Conclusion

The design of the park, from an electrical, logistical and mechanical point of view, concludes with quantitative and qualitative results.

Thus, the technical-economical study of the joint park reaches quantitative results for the location of the park, its design, the annual produced energy and the cost of this energy production per MWh. However, the study delivers qualitative results for the cost reduction opportunities, through a sensitivity analysis under the assumption of synergies between these two technologies.

Indeed, many mutualisation possibilities can be considered. However, as these parks do not exist, it remains difficult to study them quantitatively. The tool we propose in the economic part, allows, once the degree of mutualisation is known quantitatively, to calculate the exact cost reduction.

The project proposes an integrated and innovative park, that complements the recuperation of energy through a mature, competitive and fluctuant energy (wind energy) with a technology that remains experimental, more expensive but foreseeable (tidal energy). Besides indicating the possible cost reductions that the co-location of the recuperation of these energies would enable, this park implies a support to the tidal energy, and would promote its growth and allow it to become economically more competitive.

5.2 Meteorological extrapolation

The aim of our project was to test the economic viability of our innovative park. To justify this, we had to find a specific location in order to model a park and to calculate real values for this, such as:

- The number of wind and marine current turbines
- The spacing of these, according to the characteristics and specifications of the site chosen
- Calculation of the power generated by the park

In order of an offshore park to be viable, some building constraint on the location must be taken into account, like avoiding crossing maritime routes, suitability of water depth for wind turbines, distance to the coast and, of course, an optimal wind.

These constraints on our park have been multiplied, as we have to fulfil, not only the optimality of wind, but also the optimality of marine currents.
After meeting a meteorologist, Gilbert Bonneil, and the study of "Appel a Manifestations d'interets" *[18]* for both wind and current, we have found a suitable location for the building of our park. The superposition of wind speed map, marine current map, water depth and many other have confirmed our choice.

However, our project has a much wider view. Though we have imputed a specific park for a specific location, we aim at proposing a new type of offshore parks. Indeed, the superposition of global marine current maps and global wind speed maps could lead us to many other suitable locations for the implementation of joint parks.
This part has been left for a further study. The multiplicity of possible sites is a necessary condition for the justification of the creation of our new type of park. The repeatability of this project is intrinsic.

The study of maps, such as the Figure 5.1 below, enables us to find suitable sites for the implementation of tidal current parks. As seen before, the optimal tidal current speed remains around 2-3m/s. These current speeds are found near the coasts, which is a positive point for offshore park who nowadays tend not to move away into open sea. Indeed, these currents speeds (in dark blue on the map) can be found all around the world.
The complementary study of wind speed maps would lead to the selection of other suitable sites for the installation of our facility.
Even though this repeatability study has not been made, we can estimate that our park does not remain a specific case but that it can be designed and adapted to many other sites throughout the world. This study would bring a powerful and meaningful argument to our project.

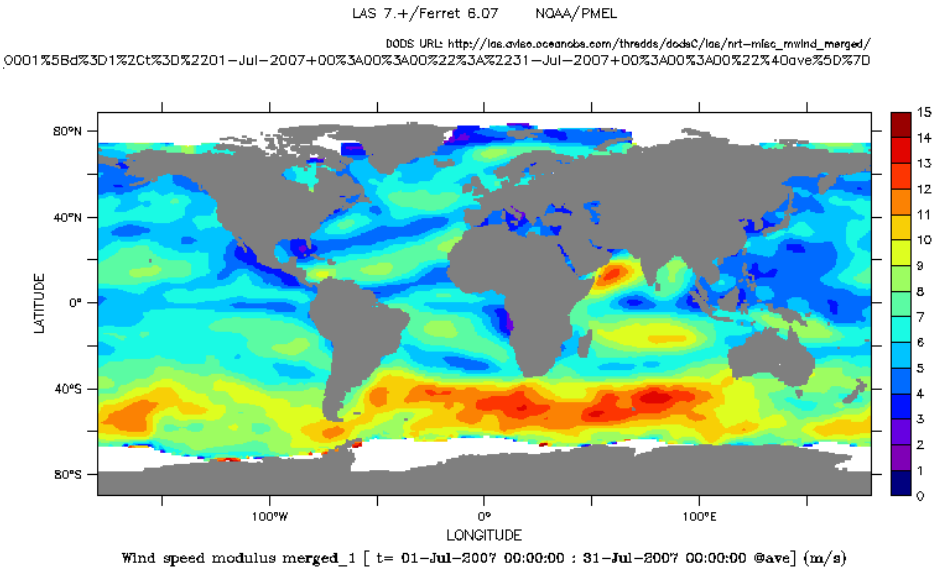

Figure 5.1: Wind speed magnitude around the world [57]

5.3 Study of the mechanical structure

In the Section *3.3.3.1 Recuperation units,* we propose the installation of a joint recuperation unit: on a same body are found a wind turbine, as well as a tidal current turbine. You may see the sketch of this unit proposed on the Figure 3.29.

This proposition has been made to improve and further the cost reductions of the joint park. However, a mechanical study of this new type of structures should be made. Therefore, have been left for a future study the trials of theoretical tiredness, tests on traction-torsion, life time, test on corrosion.

A first plan/sketch has been proposed on the Figure 3.29. This structure can surely be improved. We also advise the study of other combination possibilities of both structures on the same body –wind and tidal current turbines-, as well as the economic analysis of each combined structure possibility.

5.4 Environmental impact assessment

The construction of our park has not only an economical, but also an environmental impact. One of the advantages of the joint park is that it has positive environmental consequences, as the power recuperated has a wider spectrum. We manage to capture not only wind, but also marine current energy. On the same area, we produce a greater amount of “clean” energy.

However, we also need to specify the negative impact on its closest ecosystems. A joint park could have more negative impact points on its environment: alike costs, many impact points are common, but others not. This increases the number of negative impacts. The installation of a joint offshore park can impact on sea-life, both in the air and in the water-depths: marine mammals, sea birds, plants, seabed…

We have left this part for a further study. We advise to use the Benthic Community life cycle Analysis.

6. BIBLIOGRAPHY

[1]: Global electricity data. Available online at: http://www.planete.energies.com/en/medias/close/global-electricity-mix
[2]: Energy Production by Country . Availbale online at: https://en.wikipedia.org/wiki/Main_Page/Energy_in_Spain & https://en.wikipedia.org/wiki/Main_Page/Energy_in_Denmark
[3]:Stanford University News. Available online at: http://news.stanford.edu/news/2012/september/wind-world-demand-091012.html
[4]: Wind Turbine Types. Available online at: http://me1065.wikidot.com/types-of-wind-turbines-and-associated-advantages
[5]: Tidal turbine Technology. Available online at: http://www.climatetechwiki.org/technology/jiqweb-ro
[6]: *Profitability Assessment for a Tidal Power Plant at the Mouth of Hvammsfjörður,* Iceland. Available online at: http://www.ru.is/media/reyst/Niels-Sveinsson.pdf
[7]: Global CCS Institute. Available online at: https://hub.globalccsinstitute.com/publications/renewable-electricity-futures-study-volume-2-renewable-electricity-generation-and-storage-technologies/95-technology-characterization
[8] Subject: Cours Énergies Renouvelables, Jean- Claude Vannier. Topic: Éolien, Amir Arzandé, CentraleSupélec, 2017.
[9] Subject: Cours de Réseaux Electriques, Jean Claude Vannier, Topic: Machine Synchrone, CentraleSupélec, 2016.
[10] PAGINA WEB DE LA GEARBOX
[11] *Doubly-Fed induction generator Systems for wind turbines*, S.Muller, M.Deike and Rik W. De Doncker, 2002
[12] *Introduction to Doubly-Fed Induction Generator for Wind Power Applications*, Dr John Fletcher and Jin Yang, University of Strathclyde, Glasgow, United Kingdom
[13] Subject *:* Cours de Réseaux Electriques, Amir Arzande, Topic: Electronique de puissance, CentraleSupélec, 2016.
[14] Subject: Cours de Réseaux Electriques *,* Mohamed Bensetti, Topic: *Transformateurs*, CentraleSupélec, 2016.
[15]: 3rd International Conference on Ocean Energy. "OCEAN LIDER: Ocean Renewable Energy Leaders" J. Amate López, 2010
[16]: NTNU AMOS, Centre for autonomous marine operations and systems. Official website: www.ntnu.edu/amos/
[17] ABLE Humber Port - ABLE Marine Energy Park. Official website: www.ableuk.com/sites/port-sites/humber-port/amep/
[18] Regional database, Brittany State of the Art. www.rte-france.com/sites/default/files/be_regional_2013_bretagne.pdf
[19] Éolien en Mer, France Énergie Éolienne. Available online at : www.fee.asso.fr/politique-de-leolien/eolien-en-mer/
[20] SHOM: L'océan en reference. Database: www.data.shom.fr/donnees/

[21] Article: L'Éolien Offshore Français Monte en Puissance : Où en est-on ? Niels de Grival. Online: www.e-rse.net/leolien-offshore-monte-en-puissance-19419/amp
[22] Météo France. Available online at: www.meteofrance.com/accueil
[23] Open Ocean: Marine Data Intelligence. Official website: www.openocean.fr/
[24] A Comparison Study of Offshore Wind Support Structures with Monopiles and Jackets for U.S. Waters, R Damiani, K Dykes and G Scott. National Renewable Energy Laboratory (NREL), USA, 2016.
[25] Submarine cable map. Online: www.submarinecablemap.com/#/
[26] Visual Assessment of Windfarms: Best Practice. Scottish Natural Heritage, 2002.
[27]*:* Dong Energy website. Available online at: http://humberbusiness.com/news/dong-energy-delights-at-1-000th-offshore/story-3378-deta
[28]:MHI Offshore Website. Available online at: http://www.mhivestasoffshore.com/v164-8-0-mw-breaks-world-record-for-wind-energy-production/
[29]: Adwen Offshore Website. Available online at: http://www.adwenoffshore.com/products-services/products/8-mw-turbines/
[30]: Siemens 6.0 MW Offshore Wind Turbine Brochure
[31]: 4coffshore website. Avalailable online at: http://www.4coffshore.com/
[32]: Wikipedia, Siemens Wind Power. Available online at: https://en.wikipedia.org/wiki/Siemens_Wind_Power
[33]:Wikipedia, Seagen. Available online at: https://en.wikipedia.org/wiki/SeaGen
[34]: Greenoptimistic, John Hopkins and Johan Meyer. Available online at: https://www.greenoptimistic.com/wind-turbine-distance-doubled-meneveau-20110122/#.WKnlLhIrJhE
[35] Christophe Bassem Maalouf, *Etude des phénomènes tourbillonnaires dans le sillage éolien,* Thesis
[36] PH Alfredsson et JÅ Dahlberg : *A preliminary wind tunnel study of windmill wake dispersion in various flow conditions*. Technical Note AU-1499, 1979.
[37]: *Optimal Turbine Spacing in fully developed wind farm boundary layers*, 2011, Johan Meyers
[38]: *The wind Farm Layout Optimization Problem*, 2013, Michele Samorani
[39]: Potential Flow around a circular cylinder. Article available online at: https://en.wikipedia.org/wiki/Potential_flow_around_a_circular_cylinder
[40] *SeaGen Environmental Monitoring Programme*, 2012, Royal HASKONING
[41]: Potential Flow around a circular cylinder. Article available online at: https://en.wikipedia.org/wiki/Potential_flow_around_a_circular_cylinder
[42]: Aymeric Vie. Personal Communication.
[43]: Princeton University article https://www.princeton.edu/~asmits/Bicycle_web/blunt.html
[44]:*Wind Ener*gy. 2017; 20:465–477 Published online 4 August 2016 in Wiley Online Library (wileyonlinelibrary.com). DOI: 10.1002/we.20 http://onlinelibrary.wiley.com/doi/10.1002/we.2016/full
[45] Amir Arzandé, Personnal Communication

[46] Seawater thermophysical properties Library, MIT 2017:
http://web.mit.edu/seawater/2017_MIT_Seawater_Property_Tables_r2.pdf
[47] World Energy Perspective: Cost of Energy Technologies. World Energy Council and Bloomberg New Energy Finance, 2013.
[48] Density of air at standard atmospheric pressure and 20ºC:
http://www.engineeringtoolbox.com/air-density-specific-weight-d_600.html
[49]: MOOC: Wind Energy, Danish Technical University. Available online at:
www.coursera.org.
[50] The Economics of Wind Energy: A report by the European Wind Energy Association, 2009.
[51] Cost of Wind Energy Review, National Renewable Energy Laboratory. Christopher Moné, Tyler Stehly, Ben Maples, and Edward Settle, 2014
[52] World Energy Perspective: Cost of Energy Technologies. World Energy Council and Bloomberg New Energy Finance, 2013.
[53] Article: Europe's new record offshore LCOE forecast at 40 euros/MWh. Wind Energy Update, 2016.
[54] Article: H2 2016 LCOE: Giant fall in generating costs from offshore wind. Boomerang New Energy Finance, 2016.
[55] Methodology for Design and Economic Analysis of Marine Energy Conversion (MEC) Technologies, Sandia National Laboratories. Vincent S. Neary, Mirko Previsic, Richard A. Jepsen, Michael J. Lawson, Yi-Hsiang Yu, Andrea E. Copping, Arnold A. Fontaine, Kathleen C. Hallett, Dianne K. Murray, 2014
[56] Reference Model 1 CBS.xlsx, ReVision, 2012. Online available at:
energy.sandia.gov/energy/renewable-energy/water-power/technology-development/reference-model-project-rmp/
[57] https://www.aviso.altimetry.fr/fr/applications/atmosphere-vent-vagues/vents-et-vagues/variations-saisonniere
[58]: *Marine current turbines technical specifications report*, MCT aquisition by Siemens
[59]: *Siemens technical Specifications, pg 14.*

7. ANNEXES

Annexe 1 :Technical Specifications SeaGen 2MW (self-production) *[49]*

SeaGen S - 2MW

Twin 1MW power train

Mechanics/Aerodynamics

Rotor

	Value	Unit	
Type	Squirrel cage, no slip rings required		
Position	Upstream		
Diameter	20	m	
Sweep area	628	m^2	for 2 rotors
Sweep speed	4-11,5	rpm	
Power Regulation	Active blade pitch regulation		

Blade

	Value	Unit
Type	Composite material	

Mechanic brake

	Value
Type	Hydraulically released brake

Support structure

	Value	Unit
Weight of drive trains	60000	kg
Type	Crossbeam on tubular tower Monopile Foundation	
Tower	Steel	
Crossbeam	raised: maintain drive trains (avoiding the cost and delay of marine vessels)	

Electrical/Electronics

Generator

	Value
Type	Asynchronous

Grid Terminals

	Value	Unit
Nominal Power	1000	kW
Voltage	690	V
Frequency	---	Hz

Controller: same as wind

	Value
Type	Microprocessor
SCADA system	WPS
Controller designation	WTC 3.0

Cooling system

	Value
Gearbox	Direct to passing sea water
Generator	Direct to passing sea water

Tower

	Value	Unit
Type	Cylindrical tubular steel	
Diameter	3,5	m
Hub Height	Site-specific	
Corrosion protection	---	
Weight	Site-specific	
Height above sea level	9	m

Operational data

	Value	unit
Cut-in speed	1	m/s
Nominal power at	2,5	m/s

Annexe 2: Technical Specifications Siemens Sapiens 6MW (self-production) *[50]*

Siemens Sapiens 6MW Offshore Turbine

SWT-6.0-154

Mechanics/Aerodynamics

Rotor

	Value	Unit
Type	3-bladed, Hz axis	
Position	Upwind	
Diameter	154	m
Sweep area	18600	m^2
Sweep speed	5-11	rpm
Power Regulation	Pitch reg with variable speed	
Rotor tilt	6	degrees

Blade

	Value	Unit
Type	Self-supporting	
Blade length	75	m
Aerodynamic profile	Siemens proprietary airfoils FFA-W3-XXX	

Aerodynamic brake

	Value
Type	Full span pitching
Activation	Active, hydraulic

Mechanic brake

	Value
Type	Hydraulic disk brake

Load supporting parts

	Value	Unit
Towerhead mass	360000	kg

Electrical/Electronics

Generator

	Value
Type	Synchronous, PMG
Drive	Direct Drive

Grid Terminals

	Value	Unit
Nominal Power	6000	kW
Voltage	690	V
Frequency	50	Hz

Controller

	Value
Type	Microprocessor
SCADA system	WPS
Controller designation	WTC 3.0

Yaw system

	Value
Type	Active
Yaw bearing	Externally geared
Yaw drive	Electric gear motors
Yaw break	Passive friction brake

Operational data

	Value	unit
Cut-in speed	3-5	m/s

Hub	Nodular cast iron		Nominal power at	12-14	m/s
Main shaft	Nodular cast iron		Cut-out speed	25	m/s
Nacelle bed plate	Nodular cast iron		Maximum 3s gust	70	m/s

Tower

	Value	Unit
Type	Cylindrical	
Outer Diameter	6,9	m
Hub Height	96	m
Corrosion protection	Painted	
Weight	Site-specific	

Monopile 5 MW: Reference

	Value	Unit
Outer Diameter	6.9	m
Wall Thickness	70	cm
Pile Length	64	m
Weight	2200	t

Annexe 3 : Offshore Wind Cost portfolio (self-production)

Source: Cost of Wind Energy Review, National Renewable Energy, 2014

1. DEVELOPMENT		
Component	*% Cost of Capex*	*Value*
Permission		
Environmental study		
Discount rate (costs of burrowing money) (%)		0,098

2. IMPLEMENTATION

Capital Costs

Component	*% Cost of Capex*	*Value*
Wind Turbine	**33%**	62646964,36

	% Cost of Capex	*Value*
Nacelle	2%	3808326,101
Blades	20%	38083261,01
Gear Box	15%	28562445,76
Generator	4%	7616652,202
Controller	10%	19041630,5
Rotor Hub	5%	9520815,252
Transformer	4%	7616652,202
Tower	25%	47604076,26
Others	15%	28562445,76

Balance of Systems	**38,40%**	73119861,14

	% Cost of Capex	*Value*
Development	2,20%	4189158,711
Engineering &Managment	1,60%	3046660,881
Substructure & Foundation	9,00%	17137467,45
sight Access, Staging & Port	0,40%	761665,2202
Eelctrical infrastructure	12,90%	24563703,35
Assembly &installation	11,60%	22088291,38
Plant commissioning	0,70%	1332914,135

Financial Costs	**18,40%**	35036600,13

	% Cost of Capex	*Value*
Decommissioning	2,70%	5141240,236
Contingency	9%	17137467,45
Construction Finance	5,80%	11044145,69
Insurance	0,90%	1713746,745

Market Price Adjustment	**10,30%**	19612879,42
Total (Capex)	190416305 $	

3. OPERATION

Component	*% Cost of Opex*	*Value*
Equipment	53%	20,67
Grid Maintenance/Lease	24%	9,36
Personel Acces	9%	3,51
Labour	8%	3,12
Installation/Repair Vessels	6%	2,34
Taxes payed to local authorities/Land leasing		
Yearly (Opex) 39 $/MWh		

4. DECOMMISSIONING	
Component	*Value*
Decommissioning costs	19041630,5

Annual Energy Production	
1220617,34	MWh
Years of operation	20

Annexe 4 : Tidal Energy Cost portfolio (self-production)

source: Methodology for Design and Economic Analysis of Marine Energy Conversion Technologies, Sandia National Laboratories, 2014

1. DEVELOPMENT		
Component	*% Cost of Capex*	*Value*
Permission and Environmental Compliance	1,7%	10963502,22
Site Assesment	0,1%	527433,6892
Project Design, Engineering, and Management	1,3%	8517689,207
Discount rate (costs of burrowing money) (%)		0,098

2. IMPLEMENTATION				
Capital Costs				
Component			*% Cost of Capex*	*Value*
Infrastructure			4,5%	28778618,46
	% Cost	*Value*		
Subsea Cables	0,4%	2832484,695		
Cable Landing (Material only)	0,0%	28324,84695		
Dockside Improvements	0,0%	0		
Dedicated O&M Vessel	4,1%	25917808,92		
Other	0,0%	0		
Mooring/Foundation			**10,8%**	68384163,72
	% Cost	*Value*		
Mooring lines/chain	0,0%	0		
Anchors	0,0%	0		
Buoyancy Tanks	0,0%	0		
Connecting Hardware (shackles etc.)	0,0%	0		
Other	0,0%	0		
Pile	10,80%	68472000		
		0		
Device Structural Components			**10,20%**	64668000
	% Cost	*Value*		
Cross-arm	3,2%	20288000		
Nacelles	5,2%	32968000		
Device Access (Railings, Ladders, etc)	1,9%	12046000		
Power Take Off			**44,3%**	280829586,6
	% Cost	*Value*		
Generator	5,4%	34404825,03		
Gearbox and Driveshaft	7,9%	50260488,67		
Hydraulic System	0,9%	5799311,528		
Frequency Converter	5,8%	36595228,75		
Step-up Transformer	0,8%	4896329,589		
Riser Cable	0,4%	2690429,992		

Electrical Energy Storage	0,0%	0		
Seals	3,6%	23040991,33		
Control System	5,4%	33924757,71		
Bearings and Linear Guides	7,5%	47712931,4		
Assembly, Testing & QA	0,0%	0		
Rotors	0,5%	3153793,331		
PTO mounting	2,2%	13716964,59		
Other	3,9%	24633534,68		
Subsystem Integration & Profit Margin			**6,5%**	41412423,67
Installation			**11,4%**	72039732,4
	% Cost	*Value*		
Transport to Staging Site	0,0%	0		
Cable Shore Landing	0,7%	4128195,779		
Mooring/Foundation System	3,6%	22928845,74		
Subsea Cables	3,2%	20536143,6		
Device Installation	3,9%	24446547,28		
Device Comissioning	0,0%	0		
Contingency			**9,1%**	57636363,64
Total (Capex)	634000000	$		

3. OPERATION		
Component	*% Cost of Opex*	*Value*
Insurance	14,8%	148
Environmental Monitoring and Regulatory Compliance	11,1%	111
Marine Operations	33,3%	333
Shoreside Operations	7,4%	74
Replacement Parts	33,3%	333
Consumables	3,7%	
Yearly (Opex) 1000 $/MWh		

4. DECOMMISSIONING		
Component	*% Cost if in Capex*	*Value*
Decommissioning costs	**10%**	63400000

Annexe 5: Simulink wind turbine Model

Complete Model:

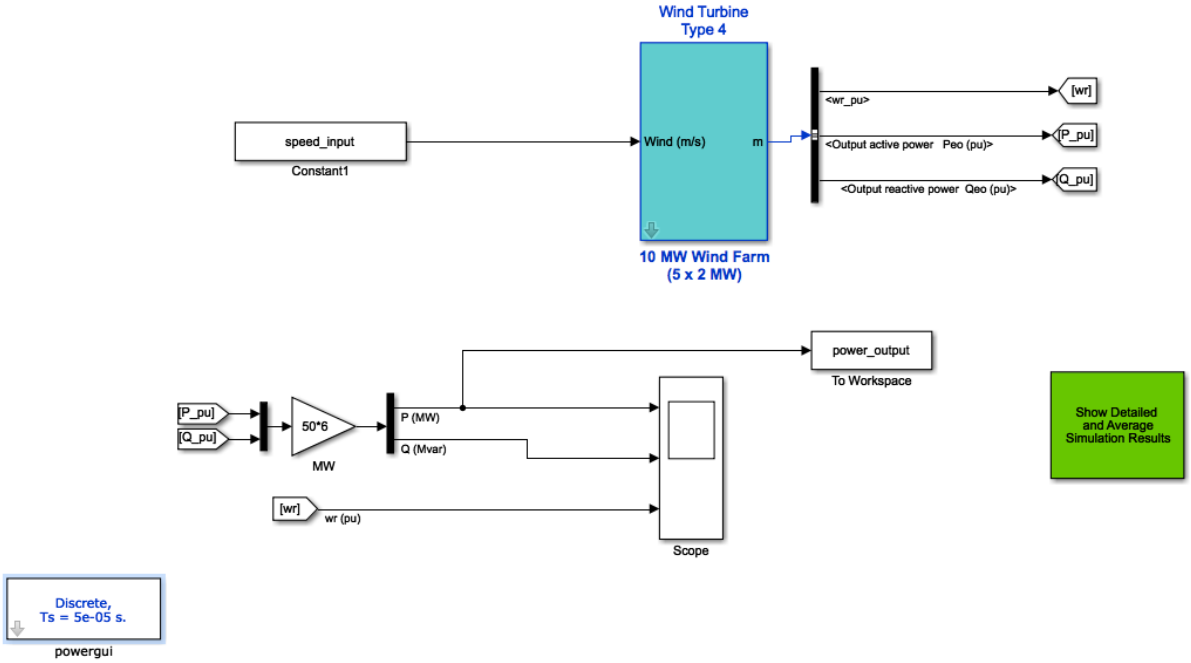

Wind turbine Type 4 Mask Parameters:

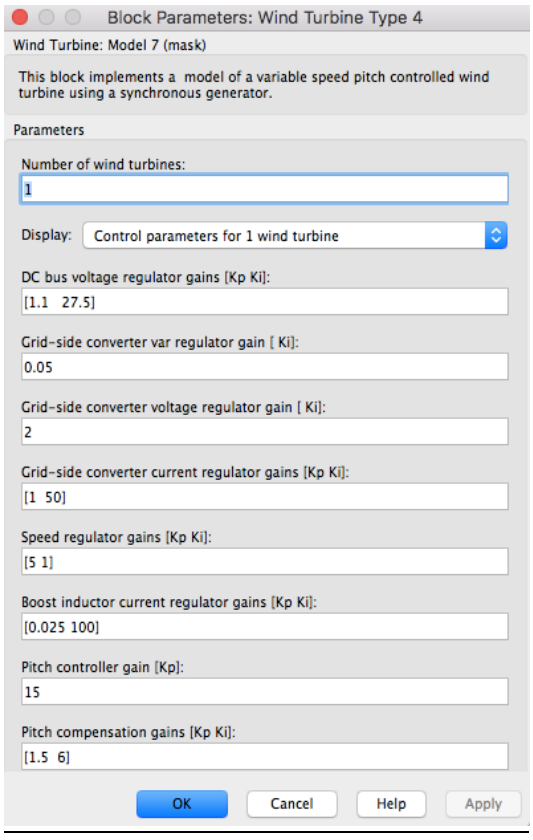

Wind turbine type 4 Mask:

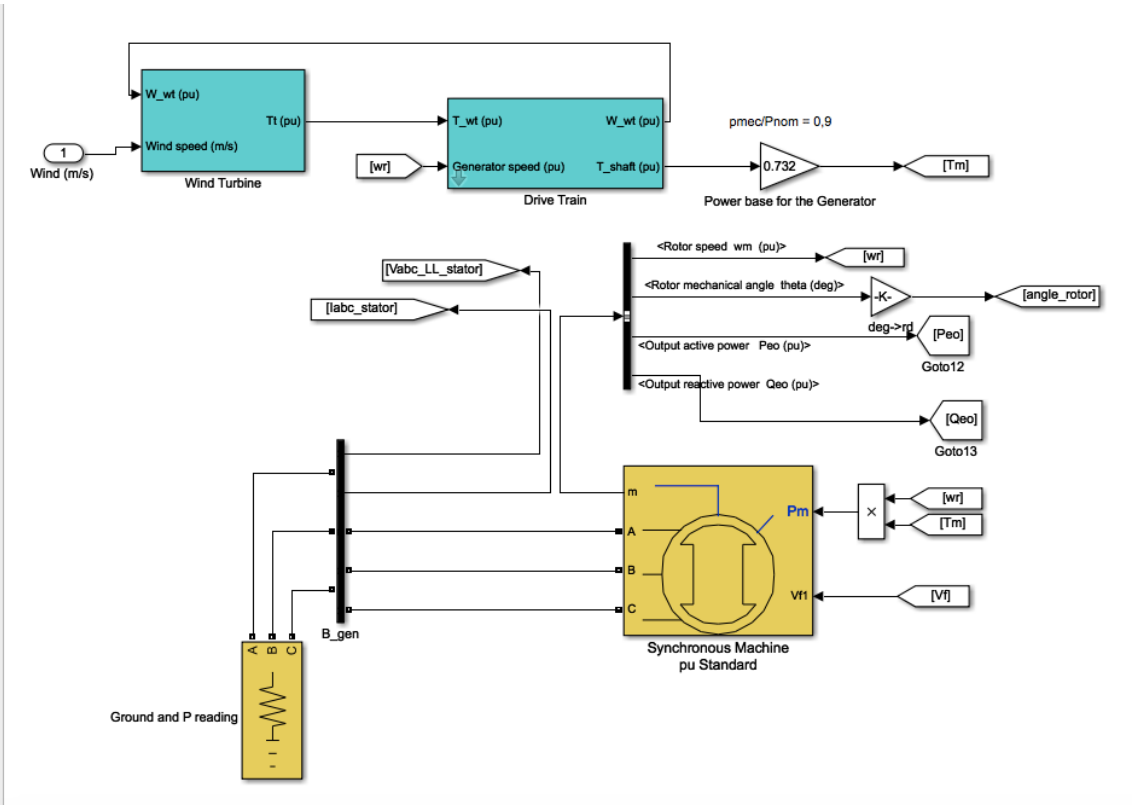

Flux estimator (calculus of Vf, input for the synchronous machine) :

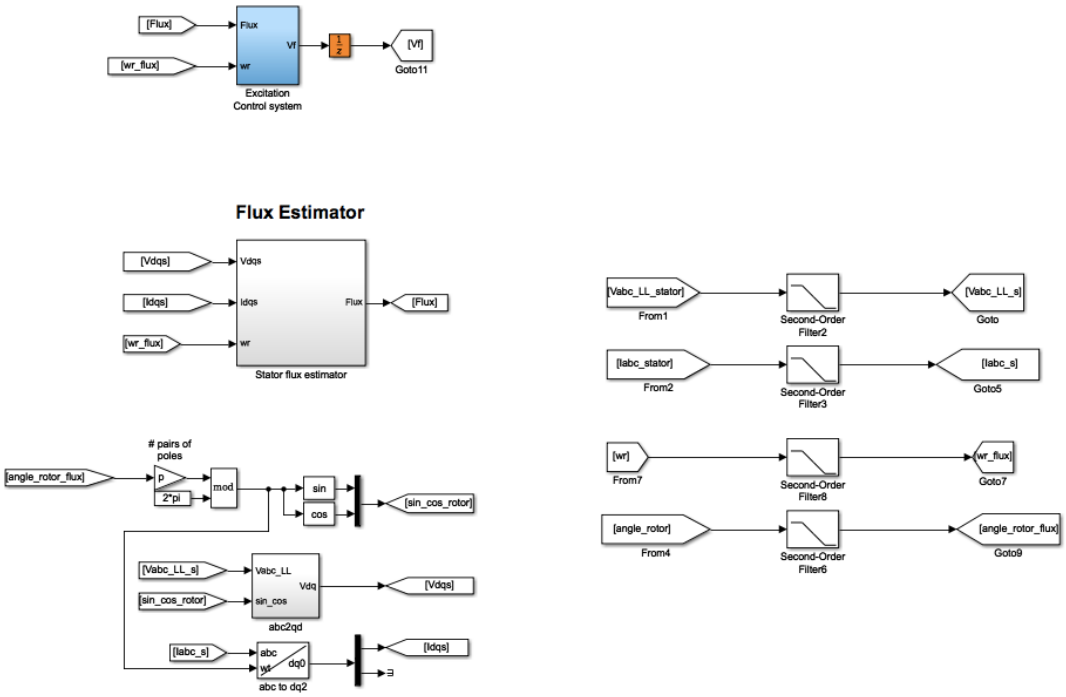

Wind Turbine Mask (left blue box):

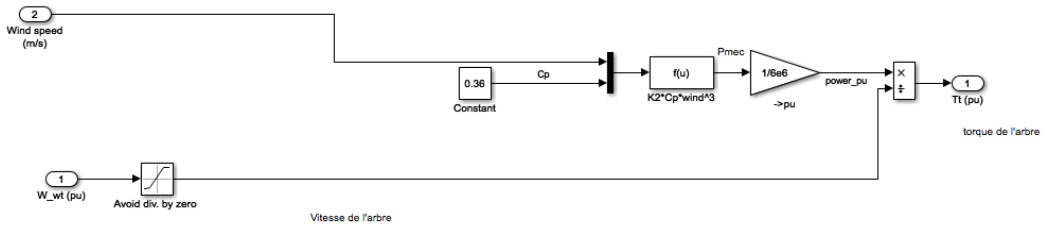

Annexe 6: MATLAB function used to run the simulation

```
%loading current speed data --> already averaged in this
case
current_trend_cut = ones(8760,1);
current_trend_cut = load('current_speed_cut.txt');

%Defining outut power vectors
current_power_trend = ones(8760,1);

%Sending current speed, retrieving power output at t=50s
n=1;
for s=1:8760
     speed_input = wind_trend_cut(s,1);
     sim('power_windgen_v4');
     current_power_trend(n,1)= power_output(2);

     s=s+1
     n=n+1;

end


% %Plotting power trends
% current plot
image(1)
plot(current_power_trend, 'b')
box off
monthlim =
[0   744   1416   2160   2880    3624    4344    5088    58
32    6552    7296    8016, 8760];
x=char('J', 'F', 'M', 'A', 'M', 'J', 'J', 'A', 'S', 'O',
'N', 'D', '');
set(gca, 'Xlim', [0, 8760], 'XTick', monthlim,
'XTicklabel', x)
set(gca, 'Ylim', [0, 400], 'yTick', [0, 100, 200, 300,
400])
set(gca,'FontSize',16)
saveas(gcf, 'current_power.jpeg')
```

Annexe 7: Simulink tidal current turbine Model

Complete Model:

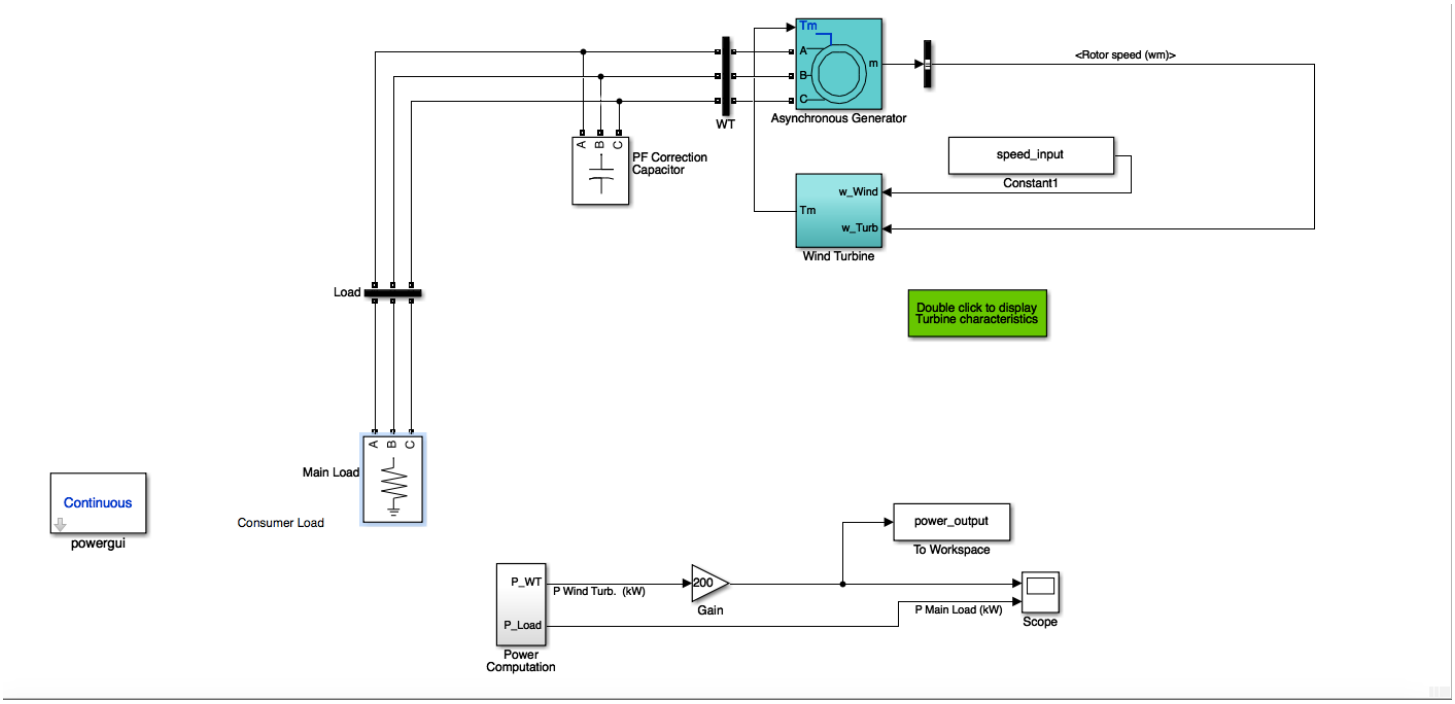

Asynchronous generator Parameters:

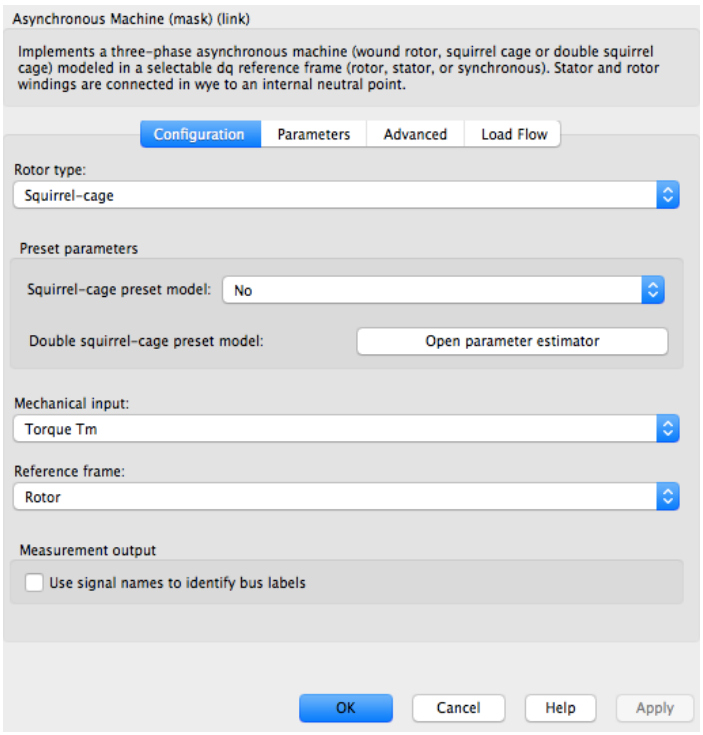

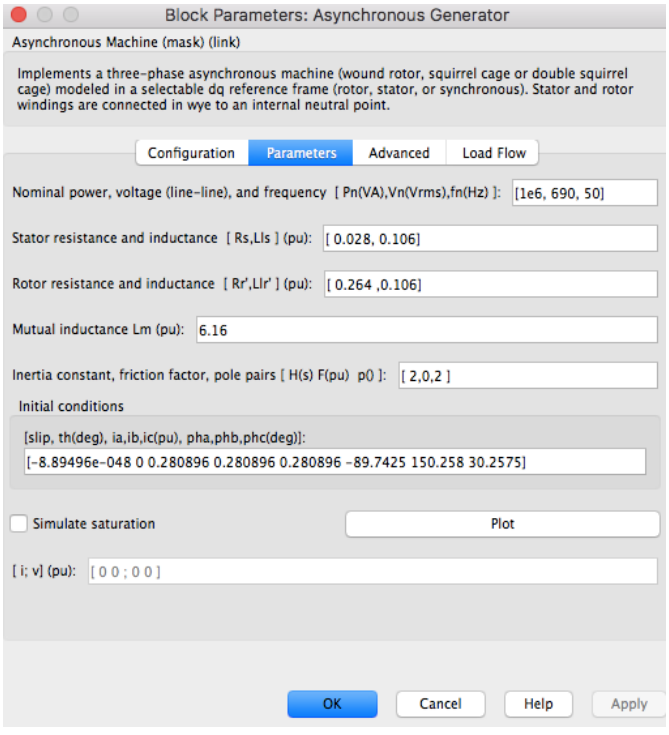

Wind turbine Mask:

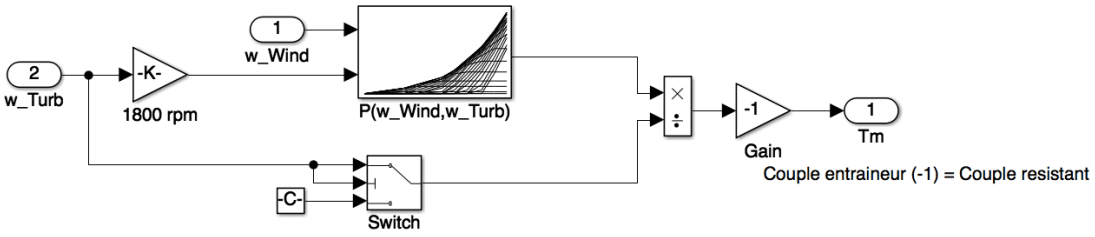

Capacity curves: